UC Santa Barbara

UC Santa Barbara Electronic Theses and Dissertations

Title

Spatial Analytics for Urban Fire Safety: Infrastructure Assessment and Planning in Fire-Prone Communities

Permalink

https://escholarship.org/uc/item/9gx8x29x

ISBN

9798186381457

Author

Heffernan, Vanessa

Publication Date

2026-06-11

Peer reviewed|Thesis/dissertation

eScholarship.org Powered by the California Digital Library
University of California

UNIVERSITY OF CALIFORNIA

Santa Barbara

Spatial Analytics for Urban Fire Safety: Infrastructure Assessment and Planning in Fire-Prone Communities

A dissertation submitted in partial satisfaction of the

requirements for the degree Doctor of Philosophy

in Geography

by

Vanessa Heffernan

Committee in charge:

Professor Alan T. Murray, Chair

Professor Richard L. Church

Professor Kathy Baylis

June 2026

The dissertation of Vanessa Heffernan is approved.

_____

Kathy Baylis

_____

Richard L. Church

_____

Alan T. Murray, Committee Chair

May 2026

Spatial Analytics for Urban Fire Safety: Infrastructure Assessment and Planning in Fire-Prone Communities

Copyright © 2026

by

Vanessa Heffernan

To God, lover of my soul.

ACKNOWLEDGEMENTS

First, I am grateful to God for being with me at every step of this process. This journey challenged me in ways I had not anticipated, and I am grateful for the strength, peace, and hope that I always found in Him.

I am incredibly grateful to my advisor and mentor, Professor Alan Murray. Professor Murray has been an exceptional mentor. He has been patient, flexible, and generous with his guidance, and I am indebted to him for helping me become the kind of researcher I am today. Not only has he inspired me to have greater research ambitions, but he has also helped me grow as a teacher and scholar. I would not have come this far without his guidance. I must admit that although it was not always easy to be mentored through a Ph.D., I now see clearly that he had my best interests in mind. His advice was always meant to make me better and to prepare me for life after this journey.

I also want to acknowledge the Wildfire Resilience Initiative, supported by Yardi Systems, for providing significant funding for a substantial portion of this dissertation. I am also grateful to the Department of Geography for its support throughout my doctoral studies. Although the work of the department often happens behind the scenes, it makes a meaningful difference in the lives of graduate students.

I am also deeply grateful to my dissertation committee. Professor Richard Church not only gave me a strong foundation in set covering models, but also offered stories and perspectives that inspired me. I am also grateful to Professor Kathy Baylis for her support, invaluable research advice, and warmth at every step of the process.

I would also like to express my gratitude to the Murray Group, especially Evgeny, Jiwon, Amelia, Su, Seonga, and Darlene, who made this journey smoother, kinder, and more collaborative. Their support, ideas, encouragement, and friendship made the challenges of graduate school much easier to carry. Another incredible source of support was my cohort. This journey would not have been nearly as fun without them, especially Kaity, Gabrielle, Em, Madie, and Caitlyn, whose friendship and adventures were refreshing in the middle of tight schedules.

To my family, thank you for your love, prayers, and emotional support. To my mother, Claudia, thank you for believing in me and supporting me as I pursued my dreams. To my brother, Julian, and my sister, Aleja, thank you for your love and encouragement throughout this process. I am also grateful to my family-in-law and my extended family in the United States. They welcomed me, supported me, and cared for me as their own. Their love and involvement helped me feel at home during a time when I was building a life far from where I began.

Finally, I am deeply indebted to my husband, Kevin, who has been my unwavering support during the most challenging times. He supported me not only practically, but also emotionally, with immense love, patience, and warmth. Kevin, no acknowledgement feels sufficient for what you have given me. Part of me wishes your name could appear beside mine on this degree, because this accomplishment also carries the mark of your love, encouragement, and sacrifice. Thank you for your unconditional love. I am endlessly grateful to share my life with you.

VITA OF VANESSA HEFFERNAN
May 2026

EDUCATION

Ph.D. in Geography, University of California, Santa Barbara, June 2026 (expected)
M.S. in Mathematical Modeling and Computing Science, Universidad de Medellín, 2021
B.A. in Economics, Universidad EAFIT, 2016

PROFESSIONAL EMPLOYMENT

2021-2025: Research Assistant and Teaching Assistant, Department of Geography, University of California, Santa Barbara.
2014: Research Assistant, Department of Economics and Finance, Universidad EAFIT.
2016-2021: Financial Analyst, Bancolombia S.A.

PUBLICATIONS

Heffernan, V., Murray, A. T., Baylis, K., & Church, R. L. (2026). Urban safety and the role of hydrant structure and configuration. *Scientific Reports*.

Murray, A. T., Rini, D., Sweeney, S. S., Roberts, D. A., Moritz, M. A., Baik, J., Echeverri, V., & Zheng, Z. (2025). Geographic fire response standards emerging from human-environment interactions. *Annals of the American Association of Geographers*, 115(9), 2048–2070.

Echeverri, V., Murray, A. T., & Funk, T. (2024). Supporting fire response: advanced spatial data analytics for hydrant access assessment. *Transactions in GIS*, 28(8), 2559–2573.

Murray, A. T., Baik, J., Echeverri, V., Rini, D., Moritz, M. A., Roberts, D. A., Sweeney, S. H., Carvalho, L. M. V., & Jones, C. (2023). Developing effective wildfire risk mitigation plans for the wildland-urban interface. *International Journal of Applied Earth Observation and Geoinformation*, 124, 103531.

Pludow, B. A., Murray, A. T., Echeverri, V., & Church, R. L. (2023). Evaluation of forest treatment planning considering multiple objectives. *Journal of Environmental Management*, 346, 118997.

PUBLICATIONS IN PROGRESS

Heffernan, V., Murray, A. T., Church, R. (2026). Strengthening urban defense through strategic hydrant additions. *Draft manuscript*.

AWARDS

Dangermond Travel Award, University of California, Santa Barbara, Winter 2023, Fall 2023, and Spring 2024.
Award for Outstanding Effectiveness in Teaching, Bancolombia S.A., 2018.
Academic Travel, Outstanding Research Assistant Performance, Georgia State University, 2014.

Full Scholarship, Universidad EAFIT, 2012-2016.

ABSTRACT

Spatial Analytics for Urban Fire Safety: Infrastructure Assessment and Planning in Fire-Prone Communities

by

Vanessa Heffernan

Fire safety in the built environment presents a paradox: advances in prevention, detection, building standards, and emergency response have reduced many fire impacts, yet structure fires continue to produce a disproportionate share of deaths, injuries, and property losses. In fire-prone coastal communities, this problem is intensified by the overlap of urban development and wildland-urban interface exposure, where fires can move from vegetation into neighborhoods and, once structures are involved, from building to building. Santa Barbara County illustrates this coupled risk context. Its coastal communities sit between the Santa Ynez Mountains and the Pacific Ocean, where dense development, complex road networks, seasonal winds, steep terrain, and wildfire exposure converge. In such settings, fire preparedness depends not only on preventing ignition or deploying firefighters, but also on whether the infrastructure that supports suppression is spatially configured to function where structures, roads, and potential losses are concentrated.

This dissertation develops a spatial analytics framework for urban fire safety that connects infrastructure assessment, empirical analysis of fire patterns and losses, and decision-support modeling for strategic investment in fire-prone communities. First, it introduces a GIS

framework using a road network approach to assess hydrant spacing compliance according to code guidelines at various spatial scales. Second, it extends this infrastructure assessment by examining historical structure-fire incidents and losses, evaluating how fire occurrence and damage are associated with urban form, hydrant infrastructure, timing, and operational conditions. Third, it translates the diagnostic and empirical findings into a spatial optimization framework for prioritizing strategic hydrant additions where infrastructure deficiencies intersect with higher structure exposure and response needs.

Results show that effective fire preparedness and planning necessitate a spatial comprehension of infrastructure readiness. This involves identifying areas with adequate access, highlighting persistent vulnerabilities, and determining the most strategic locations for investments to enhance response capacity. The road-network assessment identifies several parts of coastal Santa Barbara County where spacing deficiencies may limit fire-response readiness. Incident analysis then shows that fire occurrence and loss are shaped by a broader geography of exposure and response. Structure fires concentrate in denser activity centers, with population and housing density strongly associated with incident occurrence, while monetary losses are more closely related to suppression duration, property characteristics, and timing. These findings motivate an investment framework that considers both code-based infrastructure gaps and the places where structures and response needs are concentrated. The optimization analysis demonstrates how new hydrant locations can be prioritized to improve access for developed areas while reducing spacing deficiencies, supporting more transparent and defensible fire preparedness planning.

By linking infrastructure diagnosis, empirical fire analysis, and optimization-based planning, this dissertation contributes to GIScience, location science, and urban hazards

research. It formalizes hydrant systems as spatially structured defensive infrastructure and advances methods for assessing access, interpreting fire patterns, and prioritizing investment in fire-prone communities. More broadly, the dissertation shows how spatial analytics can support more defensible fire-preparedness planning in places where wildfire exposure and urban structure-fire risk increasingly intersect.

TABLE OF CONTENTS

1. Introduction....1

1.1. Motivation....1

1.2. Research Context and Key Problems....7

1.3. Analytical Framework....11

1.4. Research Objectives....15

1.5. Significance....15

1.6. Organization of dissertation....17

2. Supporting Fire Response: Advanced Spatial Analytics for Hydrant Access Assessment....20

2.1. Introduction....20

2.2. Background....24

2.3. Methods....28

2.4. Hydrant assessment in Santa Barbara....34

2.5. Discussion....43

2.6. Conclusions....45

3. Urban Safety and the Role of Hydrant Structure and Configuration....47

3.1. Introduction....47

3.2. Background....51

3.3. Methods....54

3.3.1. Study area....55

3.3.2. Data....57

3.3.3. Exploratory analysis....59
3.3.4. Modeling counts....61
3.3.5. Modeling fire-related losses....62
3.4. Results....63
3.5. Discussion....75
3.6. Conclusions....80
4. Strengthening Urban Defense Through Strategic Hydrant Additions....83
4.1. Introduction....83
4.2. Background....87
4.3. Methods....90
4.4. Application results....97
4.5. Discussion....108
4.6. Conclusions....109
5. Conclusions....112
5.1. Summary....112
5.2. Contributions....114
5.3. Challenges and extensions....118
References....122

LIST OF FIGURES

Figure 1.1. Shared exposure in urban environments: wildfire spread that becomes urban and fire spread that originates in urban settings. The dissertation is motivated by the overlap of WUI and urban fire-spread vulnerabilities and advances GIScience with methods to analyze how hydrant infrastructure supports community fire response. 6

Figure 1.2. Hydrant coverage and spacing distinction.....9

Figure 1.3. Conceptual framework. Progression across chapters combines diagnosis, empirical explanation, and planning response. 14

Figure 2.1. Hydrant spacing in a residential area, with the 525 ft. and 580 ft. instances exceeding the standards stipulated in Table 2.1.....26

Figure 2.2. Hydrant coverage by Euclidean distance buffers and road network distance. 28

Figure 2.3. Pseudo code for edge approach to hydrant neighbor identification. 33

Figure 2.4. Study region located in the southern part of Santa Barbara County. 35

Figure 2.5. Hydrant neighborhoods. 36

Figure 2.6. Street level hydrant spacing assessment.....37

Figure 2.7. Community hydrant spacing assessment.....37

Figure 2.8. Spacing distribution according to the regional standards in the study area. (a) Residential (500 ft). (b) Industrial/Commercial (750 ft). (c) Undeveloped (1000 ft). 39

Figure 2.9. Conformity in the study region.....40

Figure 2.10. Alternative hydrant neighborhoods. (a) Voronoi. (b) k nearest neighbors (k = 4). 41

Figure 2.11. Road centerlines and actual roads. 44

Figure 3.1. Study region in Santa Barbara County, indicating structure fires from 2014 to 2024.....56
Figure 3.2. Kernel density for the areas by subregion. (Bandwidth σ = 0.722 km; incidents per km^2).....64
Figure 3.3. K and L functions for the subregions within the study area.....66
Figure 3.4. Cross K and L functions for the study region.....67
Figure 3.5. Distribution of incident-to-nearest-hydrant distance.....73
Figure 3.6. Linear-network Cross K and L functions for the study region.....79
Figure 4.1. Steps to derive a FDS. a) Identify demand objects. b) Derive a service standard. c) Determine the FDS members based on the overlapping area of the service standard buffers. 96
Figure 4.2. Hydrant distribution in Montecito. 97
Figure 4.3. Spacing distribution in the study region and weighting scheme. 99
Figure 4.4. Spatial baseline conditions: coverage and noncompliant spacing paths. 100
Figure 4.5. Pareto frontier for 20 hydrant additions scenario. 104
Figure 4.6. Spatial tradeoff solution (star in Figure 5). 105
Figure 4.7. Spatial tradeoff solution (diamond in Figure 5). 105
Figure 4.8. Associated spatial solutions when recommending 20 hydrant additions for the best values of both objectives. 106
Figure 5.1. Dissertation contributions to fire response. 115
Figure 5.2. Current challenges and future research avenues. 121

1. Introduction

This chapter sets the stage for the dissertation, outlining its scope and focus. It provides an overview of the central issues it addresses and the broader significance of the work. The sections introduce the motivation, research context and key problems, analytical framework, research objectives, and organization.

1.1. Motivation

Fire safety in the United States represents a paradox of progress and persistence. Over the last several decades, reported fires, civilian deaths, and civilian injuries have declined substantially, reflecting advances in prevention, detection, building standards, and emergency response. Yet these improvements have not eliminated the consequences of fire in the built environment. A study by the National Fire Protection Association reported that fire departments responded to an estimated 1.38 million fires, resulting in 3,920 civilian deaths, 11,780 civilian injuries, and approximately $19 billion in direct property damage (Hall, 2025). One particularly interesting aspect of the report is that structure fires accounted for 34% of reported fires in 2024, but accounted for 81% of civilian fire deaths, 88% of civilian fire injuries, and 83% of total losses. This pattern resembles a Pareto principle, first introduced by Joseph Juran, where a relatively small proportion of events produce a significant portion of the outcomes (see Juran, 1975). In his work he identified the small proportion of events as the "vital few" and coined the rule as a Pareto principle, since his observations started with the findings of Vilfredo Pareto regarding land and wealth distribution in Italy (80% of the income and wealth was owned by 20% of the population). This principle is extremely important for the broader motivation of this dissertation, since by focusing on the 34% of the fires,

meaningful reductions in deaths, injuries, and property damage will follow. In other words, structure fires represent a “vital few” problem for life safety, property protection, and emergency planning. This makes them an especially important focus for spatial analysis because their consequences depend not only on ignition, but also on where structures are located, how urban form shapes exposure, how quickly fires can be controlled, and whether defensive infrastructure is positioned to support suppression.

The economic dimension of structure fires is also a matter of concern. Despite the number of incidents being lower in 2024 than in 1980, the average loss per structure fire, adjusted for inflation, was 1.6 times higher in 2024 than in 1980, rising from $19,700 to $32,500 in 2024 dollars. This means that fire preparedness cannot be evaluated only by whether incident counts have declined over the long term. It must also consider why damaging events remain costly, where losses occur, and what conditions shape the ability to limit damage once ignition occurs. The contemporary fire problem therefore goes beyond ignition prevention. It is a problem of loss control, response capacity, and infrastructure readiness.

Structure fires can occur in any property for various reasons, such as cooking mishaps, electrical failures, or unattended burning candles. However, there is a specific risk associated with structure fires that originate in wildlands and spread into urban areas. That problem becomes more urgent as urban development continues to expand into fire-prone landscapes. The wildland-urban interface (WUI), where housing and other development meet or mix with undeveloped natural areas, contained more than 44 million homes in 2020, or 32% of all housing in the contiguous United States. Between 1990 and 2020, the number of homes in the WUI increased by 47%, while WUI land area increased by 31% (USDA Forest Service, 2024). These numbers are especially relevant given the increased intensity and severity of wildfires

in the last 20 years, especially in the western United States. Development near vegetation, roads, and ignition sources creates places where wildland fire, structure fire, evacuation, suppression, and infrastructure systems intersect. In these settings, the boundary between wildfire and urban fire becomes blurry.

Several recent fire episodes show how wildfires can become urban conflagrations. For example, the Palisades Fire and Eaton Fire in 2025, the Tubbs Fire in 2017, and the Thomas fire in 2018 propagated into urban areas. Although California has received particular attention because wildfires have become more intense and severe there –15 of the 20 most destructive fires in the state have occurred in the last 10 years (CAL FIRE, 2025b)– this phenomenon extends to other territories. The Lahaina Fire in Maui in 2023 destroyed much of the community as it moved from wildlands to the town and stopped at the ocean. In April 2026, two large wildfires in South Georgia burned more than 40,000 acres and destroyed more than 120 homes, with officials citing extreme drought, high winds, fast spread, and evacuation orders as central concerns (CBS News, 2026). In Chile, recent wildfires have moved through forests, towns, and metropolitan edges, affecting communities such as Penco, Lirquén, and the greater Concepción area, which is the third largest metropolitan region in the country. The 2026 fires in Biobío and Ñuble killed at least 20 people, forced more than 50,000 residents to evacuate, and left forests, farmland, and hundreds of homes burned (Grattan, 2026). Similarly, Reuters reported that the fires that spread into Punta de Parra, a part of the larger Concepción area, destroyed approximately 80% of the town, with residents describing little time to evacuate as winds and embers pushed fire through the community (Reuters, 2026).

These cases of wildfire spread have something in common. These communities are near flammable landscapes with the initial hazard described as wildfire, dry and receptive fuels near developed areas, strong winds that accelerated fire spread and carried embers, rapid movement into populated communities, and conditions that complicated evacuation and suppression. Fire preparedness therefore requires attention not only to fuels and ignition, but also to the spatial readiness of the infrastructure that supports suppression once fire reaches structures, roads, and neighborhoods. Santa Barbara County meets several characteristics of the regions that were devastated by fire. The coastal Santa Barbara region is a fire-prone landscape where WUI and WUI-adjacent communities are between the Santa Ynez Mountains and the Pacific Ocean. In this dissertation, WUI communities refer to developed areas where structures meet or intermingle with wildland vegetation, while WUI-adjacent communities refer to denser developed areas that may fall outside formal WUI delineations but remain close enough to WUI areas to be affected by wildfire exposure, ember transport, constrained road networks, suppression demand, or structure-to-structure fire spread. This distinction is important because fire risk does not stop at the mapped WUI boundary.

In coastal Santa Barbara, wildfire exposure, urban structure fires, wind, terrain, road networks, water access, and development patterns intersect across both WUI neighborhoods and the urban communities extending from the WUI edge toward the coast. As mentioned before, communities in Santa Barbara County occupy a narrow and highly developed coastal corridor bounded by the Pacific Ocean and the Santa Ynez Mountains. This geography produces distinctive planning challenges. Development is concentrated in lowland and foothill areas, many neighborhoods are adjacent to vegetation and steep terrain, downslope winds, and seasonal fire weather can create conditions under which suppression resources are stressed.

Sundowner winds are characteristic of the region, which are gusty, dry downslope winds that descend the southern slopes of the Santa Ynez Mountains and affect communities along the county's slopes, foothills, and coastal areas. Events such as the Thomas Fire, which burned 281,893 acres across Ventura and Santa Barbara Counties and destroyed 1,063 structures, show how regional fire weather and development patterns can translate into major structure losses. Santa Barbara and nearby communities such as Goleta, Montecito, Summerland, and Carpinteria therefore offer an important setting for studying the spatial organization of fire-response infrastructure.

In a community like Santa Barbara, understanding whether communities are spatially prepared for fire once it reaches the built environment becomes essential. Fire response depends on a distributed defensive system that encompasses roads, hydrants, water supply, fire stations, crews, and the spatial arrangement of structures. Yet the presence of this infrastructure does not guarantee that it is configured to provide protection where it is needed most. For instance, hydrant networks may be extensive but unevenly distributed. Spacing and coverage standards regarding hydrant distribution may exist, but they can be difficult to evaluate across complex road networks. Furthermore, areas of growing exposure may not align with older infrastructure patterns. These conditions create a planning problem that is fundamentally geographic. Fire preparedness depends not only on having infrastructure, but on whether that infrastructure is accessible, spatially aligned with development, and strategically prioritized to address the most consequential vulnerabilities in terms of fire protection.

Preparedness is essential in fire-prone coastal communities like Santa Barbara since they face a coupled fire-risk context in which wildfire exposure and urban structure-fire spread are

closely connected. Wildfires can move from vegetation into developed areas, while fires that begin within the built environment can spread from structure to structure under conditions shaped by density, wind, terrain, road access, water availability, and suppression capacity. Figure 1.1 illustrates this relationship by distinguishing WUI characteristics from urban characteristics while highlighting the shared vulnerabilities that connect them. This framing motivates the dissertation's analytical framework, which develops GIScience and spatial analytic tools to evaluate fire-response infrastructure, analyze fire patterns, and support infrastructure planning in communities where WUI-related and urban fire hazards intersect.

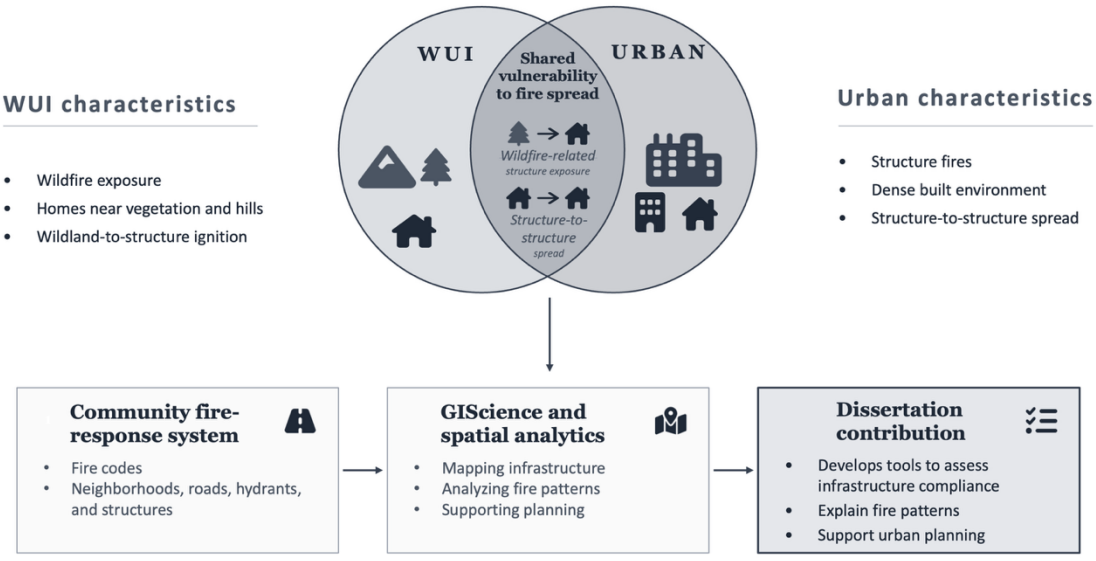


Figure 1.1. Shared exposure in urban environments: wildfire spread that becomes urban and fire spread that originates in urban settings. The dissertation is motivated by the overlap of WUI and urban fire-spread vulnerabilities and advances GIScience with methods to analyze how hydrant infrastructure supports community fire response.

This dissertation responds to that challenge by examining hydrant infrastructure as a measurable component of fire response, as it examines how hydrant networks, urban development, fire outcomes, and planning constraints interact across fire-prone communities,

focusing on problems of access, compliance, and prioritization that can be examined systematically through GIScience and spatial optimization. The methods developed in this dissertation are intended to be transferable to other urban and WUI-adjacent communities, but Santa Barbara County provides a revealing case for asking whether fire-response infrastructure is spatially configured to support suppression where people, structures, and potential losses are concentrated.

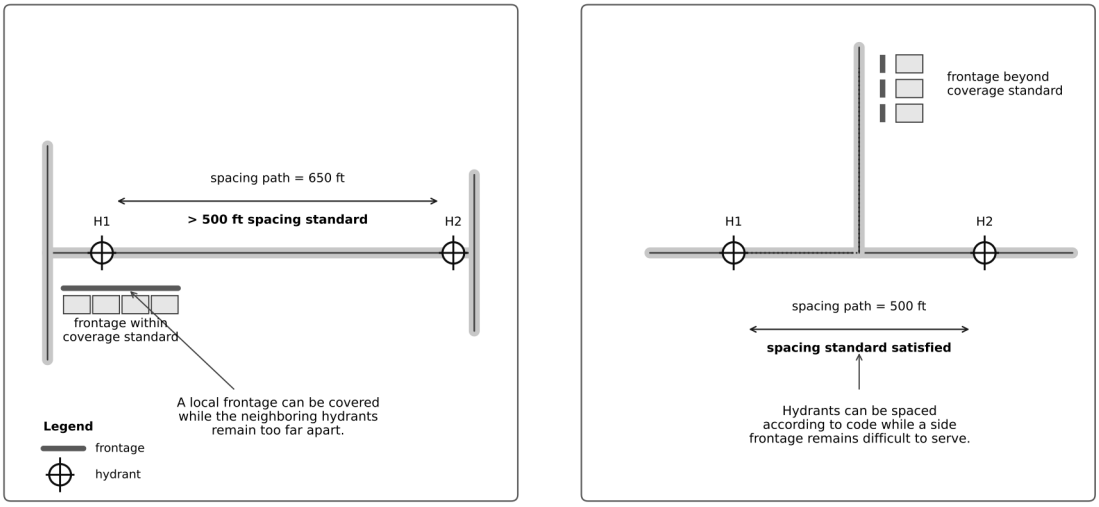
1.2. Research Context and Key Problems

Hydrants became a central feature of urban fire protection because access to water supply is necessary for suppression, property protection, and limiting fire spread. Historical work on hydrant systems and fire protection standards conveys that hydrant placement emerged from practical concerns about firefighting access, water delivery, and insurance-based assessments of urban fire defense (King, 1926; Wyss & Burns, 1958). Fire-response infrastructure is governed by standards, but standards are only meaningful if they can be translated into the geography of actual communities. Fire hydrant requirements encode assumptions about how firefighters access water, how hose can be deployed, how far apparatus can operate from a water source, and how development should be protected. In Santa Barbara County, for example, the Fire Hydrant Development Standard applies to the "selection, placement and required flow" of hydrants in conjunction with the California Fire Code, and specifies that hydrant spacing and flow requirements vary by development type, fire area, and local conditions. For buildings with fire areas below 3,600 square ft, commercial areas require 300 ft spacing, urban and rural developed areas require 500 ft spacing, and rural areas of five acres or greater require 600 ft spacing. The same standard specifies that hydrant spacing is based on distance between hydrants along an approved access road (California Fire Code, 2022).

Again, these standards reflect operational assumptions about hose reach, engine access, water supply, and fire suppression needs. Yet standards do not implement themselves. Hydrant systems are inherited from prior development decisions, modified through incremental additions, and shaped by the uneven growth of cities and infrastructure networks. Furthermore, standards create a geographic problem because fire codes can state how far apart hydrants should be, or how close a hydrant should be to a street frontage, but the built environment determines whether those standards are actually achieved. Roads curve, branch, terminate, and intersect; hydrants may be located near but not exactly at intersections; structures may be set back from the road; and access depends on the network firefighters must use. As a result, the presence of hydrants in a community does not by itself indicate whether hydrant infrastructure is spatially ready to support fire response. A jurisdiction may have many hydrants and still contain road segments, neighborhoods, or development areas where code-based spacing or frontage coverage is not satisfied.

Prior studies have used GIS to organize fire infrastructure data, identify unprotected areas in terms of service areas primarily using Euclidean distance (and to a lesser extent, road network distance), assess fire-flow capacity, map hydrant accessibility, and support planning for fire response, including work by Wielebski and Medyńska-Gulij (2019), Kaufman and Rosencrants (2015), Okon and Njoku (2018), Raškauskaite and Grigonis (2019), and Lee et al. (2021). However, the literature in hydrant assessment is limited and no works have assessed hydrant spacing as a code-based relationship among neighboring hydrants. This distinction matters. Coverage identifies whether a street segment, frontage, or structure is within a specified distance of a hydrant. Spacing evaluates the distance relationship between hydrants themselves, often along the road network. These concepts are related, but they are not

interchangeable. A road segment may appear covered by a hydrant while the surrounding hydrant network still contains excessive spacing gaps. Conversely, hydrants may be spaced according to a standard while particular frontages remain difficult to serve. Figure 1.2 illustrates these scenarios. Treating coverage and spacing as the same concept can therefore obscure different forms of vulnerability. Nonetheless, addressing spacing is complex in practice because it requires identifying actual neighboring hydrants along a road network, a task that standard GIS buffers, Voronoi diagrams, and proximity tools do not resolve well.



a) Frontage covered, spacing gap remains b) Hydrants spaced, frontage gap remains

Figure 1.2. Hydrant coverage and spacing distinction

To tackle structure fires, which concentrate the great portion of the outcomes, understanding the patterns of structure fires is essential, especially in relation to hydrant infrastructure and its role with fire outcomes. Even if hydrant coverage and spacing can be measured, that does not automatically explain where structure fires occur or why some incidents produce greater losses. Urban fire research has developed a substantial literature on incident mapping, hotspot detection, temporal patterns, socioeconomic correlates, fire-risk surfaces, and response-time analysis. Studies have used kernel density estimation, point-

pattern statistics, spatial regression, Bayesian approaches, and machine-learning methods to identify where fires concentrate and which neighborhood conditions are associated with fire incidence (Corcoran et al., 2007; Asgary et al., 2010; Ceyhan et al., 2013; Chhetri et al., 2018; Rahman Tishi & Islam, 2019; Bispo et al., 2023; Lee et al., 2025). These works provide important insight into fire occurrence, but they often represent fire protection capacity through broad proxies, such as station proximity, road access, or general service availability, rather than through the spatial configuration of hydrant networks. The spatial configuration of water-supply infrastructure remains underexamined in relation to both incident concentration and loss severity.

However, identifying service deficiencies, pockets of vulnerability, and incident patterns do not directly suggest planners where and how to invest. Fire departments and local agencies operate under budget, engineering, and feasibility constraints. Although hydrant placement is tied to roads, water mains, development patterns, and operational requirements, their main objective is to provide prompt access to water to protect people and property in case of an incident. Existing hydrant planning and optimization work has begun to explore strategic siting, including genetic-algorithm approaches for locating hydrant networks (Abrar et al., 2024; Esquivel-Saldaña et al., 2021; Kalach et al., 2020). However, there remains a need for models that explicitly connect property frontage coverage while also considering hydrant spacing compliance, exposure, road network constraints, and limited budgets in a single planning framework.

This dissertation is positioned at the intersection of these problems. It begins from the recognition that fire-response infrastructure is spatially regulated, but challenging to evaluate in practice, that structure fire incidents are spatially patterned and can provide insights to

enhance fire response to mitigate fire outcomes in urban settings, and that infrastructure deficiencies require to move from diagnosis to prescription. This dissertation therefore treats hydrant infrastructure as a measurable component of fire-response spatial readiness. Hydrants serve as a tangible infrastructure system through which this dissertation examines how communities can assess whether fire-response infrastructure is spatially configured to suppress fires effectively where exposure and potential losses are concentrated. By connecting standards, empirical fire outcomes, and investment prioritization, this dissertation develops a diagnostic, explanatory, and prescriptive framework for fire-response infrastructure planning in fire-prone urban and WUI-adjacent communities

1.3. Analytical Framework

The dissertation's analytical framework can be described as a spatial analytics pipeline for hydrant infrastructure planning. The first stage is diagnosis, which asks where hydrant spacing and coverage conditions do or do not satisfy code-based standards. The second stage is explanation, which asks how structure-fire incidents and losses are distributed and which factors are associated with those patterns. The third stage is prescription, which asks where new hydrants should be added when investment is constrained and planning objectives compete.

Thus, this dissertation is organized around the concept of spatial readiness, which refers to the degree to which fire-response infrastructure is geographically configured to support suppression where it is most likely to be needed. In this context, readiness is defined not only by the availability of resources but also by their spatial relationship to roads, structures, code standards, incident patterns, and potential losses. A community may have fire stations, hydrants, water supply, and emergency-response capacity, yet still contain places where these

systems do not align well with the geography of exposure. Spatial readiness therefore asks whether defensive infrastructure is accessible, compliant according to code standards, connected through the road network, and positioned in relation to the built environments where fire consequences are concentrated.

Defensive infrastructure is understood here as the distributed set of physical and operational systems that support fire suppression once ignition occurs. Hydrants serve as the central empirical focus because they provide a tangible and measurable infrastructure system through which broader questions of fire response can be examined. Hydrants serve as access points to municipal water supply, but their protective role depends on more than their presence. Their effectiveness is shaped by where they are located, how they relate to street frontages and neighboring hydrants, whether they satisfy spacing and coverage standards, and whether gaps occur in places where structures and potential losses are concentrated. In this sense, hydrants are treated as part of a spatial system of defense.

The framework developed in this dissertation rests on the idea that fire-response infrastructure must be evaluated through three linked forms of inquiry: diagnostic, explanatory, and prescriptive. The diagnostic dimension asks whether existing infrastructure satisfies the spatial standards intended to support suppression.

The diagnostic stage begins with the hydrant system itself. Hydrant locations, road centerlines, land use, structures, and code standards are integrated to evaluate access and spacing along the road network. This stage focuses on infrastructure compliance and spatial configuration. It asks whether the existing system conforms to standards and where noncompliance occurs. The relevant methods include network construction, hydrant snapping, edge-based neighbor identification, road-network distance measurement, and code-based

spacing and coverage evaluation. The output is a spatially explicit representation of infrastructure conditions.

The explanatory stage shifts from infrastructure configuration to observed fire incidents and losses. It uses structure-fire incident records to identify where incidents concentrate, whether clustering is statistically evident, and which variables are associated with incident counts and monetary losses. The relevant methods include kernel density estimation, Ripley's K and L functions, cross-K and cross-L functions, negative binomial count models, and Gamma loss models. This stage places hydrant infrastructure in relation to urban form, density, timing, property characteristics, and response variables. It is intentionally empirical and restrained, evaluating observable incident and loss patterns in relation to relevant spatial and operational variables.

The prescriptive stage uses the diagnostic and empirical context to support planning decisions. It asks how new hydrants can be strategically located to improve coverage and spacing outcomes under a limited budget. This stage treats hydrant placement as a location problem constrained to the road network. The relevant methods include maximal covering location modeling, finite dominating set candidate generation, demand weighting, and bi-objective optimization. The output is a set of alternatives that reveal tradeoffs between planning objectives. This is especially important because infrastructure planning rarely involves one objective alone.

Figure 1.3 summarizes the analytical framework and shows how the chapters build on one another.

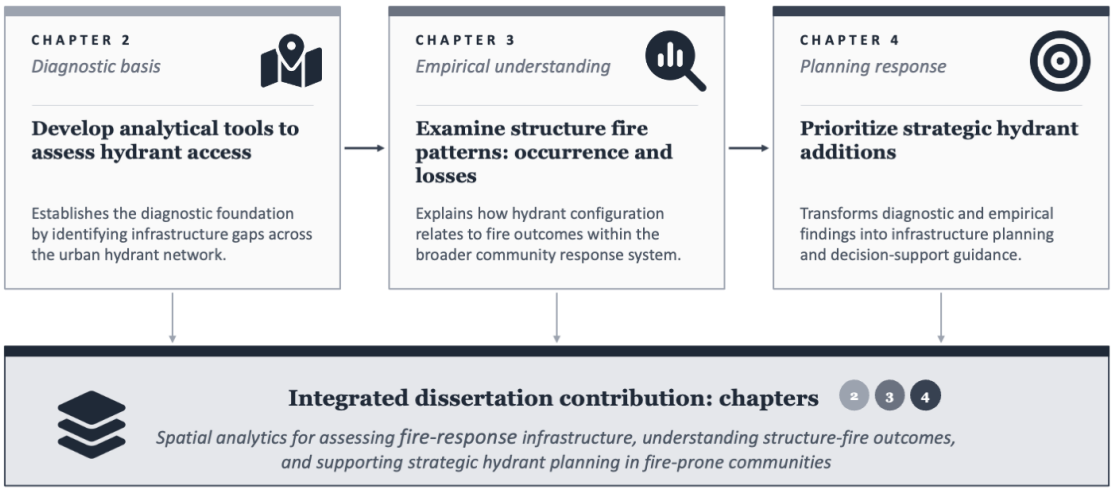


Figure 1.3. Conceptual framework. Progression across chapters combines diagnosis, empirical explanation, and planning response.

By framing hydrants through spatial readiness, this dissertation contributes to a broader planning question of how communities can evaluate whether defensive infrastructure is configured to support suppression before future fires expose existing vulnerabilities. This question is especially important in fire prone urban communities and areas adjacent to the WUI, where structure fire risk, wildfire exposure, road networks, water access, and development patterns intersect. Although the applications in the chapters focus on Santa Barbara County and Montecito, the framework is not limited to these places. It offers a transferable way to assess, interpret, and improve fire response infrastructure in communities where the spatial organization of defensive systems can shape the ability to limit fire spread and reduce losses.

1.4. Research Objectives

This dissertation aims to study and/or develop suitable methods to prevent and mitigate fire risk in communities, understand the role of defensive actions, study the methods related to improving fire response in urban environments, and propose the placement of new infrastructure to support response once vulnerabilities are identified. Specifically, the present research seeks to:

i. Formulate and propose a method to assess hydrant distribution and access in relation to the established codes to guarantee prompt fire response in urban environments.
ii. Analyze and examine past fire incidents in relation to infrastructure access in order to identify patterns and relationships in fire code compliance.
iii. Develop a spatial optimization model to support communities in strategically addressing hydrant infrastructure gaps.

1.5. Significance

The methodological significance of this dissertation lies in its treatment of hydrant infrastructure as a network-based spatial system. Conventional approaches to hydrant assessment often rely on simple buffers, nearest-neighbor calculations, or coverage summaries. These methods can be useful for exploratory analysis, but they may misrepresent service conditions when road-network geometry matters. By developing and applying methods that identify hydrant neighbors along the network and distinguish coverage from spacing, the dissertation advances GIScience approaches for evaluating distributed public safety infrastructure. Conceptually, if $G = (V, E)$ represents the road network, H represents

existing hydrants, a represents a frontage or road segment, r is the maximum allowable frontage-to-hydrant distance, then a coverage relationship can be written as:

$$C(a) = 1 \text{ if } \min_{h \in H} d_G(a, h) \leq r \qquad (1.1)$$

Where h_i and h_j are neighboring hydrants, $d_G(a, h)$ is the road network distance from frontage a to hydrant h, and s represents a relevant code standard. A spacing relationship is different and can be expressed as:

$$S(h_i, h_j) = 1 \text{ if } d_G(h_i, h_j) \leq s \qquad (1.2)$$

The methodological challenge is not only computing these distances but determining which hydrants should be considered neighbors along a complex road network. This dissertation addresses this by constructing spacing paths that reflect network connectivity, street geometry, and hydrant adjacency, rather than assuming that nearest Euclidean points or simple buffers based on Euclidean distance are adequate. In fact, Euclidean and road network approaches can produce substantially different estimates of hydrant coverage and conventional methods can obscure spacing gaps that are visible only when neighboring hydrant relationships are evaluated directly. The broader GIScience significance is that the dissertation demonstrates how infrastructure standards can be operationalized as network-based spatial objects. This approach is relevant not only to hydrants, but also to other public infrastructure systems governed by spacing or access standards, including street lighting, benches, water fountains, traffic signs, bus stops, and street trees.

A second contribution is empirical. Urban fire studies often examine hotspots, socioeconomic conditions, temporal patterns, or response but abstracted as proximity to fire stations. Hydrant infrastructure is frequently treated more indirectly, if at all. By explicitly incorporating hydrant variables into incident and loss analysis, the dissertation adds evidence

on how defensive infrastructure relates to observed urban fire outcomes. This contribution treats incident occurrence and loss severity as related but analytically distinct outcomes. Hydrants do not prevent ignition, so their relationship to incident occurrence should not be interpreted in the same way as their potential relationship to suppression and loss control.

A further methodological contribution is the formalization of hydrant improvement as a road-constrained, bi-objective location problem rather than as a post hoc mapping exercise. Existing hydrant diagnostics can identify uncovered frontages and noncompliant spacing paths, but they do not determine how a limited number of additional hydrants should be placed when coverage, spacing, exposure, and budget constraints must be considered together. This dissertation addresses that gap by weighting the road segments (demand) with uncovered frontage segments and spacing vulnerability segments, while considering that demand and feasible hydrant locations are continuous along street arcs. Drawing on covering model theory, continuous and network-based location modeling, the framework converts an otherwise large or infinite road-constrained siting problem into a tractable optimization problem that can evaluate competing infrastructure priorities. Its significance is that it connects code-based fire response standards to an explicit decision model, allowing hydrant planning to move from identifying noncompliance toward comparing defensible infrastructure improvement strategies under realistic planning constraints.

1.6. Organization of dissertation

Aligned with the research objectives stated, each substantive chapter in this dissertation examines a different dimension of fire response readiness. The dissertation begins with the assessment of existing hydrant infrastructure, then moves to the empirical analysis of patterns of fire incidence and fire outcomes, and finally develops a planning framework for strategic

infrastructure improvement. In this progression, Chapter 2 is diagnostic, Chapter 3 is explanatory, and Chapter 4 is prescriptive. Together, the chapters examine how hydrant infrastructure can be evaluated, interpreted, and improved as part of a broader defensive system in fire prone urban and WUI-adjacent communities.

As an overview, Chapter 2 develops the diagnostic foundation for the dissertation by assessing hydrant spacing and coverage along the road network in coastal Santa Barbara County. This chapter introduces a framework for assessing hydrant spacing at different spatial scales. In doing so, the chapter shows how GIScience can be used to move beyond simple buffers or Euclidean proximity and toward a more accurate evaluation of hydrant infrastructure performance.

Chapter 3 builds on this infrastructure assessment by examining historical structure fire incidents in urban areas of Santa Barbara County. This chapter evaluates where structure fires occur, whether incidents are spatially clustered, and which factors are associated with loss severity once an incident occurs. The chapter places hydrant configuration alongside population and housing density, property characteristics, time of day, season, and operational factors. This allows the dissertation to distinguish between the geography of incident occurrence and the drivers of damage, while treating hydrants as one component of a broader fire-response system.

Chapter 4 translates the diagnostic and empirical findings of Chapters 2 and 3 into a planning framework for strategic hydrant additions. This chapter focuses on Montecito and formulates hydrant placement as a road constrained spatial optimization problem with two objectives. The model prioritizes new hydrant locations under budget constraints while accounting for two related but distinct planning goals, improving frontage coverage where

structures are present and reducing spacing vulnerability where hydrant relationships exceed code-based standards. In this way, Chapter 4 moves from identifying infrastructure deficiencies to supporting investment decisions.

Finally, Chapter 5 summarizes the dissertation findings, presents broader contributions, and discusses challenges and future research avenues.

2. Supporting Fire Response: Advanced Spatial Analytics for Hydrant Access Assessment[1]

2.1. Introduction

The western United States now faces wildfire on a constant basis. The past two decades have seen a significant increase in wildfire episodes (Keeley & Syphard, 2021). In California alone, some 75% of the most destructive fires in history have occurred within the past decade, burning millions of acres, destroying tens of thousands of structures, and causing hundreds of deaths (CAL FIRE, 2025b). As an example, the Thomas and Woolsey fires, 2017 and 2018, respectively, occurring in Ventura and Santa Barbara Counties burned nearly 400,000 acres, destroyed more than 2700 structures, and witnessed 5 casualties. The reasons for this increase in wildfire activity are due to several factors, including episodes of heavy precipitation that support vegetation growth followed by periods of severe drought that turn accumulated vegetation into flammable fuel (Keeley & Syphard, 2016; Littell, 2018). Add to this human activity that extends beyond the urban core. Burke et al. (2021) estimate that, on average, 350,000 homes were constructed in the continental United States every year from 2000 to 2020 in the wildland-urban interface (see also Radeloff et al., 2023). Further, changing climate conditions too exacerbate the risk of fire, such as Santa Ana and sundowner winds in Southern California (Zigner et al., 2022). Structure fires in urban areas too are on the increase with the U.S. Fire Administration (2024) indicating that there were 374,300 occurrences in 2022 that resulted in 2720 deaths, 10,250 injuries, and total losses of nearly $11 billion.

[1] This chapter presents a revised version of a paper published in *Transactions in GIS* co-authored with Dr. Alan T. Murray and Thelonius Funk (Figueroa et al., 2024).

It is clear that efficient and effective fire hydrant infrastructure is crucial for the protection of property, structures, and life. To minimize loss and damage, the water supply system is essential in firefighting efforts, both in terms of access as well as sufficient pressure/volume. Reliable access to water influences a community's resilience against fire hazards (Wyss & Burns, 1958). Before the advent of hydrants, rudimentary methods were employed for firefighting, leading to high risks and huge losses of life and property. This drove the development of hydrant systems through public water infrastructure, and became a fundamental necessity in fire mitigation. Recognizing this, national, regional, and local agencies have established hydrant location and distribution standards (see National Board of Fire Underwriters, 1942; Jackson, 1944 Wyss & Burns, 1958). One major guideline pertains to the spacing/intervals between hydrants, which directly influences access and coverage throughout a region. In particular, King (1926) highlights the importance of hydrant spacing to provide adequate coverage, where water companies, municipalities, and fire underwriters advocate access standards. Today, such importance is latent and directly required through international, national, regional, and local code guidelines that establish specific spacings between fire hydrants (e.g., Carpinteria-Summerland Fire Protection District, 2021; California Fire Code, 2022; Montecito Fire Department, 2022; Santa Barbara County Fire Department, 2023; International Code Council, 2024). Acceptable hydrant intervals are created based on the operational range of firefighting equipment, including but not limited to distance from a hydrant to a fire engine and distance from a hydrant to a structure. The acceptable range can vary, but is generally between 150 and 450 ft., reflecting that appropriate hydrant spacing is essential for ensuring effective response coverage as water has proven successful in cooling and smothering most types of fire (Grant et al., 2000). The lack of sufficient water access was

a major factor in the deadly Maui fire in 2023 (Baker, Browning, et al., 2023). The strategic importance of hydrant spacing also extends beyond immediate fire response concerns. For example, insurance premiums and ratings are based on hydrant spacing as part of risk assessment (King, 1926; McElroy, 1865; Zampella, 2017), recognizing its role in mitigating fire-related losses. Moreover, fire departments rely on this information to formulate preparedness strategies, especially in areas where hydrant availability is sparse.

A primary emphasis of fire response has largely been on station location and associated service coverage of communities, including proximity, distribution, accessibility, and allocation (Forkuo & Quaye-Ballard, 2013). Recent research has increasingly advocated hydrant evaluation through the use of geographic information systems (GIS) to determine hydrant flow dynamics (Kaufman & Rosencrants, 2015), water accessibility to structures (Lestari et al., 2022; Raškauskaitė & Grigonis, 2019; Wielebski & Medyńska-Gulij, 2013), and flow related to socio-economic factors (Ronan & Teeuw, 2016). These studies typically employ standard GIS functions, utilizing spatial join operations, Euclidean distance, service area delineation, overlay, and buffers to assess hydrant distribution and coverage. Okon and Njoku (2018) and Y. H. Lee et al. (2021) considered network traversal in hydrant coverage along roads, seeking vulnerability posed by a lack of service. The focus in all of the above cases has been coverage because addressing hydrant spacing is complicated and difficult to undertake.

Despite the more recent interest in hydrant configuration using GIS, a notable gap persists in accurate hydrant assessment that accounts for the complexities of spacing in individual and aggregate terms along streets. A complication is that average spacing between hydrants necessitates the identification of neighbors, from which spacing can be observed and

measured. Such identification poses considerable challenges due to the complexities of street networks, barriers, and obstructions. Simplistic evaluation using Euclidean distance and buffers fails to account for the actual geographic proximity that is fundamental to being a neighbor. These limitations underscore the need for advanced GIS approaches that can adeptly navigate complex landscapes, enhancing both the accuracy and efficacy of hydrant spacing evaluation. Road network-based approaches, crucial for planning and emergency services, offer a more detailed representation of distances and connectivity within urban areas compared to Euclidean approximation (Okabe et al., 2008; Safar et al., 2009). Worth noting too is that hydrants are not the only infrastructure for which standards and guidelines are established associated with spacing as similar requirements can be found for street lights (Murray & Feng, 2016), public benches (Usui, 2022), water fountains, traffic signs, bus stops (U.S. Department of Transportation, 2015) as well as trees (City of Los Angeles Department of Public Works, 2024).

This chapter addresses important gaps by introducing an approach that enhances GIS capabilities for hydrant spacing assessment unique to road networks. The public, local authorities, urban planners, and state agencies are interested in developing strategies to protect structures, communities, and minimize economic loss. Better understanding the risk of fire and supporting response efforts at different geographical scales is vital. Across hydrant, street, parcel, neighborhood, community, and/or region spatial scales, there are two important strategic questions associated with fire risk and vulnerability:

i. Are mandated average and maximum distance hydrant access standards maintained?

ii. To what degree is coverage provided by hydrants based on established access standards?

By integrating hydrant location and road information, the proposed method enables detailed evaluation of hydrant spacing (and coverage) in accordance with established local, county, state and federal standards, tailored to the structural constraints of street infrastructure. The approach can be readily applied to other infrastructure spacing and coverage contexts, making it of broad appeal and utility. The next section provides background, reviewing the evolution of hydrant infrastructure as well as standards and guidelines that are commonly found in urban regions. This is followed by the introduction of methods to support hydrant spacing evaluation. An assessment of hydrant spacing in Santa Barbara is then carried out. The chapter ends with a discussion and concluding comments.

2.2. Background

Fire hydrant systems are now recognized as critical infrastructure, undergoing significant evolution over the past centuries. Initially, firefighting relied on the "bucket brigade," where volunteers passed water buckets from a well or source to combat a fire. By the 17th century, this response matured somewhat to the use of fire plugs to access water. When a fire would break out, excavation would be undertaken nearby around the wooden water main (pipes made of wood), creating a hole to attach a hose or water pump for use to combat the fire. Following the incident, the hole would be "plugged" for future access and/or reference (Jackson, 1944). The advent of modern fire hydrant systems coincided with the establishment of formal fire departments and the growth of the insurance industry (King, 1926; Goodhue, 1941), marking a significant leap in safety and response measures tied to fire risk. Due to demonstrated effectiveness in enhancing fire response capabilities and preparedness, guidelines for placing

and distributing hydrants were introduced. These guidelines specified intervals between hydrants as a critical factor for ensuring effective fire protection alongside other strategic measures (Jackson, 1944; King, 1926; National Board of Fire Underwriters, 1942; Wyss & Burns, 1958). The infrastructure and associated access standards were instrumental in shaping practices that safeguarded structures, property, and lives, underlining the strategic importance of hydrants in urban safety (McElroy, 1865; King, 1926Flexer, 1966).

Fire risk is heterogeneous across the United States, necessitating regional guidelines tailored to vulnerabilities faced in different areas. The western United States, particularly southern California, is highly susceptible to wildfire events due to its unique combination of weather, vegetation, and housing within the wildland-urban interface (Moritz et al., 2014; Radeloff et al., 2023), as noted previously. This region is further threatened by unique conditions, such as Santa Ana winds, that can quickly drive wildfires into urban areas. It is not surprising then that California Fire Code (2022) specifically regulates hydrant location and spacing in accordance with building materials and other considerations. For example, a residential building less than 3600 sq. ft. in size constructed with type V-B materials (wood walls and frames) requires hydrants to be spaced at 500 ft. intervals. In contrast, commercial buildings less than 50,000 sq. ft. in size with sprinklers and built with fire-resilient materials (such as types A-I enhanced or I-B basic) are required to have nearby hydrant spacing of no more than 750 ft. In non-developed areas, hydrants must be spaced every 1000 ft. to address transportation-related hazards.

In Santa Barbara, regional regulations further refine standards with respect to California Fire Code. Hydrants near structures not exceeding 3600 sq. ft. in size should be spaced no more than 300 ft. apart in commercial zones and 500 ft. in residential areas (Carpinteria-

Summerland Fire Protection District, 2021; Montecito Fire Department, 2022; Santa Barbara County Fire Department, 2023). Table 2.1 summarizes these standards for select areas. Hydrant spacing in a residential area of Santa Barbara is shown in Figure 2.1 to illustrate this issue, with instances where standards are maintained as well as two cases where it is not satisfied along streets.

Table 2.1. Regional and local standards (coastal Santa Barbara County).

Jurisdiction	Residential	Commercial	Others	No development
California (state)	500 ft	750 ft	500 ft	1000 ft
Santa Barbara County Fire District (local)	500 ft	300 ft[†]	500 ft	1000 ft
Montecito Fire District (local)	500 ft	300 ft[†]	500 ft	1000 ft
Carpinteria & Summerland Fire District (local)	500 ft	750 ft	500 ft	1000 ft

[†]Applies only to structures with a fire area of less than 3,600 sq ft.

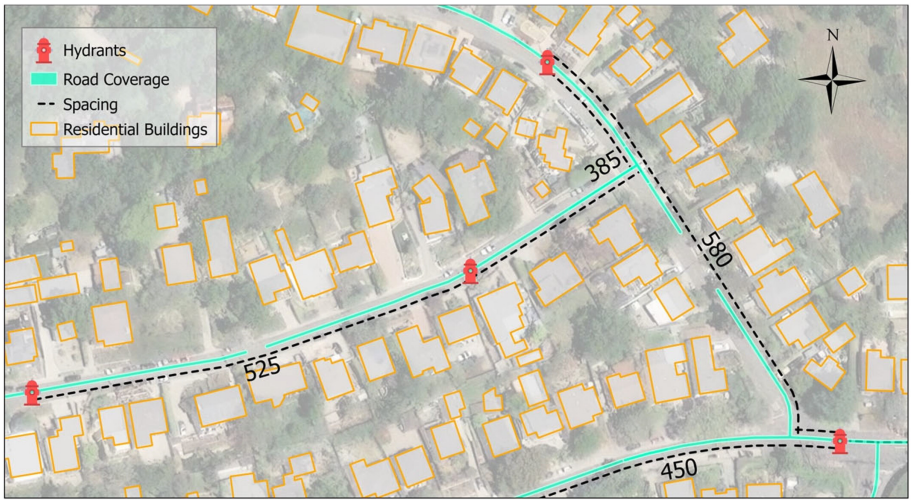


Figure 2.1. Hydrant spacing in a residential area, with the 525 ft. and 580 ft. instances exceeding the standards stipulated in Table 2.1.

Despite codes and guidelines underscoring the importance of hydrants for safeguarding life, structures, and property, there is a notable lack of literature addressing hydrant location, distribution, and service for evaluation purposes. Further, spacing and service areas of hydrants are often conflated. Spacing standards have been used to assess coverage by creating buffers as service areas based on Euclidean distance (Wielebski & Medyńska-Gulij, 2013; Kaufman & Rosencrants, 2015; Raškauskaite & Grigonis, 2019) and road network distance (Y. H. Lee et al., 2021; Okon & Njoku, 2018). These buffers are intended to enclose the street and property within the distance intervals dictated by the code guidelines. Presumably, the property and street portions within the buffers have water access provided by one or more hydrants. However, deriving buffers using Euclidean and road network distances are not the same since the latter accounts for actual travel geometry. Figure 2.2 depicts hydrant access coverage in a Santa Barbara residential area using the two approaches that have been proposed in the literature, Euclidean and road network distances. For this particular neighborhood area, road coverage corresponds to 70.5% using the Euclidean approach and 41.58% by road network distance. Of course, road network distance represents the actual access to hydrants. Thus, Figure 2.2 demonstrates the error one gets with a Euclidean approximation.

The reality is that coverage and spacing are not the same. While coverage can provide insights about where the streets are uncovered, spacing directly relates to hydrant proximity and provides specific measurements to inform better placement and preparedness strategies. While spacing and coverage concepts are related—poor coverage typically implies inadequate spacing—they are distinct and different. Code guidelines dictate that spacing between hydrants not only ensure adequate coverage but also maintain sufficient flow and water pressure during fire-fighting operations (Yadav & Patel, 2014). Regarding coverage, codes

stipulate that any point along a street frontage must be within a certain distance of a hydrant; this distance, however, is not necessarily half the mandated spacing (see Table C102 in California Fire Code, 2022). Although coverage is related to how accessible hydrants are at any given location, spacing specifically refers to the distance between hydrants.



Figure 2.2. Hydrant coverage by Euclidean distance buffers and road network distance.

2.3. Methods

A major challenge is evaluating hydrant spacing, as this requires geographic knowledge about hydrant neighbors. While seemingly a straightforward task, the geography of street networks makes hydrant neighbor identification complicated in practice. A question then is what are the GIS-oriented methods that can support the evaluation and assessment of hydrant spacing and in particular the specification of neighbors. Consider the following notation:

$\mathfrak{R}$ = region of analysis

$i =$ index of hydrants (entire set I)

$k =$ index of street intersections (entire set Ω)

$N_i = \{j | \ i \ \& \ j \in I$ neighbors$\}$ = set of neighbors to hydrant i

$P_{ij} =$ shortest distance path associated with between hydrants i and j

$d_{ij} =$ distance (shortest along network) between hydrants i and j, $\left|\left|P_{ij}\right|\right|$

$\Psi =$ spacing distance standard

$\Theta =$ set of streets in region $\Re$

Given this notation, of particular interest is the ability to assess a spacing standard for every pair of hydrant neighbors i and $j \in N_i$, with two possible outcomes:

$$d_{ij} \leq \Psi \tag{2.1a}$$

$$d_{ij} > \Psi \tag{2.1b}$$

The standard is satisfied in case (2.1a). In contrast, case (2.1b) would indicate excessive spacing between neighboring hydrants i and j, suggesting increased risk and vulnerability for some structures along the street segment path. Another consideration of interest is average spacing for a particular hydrant location, street(s) or area within a region. With the set of neighbors, evaluation of spacing, either in absolute or average terms, is possible. For a given hydrant i, the average spacing between its neighbors is:

$$\frac{\sum_{j \in N_i} d_{ij}}{|N_i|} \tag{2.2}$$

where $|N_i|$ indicates the number of members in a set. Again, this would facilitate assessment of any hydrant location, any street and/or any sub-area of the region. Of course, the ability to do this is dependent on accurately and correctly identifying hydrant neighbors to begin with.

In theory, visual inspection and evaluation would offer a definitive answer of what constitutes the neighbors of any given hydrant, but with thousands or hundreds of thousands of hydrants (e.g., 25,000 in San Diego, 118,676 in Los Angeles County, 170,000 in New York City) this is not a particularly reasonable approach. In fact, many municipalities can only inspect a small fraction of hydrants each year (Sierra & Feingold, 2022). This is indeed where GIS offers potential, both in storage and management of underlying hydrant information, street networks, structures, etc., but also in processing, evaluation, and analysis. GIS-based methods that have been automated and applied include buffer and Voronoi diagram-based approaches, as noted above. However, they are generally incapable of accurate identification of hydrant neighbors due to street network complexities. Additionally, their use has been limited to assessing approximate and/or explicit conditions reflected in (2.1a) and (2.1b) with no capacity to consider maximum or average spacing, for example, (2.2).

From a methodological perspective, the buffer approach relied upon by Wielebski and Medyńska-Gulij (2013), Kaufman and Rosencrants (2015), Okon and Njoku (2018), Raškauskaite and Grigonis (2019), Y. H. Lee et al. (2021) and Lestari et al. (2022) can be considered in the context of GIS as follows. Given hydrant i at (x_i, y_i), the buffer around it can be defined as (Murray, 2018):

$$o_i \leftarrow \{(x, y) \subset \Re | d_{(x,y)(x_i,y_i)} \leq \Psi\} \tag{2.3}$$

where (x, y) denotes any location within the region and $d_{(x,y)(x_i,y_i)}$ is the straight-line distance between (x, y) and (x_i, y_i), e.g., $\sqrt{(x - x_i)^2 + (y - y_i)^2}$. Thus, the buffer object o_i is the geographic space within region $\Re$ that satisfies half of the distance standard.

The total coverage of the hydrant system is therefore $O = \cup_i o_i$. Given Θ, the set of streets in $\Re$, one can then perform an intersection analysis in GIS with two potential outcomes:

$$\Delta = O \cap \Theta \tag{2.4a}$$

$$\Delta^c = \text{not}(O \cap \Theta) \tag{2.4b}$$

where (2.4a) identifies street segments within the buffers and (2.4b) represents street segments not within the buffer standard. Further, $\Delta \cup \Delta^c = \Theta$, or rather that all streets must be in one set or the other. Worth noting is that Okon and Njoku (2018) and Lee et al. (2020) actually derive buffer coverage along street segments only using network-based distance, differing from (2.3) in that their set $O' \subset O$.

The use of the Voronoi diagram was advocated in Wielebski & Medyńska-Gulij (2013) but only to identify service areas, not hydrant neighbors. Assuming that the hydrant locations are used as the point generator set, Voronoi polygons $V = \{v_1, v_2, \ldots, v_{|I|}\}$ are defined as (Murray 2018):

$$v_i = \left\{(x,y) \subset \Re | d_{(x,y)(x_i,y_i)} \leq d_{(x,y)(x_j,y_j)} \; \forall j \in I, j \neq i\right\} \tag{2.5}$$

where $\cup_i v_i = \Re$ and $v_i \cap v_j = \emptyset \; \forall i,j \in I, j \neq i$. While not considered in Wielebski & Medyńska-Gulij (2013), the set of hydrant neighbors identified using Voronoi polygons would be:

$$N_i^V = \{j | v_i \cap v_j \neq \emptyset \; \forall j \in I, j \neq i\} \tag{2.6}$$

Note that defining spatial neighbors based on proximity is rather common practice in geographical analysis, particularly in spatial statistics and geostatistics in terms of the spatial weights matrix. Further, the approach taken has been recognized as having a profound implication in analysis and interpretation, representing a potential source of uncertainty in model specification (Lesage & Fischer, 2008). It is not unusual to assume a spatial weights

matrix based on spatial adjacency when data are in the form of polygons, where two locations are considered as neighbors when they share a non-zero length boundary ("rook") or at least a point ("queen"). When the underlying data is in the form of points, the spatial weights matrix is often formed based on proximity between two locations being within a specified distance. Other definitions include distance decay, social or economic networks, k nearest neighbors, location statistic-based approach, lengths of shared borders divided by a perimeter as well as others (see Getis & Aldstadt, 2004; Getis, 2009; Anselin, 2022). Unfortunately, none of these alternatives is particularly helpful in defining actual neighbors in the context of hydrants along streets. This is due to the complexities of street networks but also the intent of siting hydrants at intersections, yet interpreting this in practice can be challenging.

The identification of a neighbor set in this context necessitates considering the complexities of street networks. It must account for proximity from a hydrant along the streets, or edges, to their closest hydrants. The neighboring set of hydrants is as follows:

$$N_i^e = \left\{ j \in I \mid \nexists\, l \in I, l \neq j \ \left(\left| \left| P_{ij} \cap P_{il} \right| \right| - d_{ij} \right) > \varepsilon \ \wedge \ \max_{k \in \Omega} \sqrt{\left(x_j - x_k\right)^2 + \left(y_j - y_k\right)^2} < \tau \right\} \quad (2.7)$$

where ε is a very small positive number, and τ is a tolerance threshold for proximity to an intersection. This neighbor set is defined to account for hydrant proximity in terms of network distance by considering the shortest paths between a source hydrant and other hydrants. Specifically, this set represents neighboring hydrants that have a direct shortest path from the source without passing by any intermediate hydrants (including a hydrant that is effectively at an intersection). The procedure for identifying these neighbors is detailed in Figure 2.3, referred to as the edge approach. This method involves exploring all potential shortest paths originating from a specific source hydrant and branching out to neighboring hydrants. The branching process terminates when a path encounters a target hydrant near an intersection

within a defined distance threshold τ or when a hydrant is located along the path. This condition of restricting the neighbor exploration at intersections is necessary given that historically, street intersections were favored locations for hydrants (see Section 2.5). After identifying potential paths, evaluation of edge proximity to hydrants is carried out. If an edge on a path from hydrant i to hydrant l is closer to a hydrant other than i, the path is discarded, and the candidate neighbor is excluded. This ensures that the hydrant spacing paths (or street segments) relating the hydrant source to a neighboring hydrant that can directly serve those street segments in an emergency are included. Note that there is similarity in Voronoi network diagrams. However, path inaccuracies can result.

Input: Street segments (road network), intersections and hydrants. Threshold τ. Function $C(e)$ that for a given street segment e, retrieves the closest pair of hydrants to e.
Output: A set ψ^* with individual spacing and a neighbor set for each hydrant N.

Initialize N, ψ^*

For each $i \in I$
    Initialize N_i^e
    Initialize ψ_i
    Calculate P with all shortest paths from i to all other j, where $i, j \in I \wedge i \neq j$
    Calculate d containing all the distances d_{ij}
    Sort P by d
    For each $P_{ij} \in P$:
        If P_{ij} contains a hydrant $l \in I$, $l \neq i, j$
            Pass
        Else If $N_i^e = \emptyset$
            Add j to N_i^e
            Add P_{ij}, d_{ij} to ψ_i
        Else
            Include = True
            For $P_{il} \in \psi_i$
                Calculate $||P_{ij} \cap P_{il}||$
                If $d_{il} - ||P_{ij} \cap P_{il}|| < \tau$
                    Include = False
                Else
                    Continue
            If Include ==True
                Add j to N_i^e
                Add P_{ij}, d_{ij} to ψ_i
        For $e \in P_{ij}$
            If $i \notin C(e)$
                Drop P_{ij}
    Add N_i^e to N, Add i to ψ^*
Return ψ^*, N

Figure 2.3. Pseudo code for edge approach to hydrant neighbor identification.

2.4. Hydrant assessment in Santa Barbara

The hydrant network in the coastal region of Santa Barbara County is evaluated, bounded by Gaviota State Park to the west, Carpinteria to the east, the Santa Ynez Mountain Range to the north, and the Pacific Ocean to the south. This area includes Santa Barbara, Summerland, Montecito, Goleta, and Carpinteria. The hydrant spacing guidelines for this region are municipality-specific, generally based on the California Fire Code associated with hydrant location and distribution. The data used for our analysis consists of hydrant locations and road centerlines for Santa Barbara. The study area includes a total of 5,883 hydrants and 8,413 street segments, obtained from the County of Santa Barbara. The region of study, along with the road centerlines, are depicted in Figure 2.4. Each hydrant location was assigned the primary land use around it, having implications for the applicable spacing standard that applies. Building footprints were used to represent structures, publicly available through the Conservation Biology Institute (2020), and land use information was accessed through the County of Santa Barbara. All data handling, cleaning, and analysis were done in Python 3.11.4. Networkx version 3.3 was used to create and traverse the road network as an undirected multigraph. Hydrant locations were snapped to road centerlines in order to derive distance and paths taken as well as to assess spacing guidelines. The road network consisted of 12,126 nodes and 14,040 edges. Geometric operations were handled using Geopandas and Shapely version 0.14.3 and 2.0.4, respectively. All processing was done on a desktop personal computer (12th Gen Intel CoreTM i7-12700k, CPU of 3.61GHz, 32 GB RAM) running Windows 10 (64-bit).

Fire risk and vulnerability are of great concern in Santa Barbara, and southern California more generally, given that the region is prone to wildfire along with the regular occurrence

of fires[2]. As noted previously, the public, local authorities, urban planners, and state agencies seek strategies to protect structures, communities, and minimize economic loss. The strategic questions of whether mandated average and maximum distance hydrant access standards are maintained as well as the degree of coverage provided by hydrants are critical to answer.

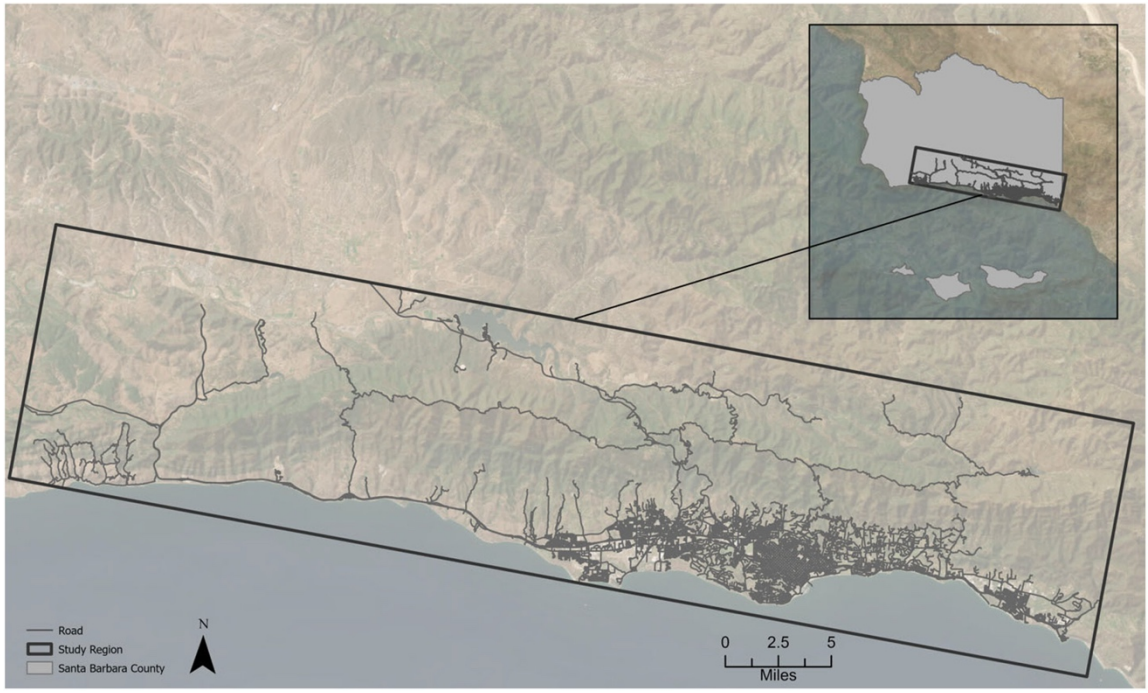


Figure 2.4. Study region located in the southern part of Santa Barbara County.

The analysis that follows focuses on each question and the fire risk and vulnerability implications for the Santa Barbara region, beginning with hydrant spacing. The proposed assessment approach (Figure 2.3) using hydrant neighbors specified in (2.7) enables the identification of maximum and average spacing at any spatial scale. Consider for example hydrant 0 shown in Figure 2.5, with neighbors defined as $N_0^e = \{1,2,3,4,5\}$. The maximum distance in this case is 502 ft. (source to 4), with an average distance of 446.8 ft.

[2] The County of Santa Barbara alone responded to 348 structure and property fires in 2022, resulting in losses exceeding $12.4 million (https://sbcfire.com/annual-statistics/).



Figure 2.5. Hydrant neighborhoods.

Spacing along a street can also be evaluated. Consider the street shown in Figure 2.6, where the maximum distance is 596 ft. (between hydrants 21 and 24), and the average distance is 589.75 ft. A community within the region is shown in Figure 2.7, where the relationships between hydrants are more complex, yet the evaluation at this scale is also possible. The analysis reveals a maximum and average spacing of 1087 ft. (between hydrants 9 and 2) and 669.5 ft., respectively.

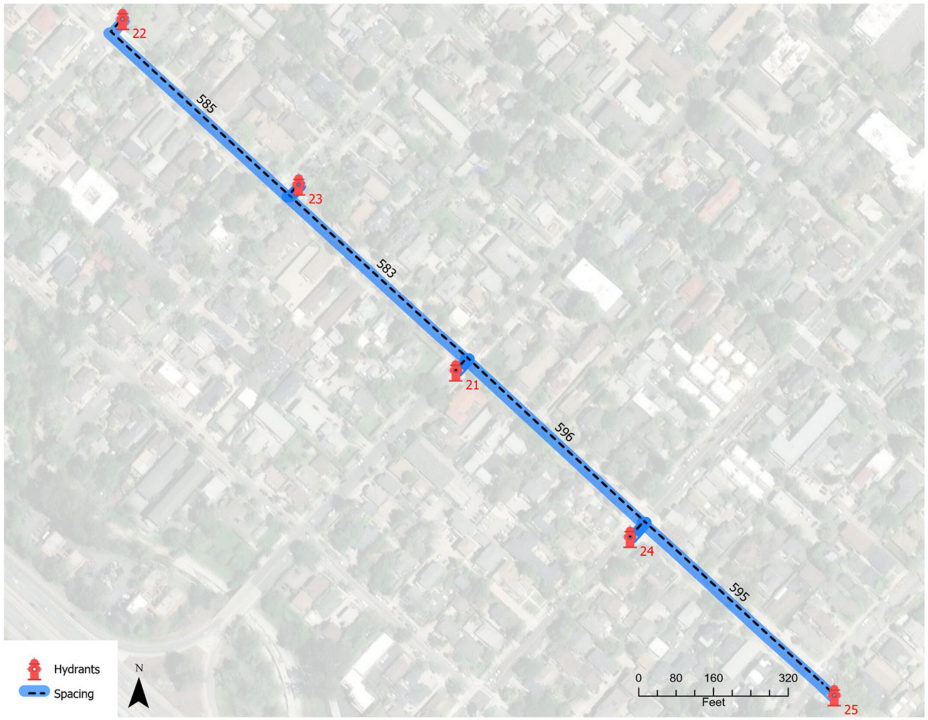


Figure 2.6. Street level hydrant spacing assessment.

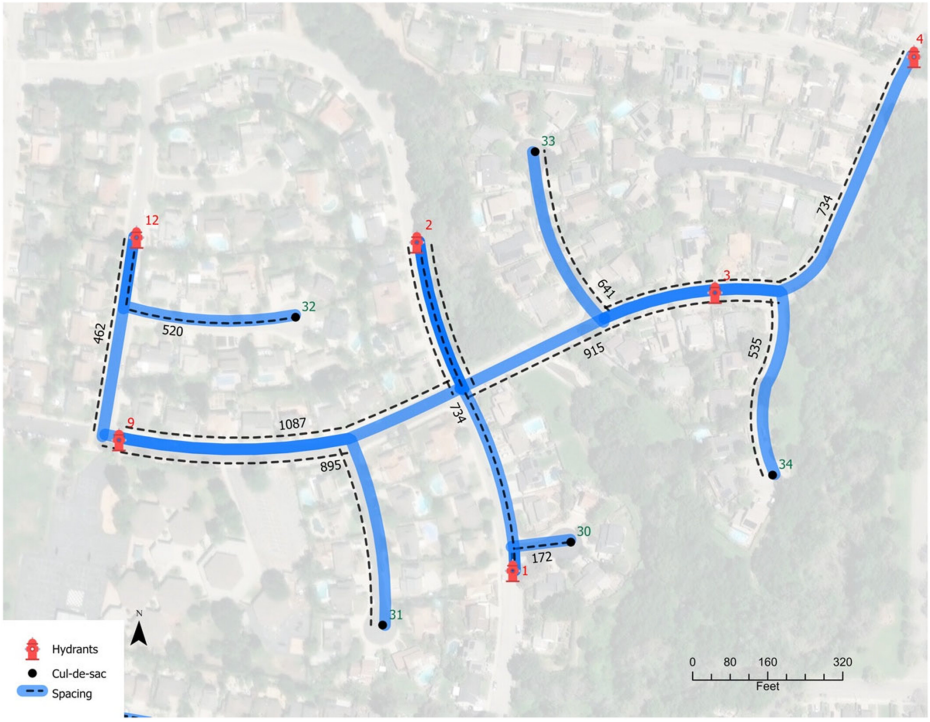


Figure 2.7. Community hydrant spacing assessment.

At the regional scale, the assessment is more nuanced because the standards vary depending on land use, structure type, and the intricacy of the road network (see Table 2.1). Nevertheless, evaluation is possible. A summary based on predominant land use is presented by associated code guidelines in Table 2.2. As an example, Table 2.2 reports that there are 7,578 unique paths between neighboring hydrant pairs that must adhere to the 500 ft. standard. The average length of these paths is 561.97 ft., exceeding the standard of 500 ft. The maximum neighboring path length in this group is 29,044.91 ft., far beyond the standard of 500 ft. In total, there are 9,242 hydrant neighbor pairs across the 500, 750, and 1,000 ft. standards-based groupings. The edge approach found the spacing pairs in 14 s. Within the Santa Barbara region, only 55.38% of the spacing standards are maintained, with 52.26% conforming when the standard is 500 ft., 92.61% when the standard is 750 ft., and 52.71% for the 1,000 ft. standard (Table 2.2). Lack of conformity is more commonly found in residential and undeveloped areas. For instance, in the residential community shown in Figure 2.6, the standards dictate a maximum and average spacing of no more than 500 ft., yet this standard is mostly violated. For commercial areas in the region, the average spacing of 394.57 ft. is quite low compared to the 750 ft. regional standard. The least conformance is for the 1,000 ft. standard (undeveloped) instances, with only 52.71% of hydrant neighbor pairs being within the standard. Figure 2.8 histograms show that within each standard group, some spacings are relatively close to their respective requirements. For residential areas, while some spacings exceed the 500 ft. standard, the highest density is near this threshold. Similarly, for commercial areas, most spacings fall below the 750 ft. standard.

Table 2.2. Regional hydrant spacing summary.

Spacing Standard	Count (spacing paths)	Mean (distance in ft)	Conformity	Conformity (%)	Max (distance in ft)
Residential (500 ft)	7,578	561.97	3,960	52.26	29,044.91
Industrial/Commercial (750 ft)	704	394.57	652	92.61	2,695.89
Undeveloped areas (1000 ft)	960	4,942.70	506	52.71	187,272.77

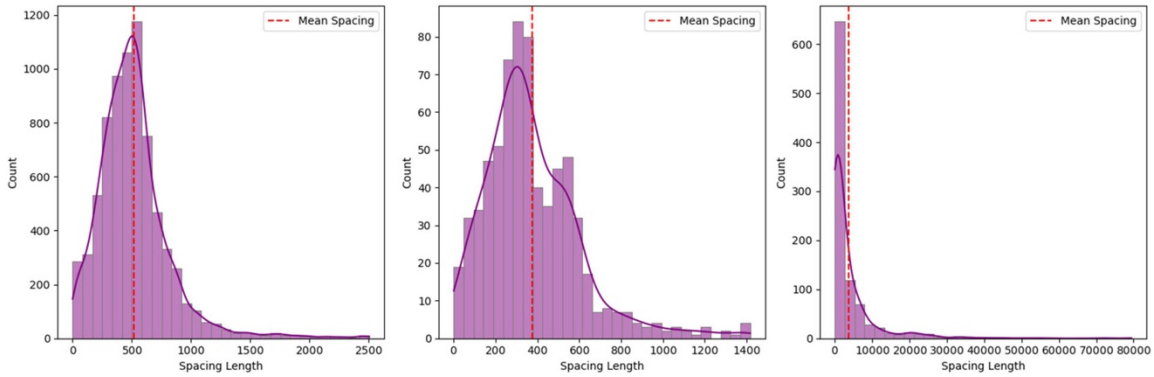


Figure 2.8. Spacing distribution according to the regional standards in the study area. (a) Residential (500 ft). (b) Industrial/Commercial (750 ft). (c) Undeveloped (1000 ft).

Figure 2.9 presents the spacing assessment for the entire region under analysis, where the conformities and violations are displayed in yellow and purple, respectively. As expected, some areas, such as downtown Santa Barbara and downtown Goleta are highly compliant given the commercial activity. Conversely, some residential areas, the zoomed inset of Figure 2.9, lack conformity. Several residential areas in Goleta and northern neighborhoods in Santa Barbara stand out, particularly the roads of Camino al Cielo, Paradise and Chumash Highway, have exceptionally large hydrant spacings, including the observed maximum of 187,272.77 ft. reported in Table 2.2 for undeveloped areas.

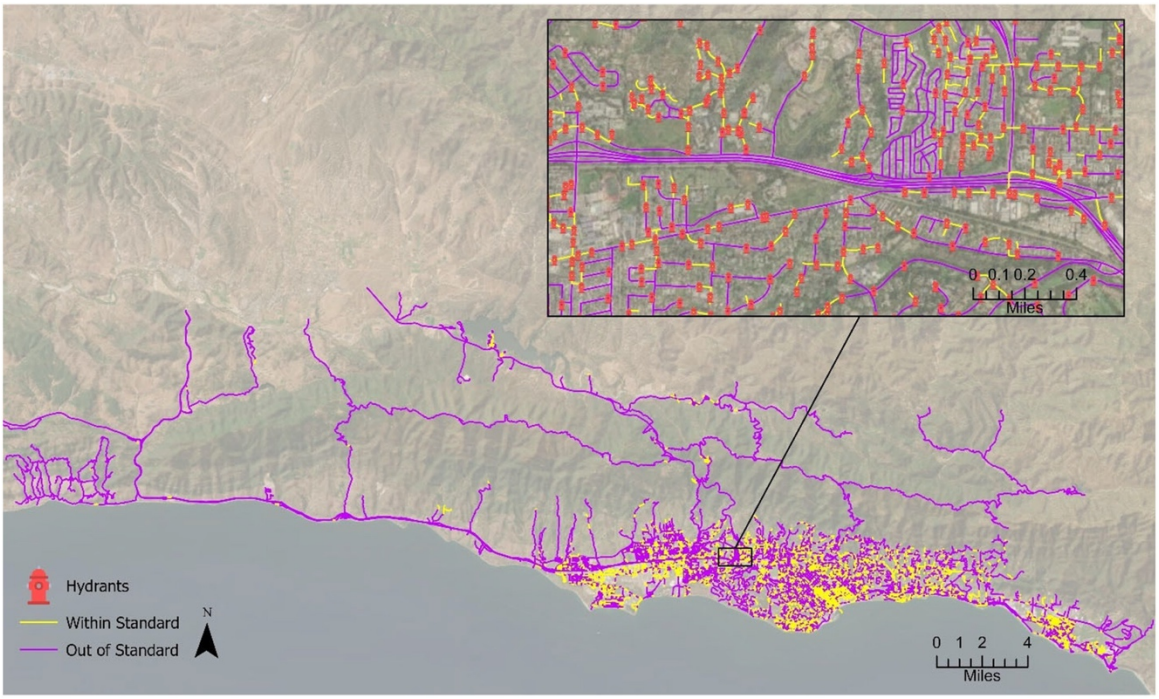


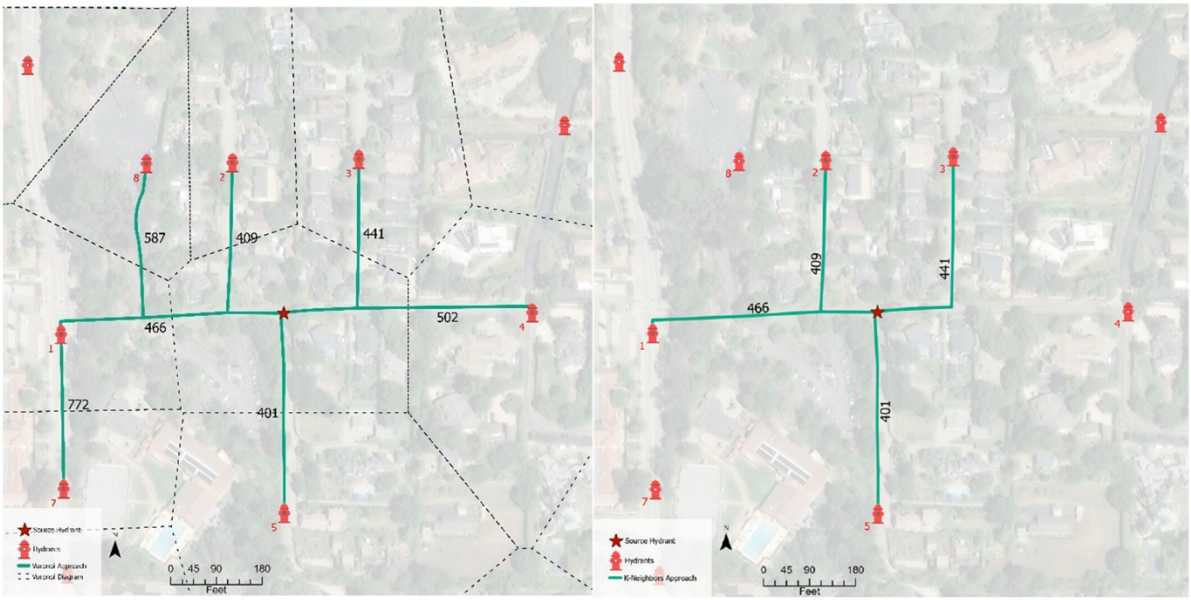
Figure 2.9. Conformity in the study region.

As previously mentioned, there are alternatives to finding spatial neighbors, e.g., k nearest neighbors[3] and Voronoi, (2.5) and (2.6), approaches. From any defined neighborhoods, it is possible to derive associated spacings. Figure 2.10 illustrates neighbors identified using the Voronoi and k nearest neighbor approaches, offering a comparison to Figure 2.5 showing the actual neighbors using the edge approach. The Voronoi approach identifies seven neighbors, $N_0^v = \{1,2,3,4,5,7,8\}$, with a maximum spacing of 722 ft. and an average spacing of 511.14 ft. The k nearest neighbors' approach $k = 4$)[4] identifies four neighbors, $N_i^{kNN} = \{1,2,3,5\}$, with a maximum and average spacing of 466 ft. and 429.25 ft., respectively. Clearly, this differs from the actual in Figure 2.5, suggesting error and uncertainty. This is not simply an isolated

[3] While not formally defined in the previous section, this is simply the k closest hydrants to a given hydrant, where k is a value set in advance.

[4] $k = 4$ was selected given that beyond four neighbors, the number of relationships (spacings) found increased, but the number of conform spacings slightly changed.

instance but rather can be observed at the street, community, and regional levels as well. Table 2.3 summarizes hydrant spacing using these two alternative methods for Santa Barbara. A very different picture of average spacing and conformity emerges that is inconsistent with the actual case shown in Table 2.2. It is clear then that correct identification of hydrant neighbors is critical for carrying out assessment at any scale.



(a) Voronoi (b) k nearest neighbors (k=4)

Figure 2.10. Alternative hydrant neighborhoods. (a) Voronoi. (b) k nearest neighbors (k = 4).

Table 2.3. Comparison with alternative methods.

Method	Spacing Standard	Count (spacing paths)	Mean (distance in ft)	Conformity	Conformity (%)	Max (distance in ft)
Voronoi	Residential (500 ft)	15,212	1,621.41	4,159	27.34	104,254.25
	Industrial/Commercial (750 ft)	1362	839.02	905	66.44	8441.39
	Undeveloped areas (1000 ft)	2,496	7,836.06	668	26.76	285,262.18
k Nearest Neighbors	Residential (500 ft)	10,183	693.14	4,065	39.92	29,044.91

(k=4)	Industrial/Commercial (750 ft)	923	452.41	816	88.41	2,695.89
	Undeveloped areas (1000 ft)	1,145	3,987.89	625	54.59	139,246.18

The second analysis question posed above was associated with coverage provided by hydrants. This is along the lines posed by researchers previously, namely Kaufman and Rosencrants (2015), Wielebski and Medyńska-Gulij (2013), Raškauskaitė and Grigonis (2019), Okon and Njoku (2018), and Lee et al. (2020). Hydrant coverage, (2.3), relative to standards is a relevant issue in fire risk and vulnerability. Just as spacing evaluation and standards assessment are possible, coverage at the street, community/neighborhood, and regional levels can also be observed. For instance, from Figure 2.2, previously shown in Section *B*, hydrant access coverage can be assessed and measured at the community level using the two approaches, Euclidean and road network distance, for which coverage resulted in 70.5%, and 41.51%, respectively. Figure 2.2 demonstrates the error one gets with a Euclidean approximation, but also that this inaccuracy is rather significant across an area. Table 2.4 summarizes hydrant coverage across the Santa Barbara region, with rather pronounced differences in access suggested by the Euclidean of 58.40% of roadway whereas the actual coverage is 49.52%.

Table 2.4. Hydrant road coverage in Santa Barbara.

Buffer	Coverage (%)
Approximate (Euclidean)	58.40%
Exact (Road Network)	49.52%

2.5. Discussion

Several points merit further attention regarding the differences between spacing and coverage, the uncertainty inherent to spatial data, and some spatial contexts where the edge approach offers a possibility for evaluation. The literature does not directly assess hydrant spacing but rather focuses on street coverage. The application results highlight that there is a distinction between spacing and service coverage. While coverage of streets within a region is important and can be summarized for a region as done in Table 2.4 for Santa Barbara (49.52%), this is an incomplete picture. Further, it ignores the specifics of standards and guidelines that outline spacing in terms of observed distances, averages, and maximums. Regional coverage does indicate portions of road segments that are within standards, but there is nothing about specific spacing nor any way to summarize roads that do not conform to standards. Hydrant spacing is a richer approach offering greater insights in terms of potential risk and vulnerability. Fire departments, local agencies, and urban planners can benefit from this approach to evaluate spacing at different scales—hydrant, street, community, and regional levels—to assess hydrant spacing status, have a complete picture of the hydrant network, and plan accordingly based on the detected vulnerabilities.

There are many sources of potential uncertainty associated with geographic data. In order to evaluate hydrant spacing, locational coordinates and road centerline data were necessary. However, road centerlines are an abstraction of the actual road network, as depicted in Figure 2.11. Centerline information lacks precision as well as detail, including separations, sidewalks, width, and number of lanes, which may be important to spacing guidelines. One example is that hydrant installation typically has favored being near street intersections, when possible (see King, 1926; Kimmel et al., 2004) and remains the case for many cities (e.g.,

(City of Los Angeles, 2016; City of Medford, 2024). The hydrant shown in Figure 2.11 is an example of this. Once street widths and sidewalks are considered, the hydrant in Figure 2.11 is effectively at the intersection, but in technical terms, it is interpreted differently in a GIS environment since it is not exactly at or on the centerline intersection.



Figure 2.11. Road centerlines and actual roads.

Another source of uncertainty is linked to information unavailability. Fire hydrants are required based on surrounding structures in California. Fire response agencies have boundaries that determine specific hydrant spacing in rural areas according to property acreage. Additionally, the service provided by water purveyors determines whether alternative sources, such as ponds or cisterns, are necessary to combat potential fire. Private companies do not make the associated information or safeguards available for analysis, potentially creating some degree of uncertainty.

While the focus of this chapter was on hydrant spacing, there are actually many different contexts where services are required or encouraged to satisfy similarly stipulated standards

and guidelines. For example, Murray and Feng (2016) discuss the importance of street lights in public safety and propose a model for street light location, noting that local codes indicate that spacing intervals should not exceed 300 ft. Another example is the installation of benches, with Usui (2022) indicating that the maximum allowed distance is 1148 ft. between benches. The International Building Code, as another example, suggests that the distances between water fountains shall not exceed 500 ft. over a walkable path. Traffic signs too have spacing standards. The U.S. Department of Transportation (2024) specifies spacing guidelines and distributions depending on the type of road, mandating spacing of 10 to 20 miles. Bus stops also have spacing mandates depending on the city, with Memphis designating a spacing maximum of 931 ft. (see U.S. Department of Transportation, 2015), as an example. Finally, the City of Los Angeles Department of Public Works (2024) designates a desirable distance between street trees to range from 25 to 40 ft.

2.6. Conclusions

Water accessibility is essential for effective fire response, protecting structures, property, life, and limiting overall damage. Hydrants play a vital role in providing accessibility, with national, regional, and local placement guidelines designed to decrease risk and vulnerability and support emergency response. Given population growth and new development, regions require regular and continued evaluation, yet this is often not done. Comprehensive hydrant spacing evaluation is a challenging task. The literature has noted and discussed the importance of spacing for urban safety and emergency response (McElroy, 1865; King, 1926), and some work has attempted assessment (e.g., Wielebski and Medyńska-Gulij, 2013; Kaufman and Rosencrants, 2015; Okon and Njoku, 2018; Raškauskaitė and Grigonis, 2019; Lee et al., 2020). These works, however, have focused on coverage not spacing per se. To the best of

our knowledge, a direct method has not yet been proposed to measure and observe spacing between features along a road network. Furthermore, traditional GIS techniques, such as service area mapping, proximity analysis, and flow measurement, are helpful but fall short of enabling direct assessment of hydrant spacing. Calculating spacing requires the accurate identification of neighboring hydrants from a given source, but this is not easily accomplished.

To directly measure and assess hydrant spacing, an approach that accurately identifies hydrant neighbors was developed, extending GIS capabilities to support assessment. Evaluation of hydrant spacing in Santa Barbara demonstrated that the edge approach was both effective and flexible. It was found that hydrant coverage of streets in the region was nearly 50%. More detailed analysis demonstrated that spacing varied across the region, with some areas more vulnerable than others. Query and investigation by hydrant, street, neighborhood/community, etc. are possible to explore risk and vulnerability based on the developed methods. This chapter lays a foundational framework for urban safety assessment, fire preparedness, and emergency response. Urban planners, fire departments, and local agencies can use the insights from this study to identify vulnerabilities and enhance planning efforts, particularly in fire-prone areas. In particular, instances where spacing is excessive may suggest that supplemental infrastructure is needed, such as dry hydrants, water tanks, shuttle service, water trucks, and/or drawing water from pools/ponds. However, planning along these lines must be done in advance, making risk and vulnerability assessment critical. Detailed characterization of vulnerable areas is essential for effective planning, factoring in variables for preparedness and prioritization. For instance, considering socioeconomic and social vulnerability factors can help prioritize areas with hydrant service deficiencies, ensuring that populations more profoundly impacted by fires receive the necessary attention.

3. Urban Safety and the Role of Hydrant Structure and Configuration[5]

3.1. Introduction

Fire hazards are prevalent in urban environments and pose significant threats to communities worldwide. Structure fires in particular cause substantial loss of life, injuries, and property damage. The U.S. Fire Administration (2024) indicates that there were 344,600 residential building fires in the United States in 2023, resulting in 2,890 deaths, 10,400 injuries, and nearly US $11.27 billion in losses. Water is the primary extinguishing agent, and access to water is essential for limiting fire loss and spread based on lessons learned from the Great Fire of London in 1666, where thousands of buildings were lost (see Garrioch, 2016), the Great Chicago Fire in 1871, and more recently the Lahaina fire in Hawaii in 2023 and the Los Angeles fires in January 2025. During the Great Chicago Fire, the Chicago pumping stations were compromised, resulting in days of destruction across some three square miles that left nearly 100,000 residents homeless (Smith, 2020). The Chicago Architecture Center (2025) reports that widespread water pressure failure resulted in an estimated 300 deaths and 18,000 structures lost. Early large-scale fires, such as those in London and Chicago, led to the development of water mains and the standardization of hydrant networks that exist today. Guidelines exist at many geographic scales, including international (e.g., International Code Council (2024), national (e.g., (National Fire Protection Association, 2024), state (e.g., (California Fire Code, 2022)), and municipal (e.g., (Carpinteria-Summerland Fire Protection

[5] This chapter presents a revised version of a paper published in *Scientific Reports* co-authored with Dr. Alan T. Murray, Dr. Kathy Bailys, and Dr. Richard Church (Heffernan et al., 2026).

District, 2021). Yet, despite standardized guidelines for incident response, structure fires persist and conflagrations continue to occur.

In the past, inadequate infrastructure facilitated the rapid spread of fires, resulting in significant losses. However, with the advancement of firefighting infrastructure and response measures, one might assume that such devastation would not be observed today. Unfortunately, large-scale losses by fire continue, often in and around urban areas where spread from the wildland is assisted by favorable environmental conditions, such as strong winds, dry vegetation, flammable building materials, and the close spatial arrangement of structures.

While it is commonly believed that fire spread is less prevalent in densely developed environments, this does not mean that urban areas are immune. There have been several documented cases of wildfires devastating communities in urban regions. One example is the Lahaina fire in 2023, where a wildfire jumped to properties and spread relentlessly throughout the town, stopping only when it met the ocean (Baker, Browning, et al., 2023). Similarly, the Coffey Park neighborhood in Santa Rosa, California, was destroyed in 2017 by the Tubbs Fire (Maranghides et al., 2022). More recently, the Palisades and Eaton fires in Los Angeles County burned for 24 days, and devastated the communities of Altadena, Pasadena, Pacific Palisades, Topanga, and Malibu, claiming 30 lives, injuring 13 people, destroying 16,251 structures, damaging 2,047 structures, and burning 37,469 acres (CAL FIRE, 2025a). Although fire events in densely populated urban environments may be easier to contain due to better water access, less flammable building materials, and less dry, dense vegetation, significant destruction still occurs (Maranghides et al., 2022). The above events highlight that significant vulnerabilities remain, and under the right conditions, massive fire spread is possible. This means communities need to be well prepared, understand where and when incidents concentrate,

which conditions are associated with larger losses, and how defensive infrastructure relates to those outcomes.

The County of Santa Barbara, known for its scenic beauty and decorated landscape, situated between the Santa Ynez foothills and the Pacific coast, faces significant wildfire vulnerabilities due to the combination of conditions that favor fire ignition and spread. Its Mediterranean climate, Sundowner winds, flammable vegetation, and other factors that contribute to wildfires make this area particularly vulnerable (Moritz et al., 2014; Murray et al., 2021). With wildfire events over the last couple of decades demonstrating greater intensity and severity, and the growing population in wildland-urban interface (WUI) communities, not only are people at risk of exposure and potential spread to urban environments, but also, human activity increases this risk. In the last century, about 95% of fires in California were human-caused (Syphard et al., 2007). Combined with a growing WUI population in California, 41% between 1990 and 2010 (Li et al., 2022), inhabited areas are exposed to increasing levels of wildfire risk. It is imperative to conduct a thorough examination of the behavior of fires that occur in urban environments to assess defensive measures that may explain factors contributing to the structural losses experienced in fire-prone regions.

Prior work on incident patterns and structure loss spans two largely separate threads. One is urban fire-incident studies where researchers have: (i) mapped risk and hotspots, often with kernel density and related spatial tools (Corcoran et al., 2007a; Corcoran et al., 2007b; Jeong et al., 2018; Rahman Tishi & Islam, 2019); (ii) linked incident counts to socio-demographic context via regression (Corcoran et al., 2007a; Corcoran et al., 2011a); and (iii) modeled spatio-temporal dependence with point-process or Bayesian approaches (Corcoran et al., 2007b; Asgary et al., 2010; Corcoran et al., 2011b; Ceyhan et al., 2013; Chhetri et al., 2018).

The other is WUI structure-loss studies, where analyses emphasize parcel/structure and landscape factors, including defensible space, materials, topography, and housing arrangement (Maranghides & Mell, 2011; Alexandre et al., 2016; Syphard et al., 2017; Maranghides et al., 2022; Price et al., 2021).

Nonetheless, fire protection capacity has been typically represented through broader conceptual factors or proxy measures, such as proximity to fire stations, but has been less studied in terms of the spatial configuration of defensive infrastructure, specifically directly accounting for hydrant networks. Moreover, although fire incidents have been studied in different contexts, they have been tailored to specific objectives, mostly focusing on characterizing fire risk hotspots, identifying possible causes of higher incidence, predicting fire spread, or understanding the contributing factors to structural damage in the WUI. Despite advances in spatial statistics and analytical tools, the literature still lacks a more comprehensive analysis that moves beyond the descriptive characterization of fire incidence to formal tests of clustering, identifies factors associated with spatial concentration, and examines the determinants of losses while directly accounting for defensive infrastructure such as hydrant networks. This chapter addresses that gap by explicitly examining hydrant infrastructure as a component of urban fire protection and by evaluating its relationship with fire incidence and structure damage in an urban region. Although this study is not designed to produce a fire-risk measure, it focuses on two empirically observable dimensions: the spatial concentration of urban structure-fire incidents and the severity of losses once incidents occur.

Hydrant code guidelines have been studied previously, delving into compliance with respect to structure access (Baik & Murray, 2024) and spacing (Figueroa et al., 2024). These evaluations identified vulnerabilities and revealed differential levels of code compliance,

namely that commercial areas have higher compliance than certain residential neighborhoods. With spacing and structure access information combined with past fire incidents, relevant information regarding urban fire spread, patterns, damage, and response can support analysis and provide insights on response alternatives and mitigation strategies for future events. Likewise, assessing access to hydrant infrastructure is important for limiting fire spread, particularly in at-risk environments. Finally, identifying factors that make some areas more susceptible to fire and estimating expected losses can provide valuable guidance for urban planners and policymakers.

This chapter introduces a framework for examining historical structure-fire incidents by examining their spatial distribution and their association with hydrant infrastructure. The analysis assesses the effectiveness of defensive actions while also characterizing patterns associated with fire-spread potential. Additionally, insights regarding the patterns of fires are sought relative to how they behave in space and how structures are destroyed based on response. The next section presents a review of the scope of this study. Then, methods and framework to analyze past incidents and their relationship with defensive infrastructure are presented. Results are detailed in the assessment of historical fires in Santa Barbara County. Finally, a discussion and concluding remarks are offered.

3.2. Background

Most urban fire studies start with description and mapping. Official incident records are often analyzed to answer *where* and *when* events concentrate by mapping spatial hotspots and documenting temporal regularities in fire occurrence Kernel density estimation (KDE) has been used to identify hotspots and characterize them as risk surfaces (Corcoran et al., 2007a; Corcoran et al., 2007b; Asgary et al., 2010; Gilbert & Butry, 2018; Rahman Tishi & Islam,

2019; Guldåker, 2020; Zhang et al., 2020; Shuo et al., 2021; Singh et al., 2021; Wang et al., 2021;Bispo et al., 2023). In several studies, these KDE-based hotspot surfaces have been paired with additional analytical methods to develop a more comprehensive understanding of urban fire patterns. For example, KDE surfaces have been combined with count models to relate spatial patterns of fire incidence to socioeconomic context (Corcoran et al., 2007a; Corcoran et al., 2011a), with spatial econometric approaches to identify the socioeconomic factors associated with fire occurrence (Bispo et al., 2023), and with inferential spatial statistics, such as Diggle's D-function and the spatio-temporal K-function to detect clustering across space and time (Ceyhan et al., 2013). Other studies have paired KDE mapping with average nearest-neighbor methods to characterize spatio-temporal fire patterns (Jeong et al., 2018; Mohammadi et al., 2023), and with Getis-Ord Gi* and interpolation methods (Singh et al., 2021).

Studies examining incident outcomes have focused on factors contributing to fire casualties through logistic regression (Xiong et al., 2015). To complement these views, ecological Poisson risk models with exposure offsets and Bayesian approaches reveal that deaths and injuries arise from disjoint populations (Gilbert & Butry, 2018; Taylor et al., 2024). Separately, research on spatial coupling of fire incidents with surrounding infrastructure and other spatial features has combined Cross-K and Cross-L functions with global and local colocation quotients to examine relationships between fire types and adjacent facilities (Xia et al., 2019).

Beyond KDE-based hotspot mapping, K- and L-function analysis, count models, and spatial coupling, researchers have used a range of approaches to characterize urban fire patterns and relate them to neighborhood, temporal, and operational conditions. Composite-indicator methods, such as AHP-based indices, and machine-learning approaches, including supervised

self-organizing maps, have been used to generate explicit fire risk assessments (Asgary et al., 2012; Zhang, 2013). Other studies have used quad-plots and Dirichlet-multinomial models to examine how temperature, socioeconomic conditions, and temporal patterns interact with different incident types (Corcoran et al., 2011b). Additional spatio-temporal studies have taken a descriptive perspective focusing on spatial dependence, correlations, and clustering, and have shown that intentional or suspicious fires are associated with living condition indices and economic indicators (Guldåker & Hallin, 2014; Kelly et al., 2019). Related work has also examined operational outcomes, with quantile models showing slower seasonal response times (e.g., winter) in areas with lower socioeconomic status and more complex street networks (KC & Corcoran, 2017). More broadly, studies associating fire incidents with neighborhood characteristics have progressed from basic regression to spatial econometric and geographically weighted regression approaches, allowing effects to vary across the urban fabric (Todorović, 2020), and to panel models that separate cross-sectional structure from temporal change at city or tract scale (Wang et al., 2015; Hu et al., 2019; Hossain & Smirnov, 2023).

Another strand of the urban fire literature emphasizes fire forecasting, operational deployment, and emergency response. Bayesian and stochastic models have been used to predict where fires are likely to occur using building footprints and past incidents, thereby avoiding some of the information loss associated with coarse spatial aggregation (Rohde et al., 2010). Markov-chain approaches indicate short-term temporal dependence, where risk tends to dip for roughly two months after a local fire, and the absence of a recent nearby event can increase short-term risk, creating windows for prevention across a region based on location (Ardianto & Chhetri, 2019). Response times exhibit distinct spatial patterns. Recent predictive

work integrates GIS-derived spatial features with machine learning to estimate the likelihood that an urban fire escalates, explicitly linking spatial context to response resource allocation (S. L. Lee et al., 2025). Fire spread simulation in urban environments has also been a focal point, with several studies modeling fire dynamics in dense urban settings (Halim et al., 2021; Himoto & Tanaka, 2008; Jain & McLean, 2006). Related research has also addressed evacuation preparedness, including the development of open-source simulation frameworks (Ronchi et al., 2019).

Across these streams, important gaps remain. Few studies have examined urban fire incidents through a framework that moves from hotspot identification to formal clustering analysis and then to the consequences of fire in terms of structural loss, while directly accounting for defensive infrastructure. In particular, the spatial configuration of water supply infrastructure, especially hydrant networks, remains underexamined in relation to both incident concentration and loss severity. Urban studies sometimes proxy response with station proximity or road accessibility, but direct analysis of incident-hydrant interaction remains limited. This chapter bridges the existing gap by combining an exploratory point-pattern analysis (KDE; univariate and cross-K and cross-L diagnostics) with count and loss models to separate where incidents happen from what drives losses, placing hydrant availability, spacing, and reach alongside density, land use, timing, and season. Thus, this chapter connects urban fire analytics to the defensive infrastructure that ultimately enables suppression and limits damage in fire-prone regions.

3.3. Methods

The goal of this chapter is to examine how the availability and configuration of defensive infrastructure, specifically fire hydrant networks, influence the spatial patterns of structure-

fire incidents and the magnitude of losses when fires occur. To address these objectives, the analytical framework combines exploratory spatial analysis with two complementary inferential components: (i) modeling the intensity of incident counts across areal units, and (ii) modeling fire-related losses at the property level. Both components make use of generalized linear (mixed) models tailored to the distributional nature of the outcomes, incorporating covariates that capture demographic, infrastructural, and spatial factors.

3.3.1. Study area

The study region encompasses urban areas within Santa Barbara County, as shown in Figure 3.1. The area is aligned with the Santa Barbara County Fire Protection District's operational scope. Incidents that occurred within jurisdictions with their own fire departments, which provide primary protection and incident reporting, were excluded since records for those jurisdictions were not available in a form that allowed a complete sample for those areas.

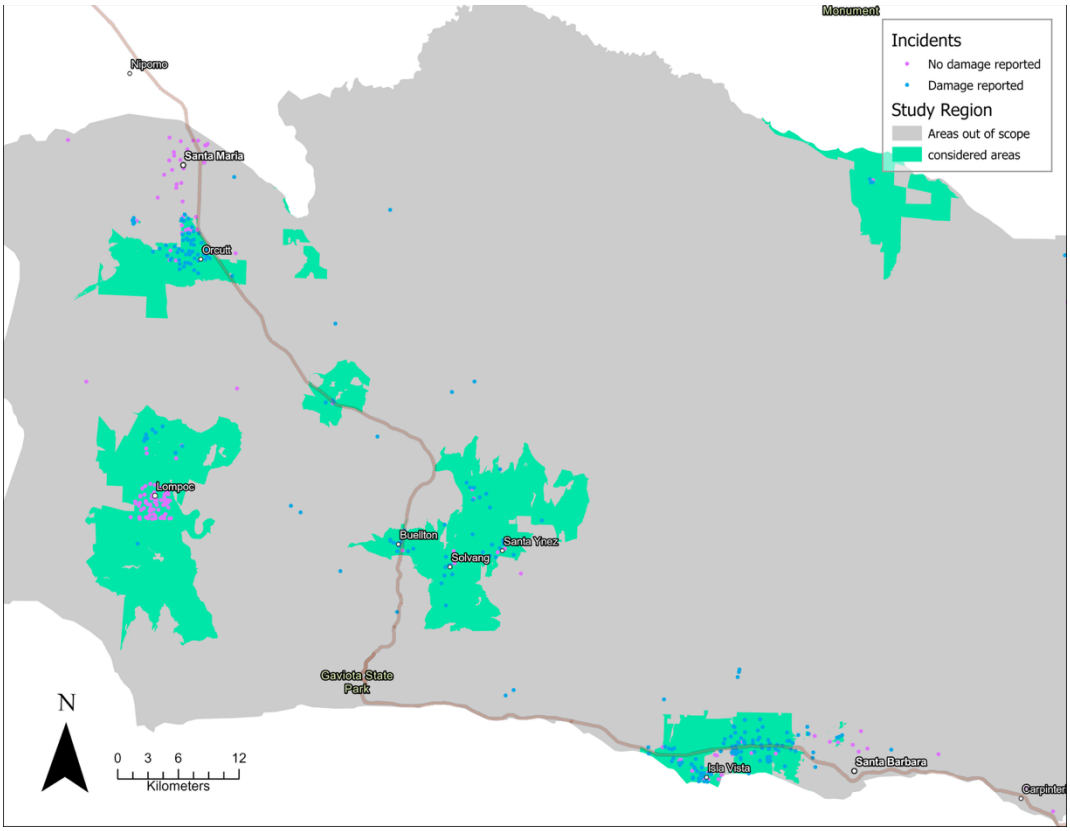


Figure 3.1. Study region in Santa Barbara County, indicating structure fires from 2014 to 2024.

The urban areas in Santa Barbara County are diverse, ranging from small rural communities, such as Los Alamos and New Cuyama, to larger urban centers, such as Orcutt, Lompoc, Solvang, Goleta, and Isla Vista. For interpretation and mapping, several adjacent towns are aggregated into regional groupings. This is the case for Goleta and Isla Vista, Lompoc (including Lompoc, Vandenberg Village, Mission Hills), and Solvang (including Solvang, Buellton, Ballard, Los Olivos, Santa Ynez). These subregions differ in population size, socioeconomic composition, and settlement form, and this heterogeneity relates to the spatial patterns and model results reported in section 4. Population by area is shown in Table 3.1 (2020 decennial census counts). Based on recent American Community Survey income estimates, Goleta, Orcutt, and the Solvang region tend to have median household incomes near

or above $100k, whereas Lompoc is lower (roughly between $60 and $70k). Isla Vista is a student-dominated community (median age of approximately 21 years old), with a lower median household income of around $24,000, which is typical of college towns and reflects student composition. Ethnically, Lompoc is majority Hispanic/Latino. Goleta and Orcutt are mixed with substantial Hispanic/Latino populations. Much of the Solvang region remains predominantly non-Hispanic White. These differences matter for fire risk analysis since socioeconomic conditions and household composition can shape ignition opportunities, prevention practices, and recovery capacity (Corcoran, Higgs, Brunsdon, Ware, et al., 2007).

3.3.2. Data

The incident dataset comprises records of structure fire responses collected by the Santa Barbara County Fire Department from January 2014 to June 2024 and was available upon request. The count of incidents in each region is reported in Table 3.1. Each record includes the fire's geographic location, the number of structures involved, the incident date and time, suppression duration, and the assessed value of the affected property. Table 3.1 shows incident counts per region within the study area. Los Alamos and New Cuyama are excluded from the analysis due to a low incident count (eight incidents), which did not support stable spatial inference for the subregion. Hydrant locations were obtained from the Santa Barbara County Fire Department, and socioeconomic indicators (population density, housing density, median income) were derived from the American Community Survey at the census block group level. For the count models, the observation units are irregular polygons defined by the census block groups. As for the loss models, the unit of analysis is the individual fire incident.

Table 3.1. Incidents and population by region. Population: 2020 decennial census.

Region	Population	Incidents

Lompoc region	55,323	90
Goleta and Isla Vista	48,190	120
Solvang region	17,747	52
Orcutt	32,034	68
Total	**153,294**	**330**

Prior to modeling, the data underwent several derivation, cleaning, and transformation steps. The distance to the closest hydrant from each incident was calculated using road-network distance, as well as the distance to the closest fire station. Hydrant spacing was derived using the previously proposed edge approach (Figueroa et al., 2024), which also uses road network distance. Hydrant-to-structure access compliance was also based on an approach devised in previous work (Baik & Murray, 2024). Variables prone to infinite values (e.g., logarithms of densities) were filtered to retain only finite observations. Reported economic losses include property losses and content losses in U.S. dollars (USD). Continuous covariates with heavy skewness were log-transformed using either the natural logarithm or the transformation $\log(1 + x)$ to preserve zero values. For instance, the distances to the nearest hydrant (*lh*) and fire station (*lf*), the total suppression time (*lt*), and the structure area (*la*) were all computed using the aforementioned logarithmic transformation. Categorical variables were encoded as factors, with clear baseline categories (e.g., residential for property type, afternoon for time of day, Friday for day of week, and winter for season). All analyses were conducted in R 4.3 with dplyr, tidyr, purrr, and ggplot2 packages for data processing, analysis, and visualization. All spatial layers were transformed to a common projected coordinate reference system, NAD83 / California zone 5 (EPSG:26945).

3.3.3. Exploratory analysis

A distribution of points in two-dimensional space, as in the case of structure fire incidents, can be characterized and analyzed using point pattern analysis. Such analyses can describe whether incidents are clustered, randomly distributed, or dispersed relative to complete spatial randomness (CSR). CSR corresponds to a homogeneous Poisson process and serves as the null model for inferential tests. Structure fire incidents have been studied by characterizing hotspots of incidence as a way to visualize and use the returned intensity to predict future fire incidence. The way to visualize the concentration of incidents or hotspots is commonly done by estimating an intensity surface using a two-dimensional Gaussian KDE, which generalizes the univariate KDE introduced in the statistical literature (Silverman, 1986; Scott, 1992). Given incident locations $\{x_i\}_{(i=1)}^{n}$ inside a window $W \subset R^2$, the KDE at location x is defined as:

$$\hat{\lambda}(x) = \frac{1}{2\pi\sigma^2}\sum_{i=1}^{n}\exp\left(-\frac{\|x-x_i\|^2}{2\sigma^2}\right) w_i(x)\,, x \in W \qquad (3.1)$$

where σ is a bandwidth that controls the degree of smoothing and $w_i(x)$ is an edge-correction weight that compensates for boundary bias. This intensity surface forms the basis for hotspot maps. The choice of σ controls smoothness. Smaller bandwidths amplify local noise, whereas larger bandwidths can obscure compact clusters (Diggle, 2013). In the kernel density estimations, a $\sigma = 0.722$ km was selected based on likelihood cross-validation and corroborated by a plug-in bandwidth criterion (Diggle, 1985; Sheather & Jones, 1991). Although KDE is essential for localizing hotspots, it does not provide a formal test to assess the concentration, dispersion, or randomness of the point pattern-generating process. For this reason, although there are several ways to test against CSR (e.g., quadrat count methods and nearest neighbor point pattern measures), distance-based measures, such as Ripley's K function

and its variance-stabilized transformation, the L function, are commonly utilized to formally quantify departures from CSR across multiple spatial scales (Ripley, 1976; Besag, 1977, 1977). The K function at radius r is defined as the expected number of additional events within distance r of a typical event divided by the overall intensity. An unbiased estimator with edge correction is:

$$\widehat{K}(r) = \frac{|W|}{n(n-1)} \sum_{i=1}^{n} \sum_{j \neq i} \frac{I(d_{ij} \leq r)}{e_{ij}}, \tag{3.2}$$

where I(.) is the indicator function, d_{ij} is the distance between events i and j, e_{ij} is an edge-correction factor, and |W| is the area of the observation window. Because the variance of $\widehat{K}$(r) increases with r, the L function was proposed (Besag, 1977):

$$\hat{L}(r) = \sqrt{\frac{\widehat{K}(r)}{\pi}}, \tag{3.3}$$

which stabilizes the estimator's variance. Under CSR, the theoretical value of L(r) is r. It is therefore common to examine the centered function $\hat{L}(r) - \mathrm{r}$. Positive values indicate clustering, whereas negative values indicate dispersion. Monte Carlo simulation envelopes are used based on CSR to assess the significance of observed deviations(Ripley, 1979). In addition to analyzing incident clustering alone (univariate case), the bivariate cross-L function is used to assess bivariate patterns (the relationship between two point patterns) by examining the spatial relationship between incident and hydrant locations. The cross-K function K_{IH}(r) measures the expected number of hydrants within a distance r of a typical incident, standardized by the mean density of hydrants. The cross-L function is defined analogously as $L_{IH}(r) = \sqrt{K_{IH}(r)}/\pi$. Comparing $\hat{L}_{IH}$(r) with its CSR expectation r allows for testing

whether hydrants are randomly located relative to incidents or whether there is evidence of attraction (clustering) or repulsion (dispersion). Throughout, cross functions are computed using Euclidean distance. An important consideration for analysis and interpretation concerns the assumption of the null model, since it implies a homogeneous Poisson process. In the present context, CSR should not be interpreted as a literal model of urban structure. Urban fire incidents arise in a built environment shaped by land use, road geometry, and uneven settlement patterns. Rather, CSR should be used as a benchmark to test whether the observed point pattern is more clustered or more dispersed than expected under spatial homogeneity. Departures from CSR, therefore, indicate non-random spatial structure, but do not by themselves identify the mechanism producing that structure.

3.3.4. Modeling counts

Fire incidence in urban areas is associated with socioeconomic factors, including low income, high unemployment rates, household overcrowding, and ethnicity, where higher incidence and casualties are more prevalent in economically deprived areas (Corcoran et al., 2007a). Given the importance of socioeconomic variables in fire incidence, Poisson regression provides a way to assess variables related to spatial clustering or perceived spatial distribution of incidents. A Poisson model is suitable because the response variable is the number of incidents observed in each census block group. Thus, a count regression provides the natural starting point. Let Y_i denote the number of structure fire incidents observed in polygon i during the study period. A Poisson regression is defined as:

$$\log(\lambda_i) = \beta_0 + x_i^{\top}\beta + \log(a_i) \tag{3.4}$$

where $Y_i|x_i \sim \text{Poisson}(\lambda_i)$, $\lambda_i = \mathbb{E}(Y_i|x_i)$, x_i is a vector of covariates, a_i is the polygon area in square feet used as an offset, and β are parameters to be estimated. However,

inspection of the Poisson model residuals reveals that substantial overdispersion exists when the Pearson dispersion $\phi > 1$, indicating that the variance greatly exceeds the mean. Conventional guidance suggests the adoption of negative binomial (NB) models to resolve this issue:

$$\mu_i = \exp(\beta_0 + x_i^\top \beta) a_i \tag{3.5}$$

where $Y_i \sim NB(\mu_i, \kappa)$. Count models are estimated in R using the glm() function for the Poisson specification, the glm.nb() function from the MASS package for the negative binomial specification, and the glmmTMB() function from the glmmTMB package for the mixed negative binomial specification.

3.3.5. Modeling fire-related losses

The second modeling task seeks to explain variation in monetary losses and the importance of the hydrant infrastructure, measured by distance to the incident and by hydrant-to-structure access compliance, conditioned on incident. Let L_j denote the total economic loss for incident j in U.S. dollars. Because fire-related losses are positive, continuous, and strongly right-skewed, a Gaussian model would be inappropriate. Accordingly, losses are modeled using a Gamma specification with a log link, and a block-group random intercept is included to account for clustering and unobserved area-level heterogeneity. Specifically:

$$L_j \mid x_j, b_{g(j)} \sim \text{Gamma}(\mu_j, \phi),\ \mu_j = \mathbb{E}[L_j \mid x_j, b_{g(j)}],\ \log(\mu_j) = \beta_0 + x_j^\top \beta + b_{g(j)} \tag{3.6}$$

where $g(j)$ indexes the census block group corresponding to incident j. A random intercept $b_{g(j)} \sim N(0, \sigma^2)$ captures unobserved heterogeneity across block groups, reflecting that nearby properties may share latent risk factors (e.g., building codes or vegetation). Here, μ_j denotes the conditional mean loss for incident j, ϕ is the Gamma dispersion parameter, and

x_j is the vector of covariates. The log link ensures that multiplicative effects of covariates on expected loss translate into additive effects on $\log(\mu_j)$. Covariates in x_j include the log of the distance from incident j to its closest hydrant, the log of the distance from incident j to its closest fire station, the log of total suppression time in minutes, and the log of the area of the property where the incident occurred. Some categorical variables are included, such as hydrant-to-building code compliance (1 if structure where the incident occurred was compliant and 0 otherwise), building type (residential, commercial, outdoors building, etc.), spatiotemporal variables, such as time of the day in which the incident occurred (dawn, morning, lunch time, afternoon, evening, and night), day of the week (Monday to Sunday), and season (winter, spring, summer, and fall). Loss models are estimated in R using glmmTMB() from the glmmTMB package, specifying a Gamma distribution with a log link.

3.4. Results

This section reports the findings in three stages aligned with the research aims. First, an exploratory point pattern analysis shows incident clusters and spatial scale. Second, count models show the relationship between hydrant presence and fire intensity, as well as which factors are associated with incident intensity. Lastly, loss models identify factors associated with economic loss during an incident, including hydrant infrastructure. The estimates, shown in Figure 3.2, reveal incident concentrations, or hotspots, within the study region, with these hotspots primarily around the principal activity centers.

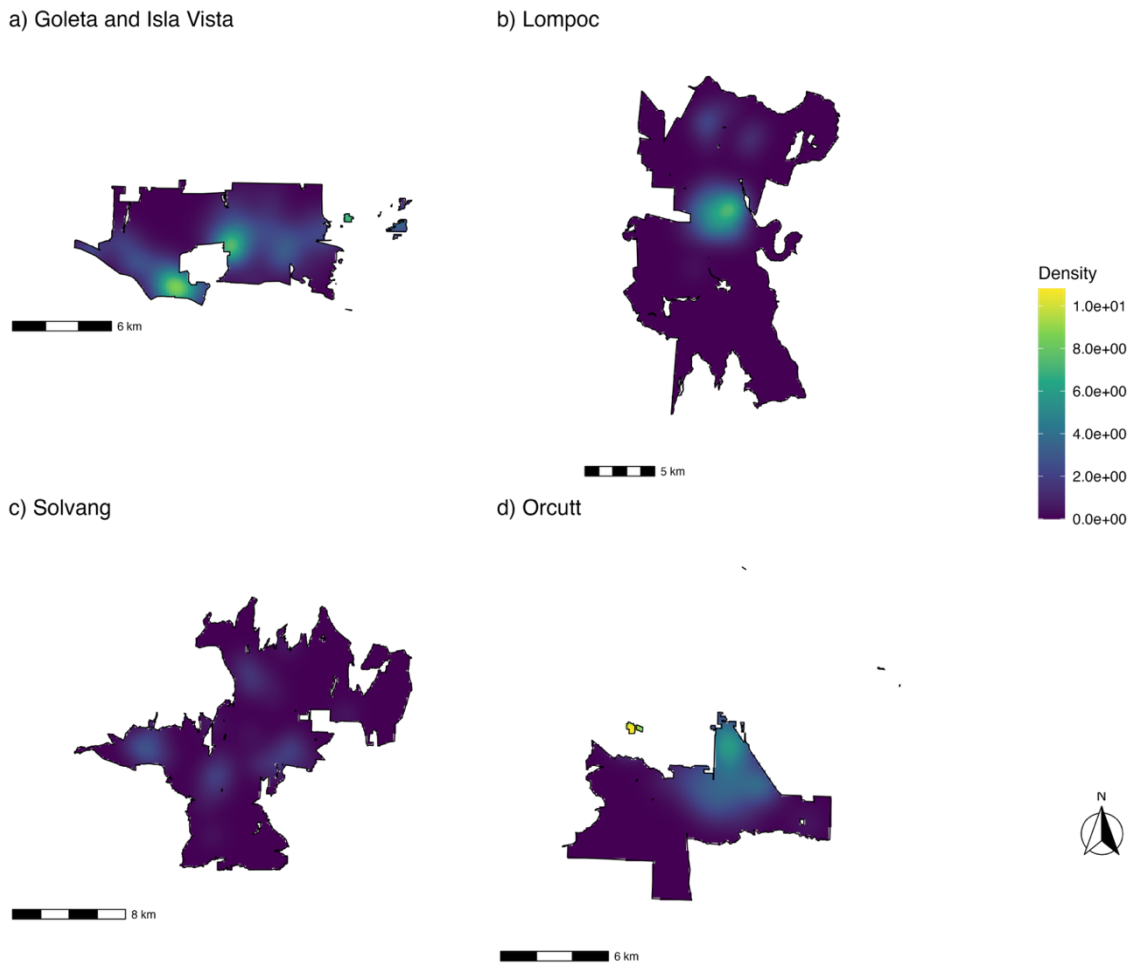


Figure 3.2. Kernel density for the areas by subregion. (Bandwidth σ = 0.722 km; incidents per km^2).

For example, the area of Isla Vista and Goleta presents a couple of compact core hotspots with density $\lambda(x)$ peaking near 9 incidents per square kilometer in Isla Vista and downtown Goleta, while incidents decline to less than 1 per square kilometer towards the peripheries of those hotspots. Similarly, in the Lompoc region, the incidence is concentrated in downtown Lompoc, with density $\lambda(x)$ peaking at nearly 7 incidents per square kilometer. In the Solvang region, the highest density peaked in Buellton at 3 incidents per square kilometer, where the hotspots were present in downtown Buellton (see Figure 3.1 to locate these towns within the study region), and with less density in downtown Solvang, downtown Santa Ynez, and Los

Olivos. The highest density was found in the Orcutt region, within Tanglewood, with an intensity of nearly 11 incidents per square kilometer, followed by a hotspot in the northern part of Orcutt.

Since KDE is merely descriptive, departures from CSR were formally evaluated within each subregion using Ripley's K and L functions with simulation envelopes (see subsection 3.3.3). Figure 3.3 shows that clustering within each subregion is statistically significant across a range of distances. Across the four subregions, the observed $L(r)$ consistently departed from the theoretical CSR expectation, confirming the nonrandomness of the incident's spatial distribution. These subregions exhibited clustering at characteristic spatial scales, with the magnitude and spatial extent of clustering varying with settlement size and morphology, whereas no envelopes suggested dispersion. Particularly, in the subregion of Isla Vista and Goleta, the $L(r)$ curve lay substantially above the CSR envelope across nearly the full distance range shown, indicating persistent clustering from local to broader neighborhood scales. This is consistent with the hotspots revealed by the kernel density analysis. Likewise, in the Lompoc region, the $L(r)$ curve exceeds the envelopes up to 2 km. This indicates statistically significant clustering across local and neighborhood scales. This scale-wide departure is consistent with multiple local hotspots superimposed on a broader urban concentration. In the Solvang region, the observed $L(r)$ exceeds the CSR band up to 1.2 km, indicating statistically significant clustering at short- to medium-range scales, consistent with the multiple centers contained in this region. In Orcutt, the clustering is statistically significant up to 1.5 km. This shows the concentration at the local scale and neighborhood scale.

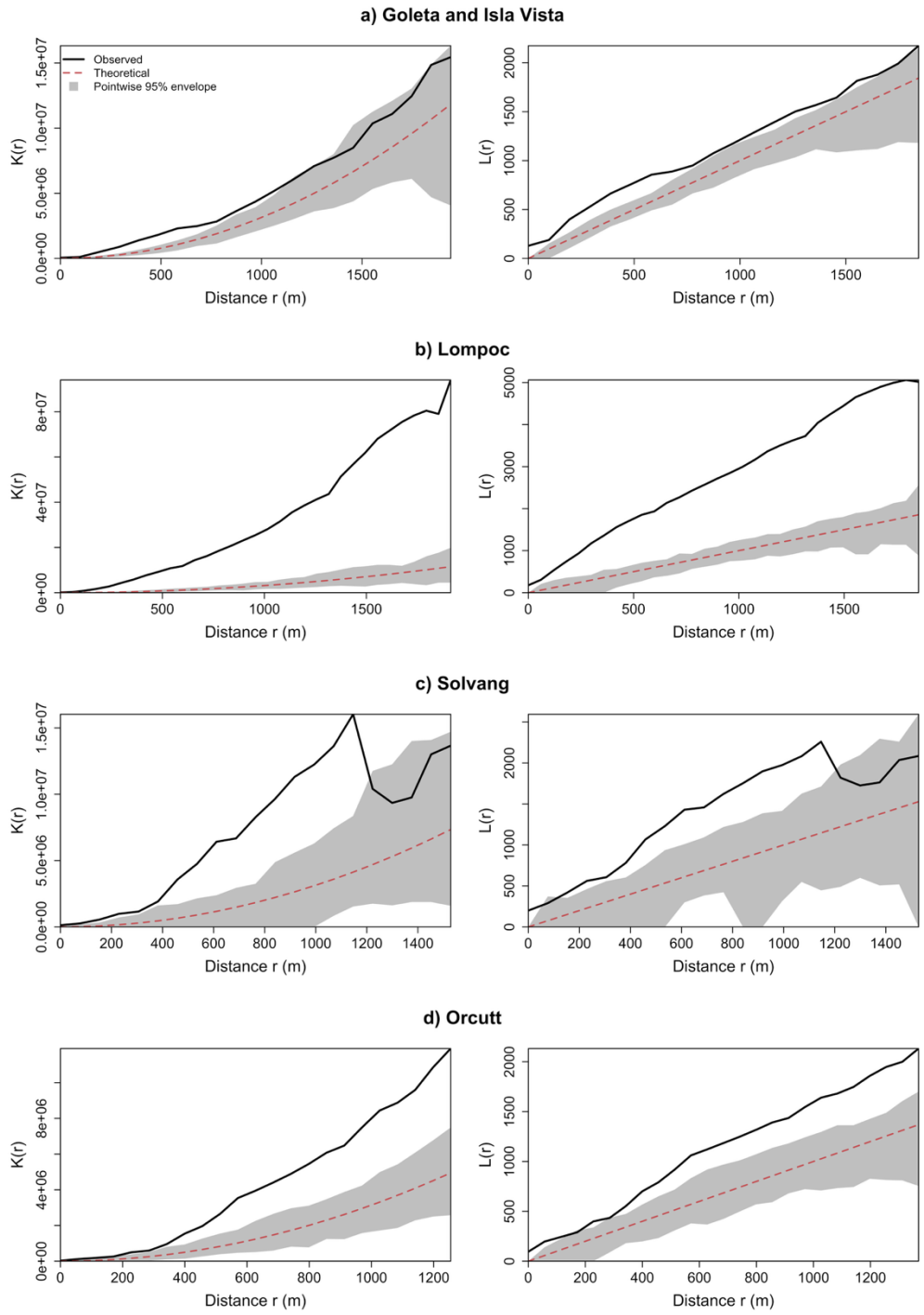


Figure 3.3. K and L functions for the subregions within the study area.

Now that the clustering of the incidents is statistically confirmed, the subsequent analyses examine whether hydrant locations are spatially associated with incidents and whether hydrant-related, demographic, and operational factors help explain incident intensity and loss

severity. Hydrants, as the first line of defense, are a mitigation tool rather than a preventive method. Figure 3.4 displays the cross-K and L functions, which consider a bivariate pattern between incident and hydrant locations to statistically test whether the locations of hydrants and incidents exhibit clustering or dispersion across space, or whether their locations are uncorrelated.

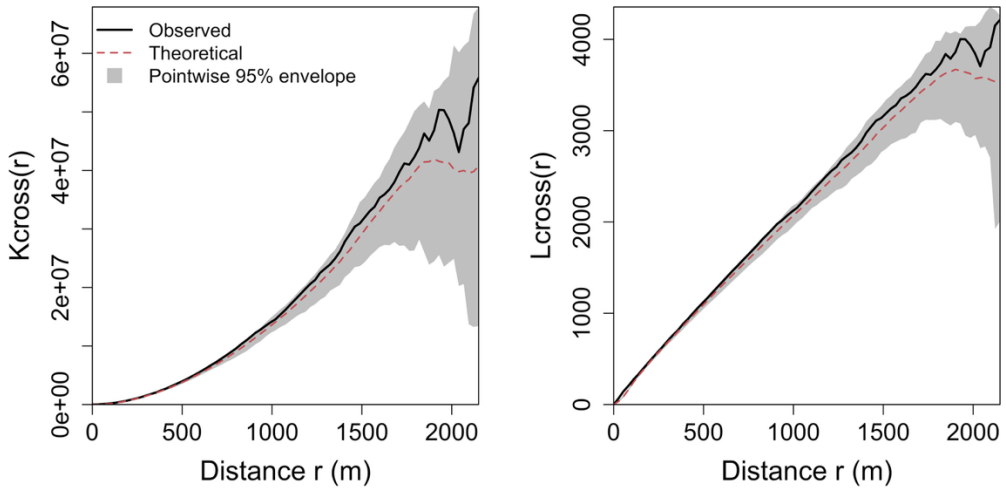


Figure 3.4. Cross K and L functions for the study region.

The cross $K(r)$ and $L(r)$ functions remain within the simulation envelope across the distance range considered, indicating no statistical evidence of departure from the baseline null model of spatial independence between incident and hydrant locations. In other words, the observed incident and hydrant point patterns do not exhibit detectable attraction or repulsion in the baseline planar analysis. This is consistent with the count models shown in Table 3.2, where hydrant covariates were not statistically significant.

Table 3.2. Negative Binomial (NB) regression models for incident intensity.

Term	Model 1 (NB)	Model 2 (NB)
Intercept	-16.963***	-17.725***
	(1.771)	(1.510)
Hydrant count	0.002	0.004
	(0.004)	(0.004)

log(Income)	-0.183 (0.144)	-0.196 (0.144)
log(House density)	0.834*** (0.048)	—
log(Pop. density)	—	0.833*** (0.047)
AIC	569.3	565.7
BIC	584.3	580.7
logLik	-279.6	-277.9
Dispersion (Pearson φ)	1.307	1.245
DHARMa KS (D, p)	0.048, 0.891	0.091, 0.170
DHARMa Disp (stat, p)	0.929, 0.784	0.946, 0.896
DHARMa Zero inf. (stat, p)	0.934, 0.768	0.917, 0.664
DHARMa Outlier (stat, p)	0.000, 0.940	1.000, 1.000
Pseudo-R^2 (McFadden)	0.188	0.193
Pseudo-R^2 (Nagelkerke)	0.588	0.598
Residual Moran's I (stat, p)	0.073, 0.066	0.135, 0.004

Standard errors in parentheses. Significance *$p < 0.05$ *, $p < 0.01$ **, $p < 0.001$ ***.*

Following the spatial point pattern analysis, regression models were estimated to assess whether hydrant infrastructure, income, and density measures (house and population) systematically explained the observed variation in incident counts at the census block group level. A Poisson GLM was first fitted but exhibited severe overdispersion (Pearson $\varphi = 3.29$), confirming that it was an inadequate baseline model. For clarity and parsimony, results from the Poisson GLM are not displayed, as subsequent models provide more reliable inference.

A suite of models was estimated with different combinations of covariates to probe the drivers of incident counts, and the two most relevant are shown in Table 3.2. Explanatory variables included hydrant count within each census block group (Hydrant count), population density (Pop. Density), housing density (House density), and median household income (Income). All density measures were expressed in logarithms to linearize elasticities, and a logarithmic area offset ensured that intensity is modeled, i.e., incidents per unit area. Model

selection relied on AIC/BIC and DHARMa residual diagnostics (uniformity and dispersion). Across specifications, density is the only strong predictor of incident intensity, i.e., house density in model 1 and population density in model 2. The two density measures are highly correlated at the census block-group level (Pearson $r = 0.973$), indicating that they capture closely related aspects of spatial concentration. Whether operationalized as housing density or population density, the density coefficient remains positive, similar in magnitude, and highly stable across the two specifications. For example, in the population density model, the coefficient is $\beta = 0.833$ statistically significant, suggesting that a 1% increase in population density is associated with a 0.83% increase in expected incident intensity, holding other factors constant. By contrast, hydrant count and income were not statistically significant in either specification. This suggests that hydrant availability, as represented here by hydrant count at the census block-group level, does not explain incident intensity once density and income are taken into account. Similarly, income does not explain where incidents occur at this spatial scale (see section 3.5), even though it may affect the economic magnitude of losses. DHARMa diagnostics indicate well-behaved residuals and no evidence of residual overdispersion in either model. Residual spatial autocorrelation was evaluated using Moran's I with queen-contiguity weights at the census block-group level. Model 1 showed weak residual spatial autocorrelation, while Model 2 retained modest positive residual spatial autocorrelation. A spatial negative binomial model was estimated as a robustness check, but it was not reported because the coefficient values and significance did not depart significantly from the models reported in Table 3.2.

Since the presence of hydrants did not seem to influence the location of incidents or their intensity, it is crucial to examine how hydrants contribute to fire damage, i.e., once an incident

occurs. Table 3.3 presents the estimates of the Gamma models with a log link, estimated as a sequence of specifications that progressively add covariates while retaining a random intercept for census block group (GEOID) to capture unobserved location-level heterogeneity. The loss-model sample includes 90 incidents ($n = 90$) for which complete positive-loss information was available. Because this complete-case loss sample is substantially smaller than the full incident dataset, the loss-model results should be interpreted cautiously. Coefficients are presented on a log scale, and all models include a random intercept. AIC and BIC were computed for each specification, along with the log-likelihood. Marginal and conditional R^2 values were obtained using the approach of Nakagawa and Schielzeth. The marginal R^2 reflects the variance explained by fixed effects alone, while the conditional R^2 accounts for fixed and random effects. The intraclass correlation coefficient (ICC) measures the proportion of total variance attributable to the random intercept. DHARMa residual diagnostics for uniformity, dispersion, and outliers, as well as quantile tests, were conducted to assess model adequacy. Models with lower AIC/BIC, higher R^2, and acceptable DHARMa diagnostics were considered to provide a better overall fit. Model 3 provides the best overall balance of fit and parsimony. However, because the fully adjusted specification includes the largest number of parameters relative to the available loss sample, bootstrap-based stability checks were applied to Model 5 to assess the robustness of its coefficients under finite-sample conditions.

Table 3.3. Gamma regressions with a log link.

$Y =$ Loss (USD); Gamma(log); $n = 90$	**Model 1**	**Model 2**	**Model 3**	**Model 4**	**Model 5**
(Intercept)	2.956 (3.151)	4.770 (3.354)	4.098 (3.215)	4.537 (3.174)	4.724 (3.385)
lh	-0.038 (0.257)	-0.243 (0.273)	-0.393 (0.259)	-0.435 (0.250)	-0.495 (0.258)

la	0.542** (0.172)	0.408** (0.182)	0.310 (0.174)	0.260 (0.170)	0.215 (0.177)
lf	-0.076 (0.350)	-0.024 (0.357)	0.202 (0.320)	0.176 (0.301)	0.233 (0.314)
lt	1.213*** (0.185)	1.228*** (0.188)	1.220*** (0.181)	1.330*** (0.187)	1.326*** (0.189)
Hyd-to-str (baseline: noncompliant)	0.001 (0.411)	—	—	—	—
Type of building (baseline: residential)					
Commercial	—	0.260 (0.636)	0.350 (0.581)	0.344 (0.546)	0.223 (0.550)
Institutional	—	1.540 (1.674)	1.529 (1.584)	1.576 (1.510)	1.990 (1.545)
Outbuilding	—	-1.317* (0.669)	-1.431* (0.633)	-1.739** (0.643)	-1.799** (0.686)
Time of the day (baseline afternoon)					
Dawn	—	—	1.454* (0.607)	1.363* (0.616)	1.463* (0.651)
Morning	—	—	0.200 (0.554)	0.303 (0.577)	0.386 (0.579)
Lunch Time	—	—	0.100 (0.726)	-0.063 (0.738)	-0.061 (0.767)
Evening	—	—	-0.952 (0.625)	-1.116 (0.667)	-0.941 (0.689)
Night	—	—	0.393 (0.554)	0.426 (0.591)	0.424 (0.596)
Day of the week (baseline Friday)					
Monday	—	—	—	-0.134 (0.792)	-0.101 (0.829)
Tuesday	—	—	—	-0.153 (0.691)	0.025 (0.688)
Wednesday	—	—	—	0.023 (0.657)	0.193 (0.656)
Thursday	—	—	—	0.510 (0.670)	0.693 (0.676)
Saturday	—	—	—	1.304 (0.762)	1.634* (0.802)
Sunday	—	—	—	-0.337 (0.734)	-0.186 (0.722)
Season of the year (baseline Winter)					
Spring	—	—	—	—	-0.373 (0.502)

Summer	—	—	—	—	0.189 (0.543)
Fall	—	—	—	—	-0.421 (0.441)
AIC	2084.9	2084.29	2080.51	2083.94	2088.17
BIC	2104.9	2109.29	2118.01	2136.43	2148.17
logLik	-1034.4	-1032.15	-1025.25	-1020.97	-1020.09
R^2 (marginal)	0.432	0.457	0.571	0.638	0.648
R^2 (conditional)	0.774	0.768	0.796	0.781	0.787
ICC (adjusted)	0.602	0.573	0.524	0.397	0.395
DHARMa KS (D, p)	0.11, 0.26	0.07, 0.72	0.08, 0.61	0.06, 0.88	0.07, 0.80
DHARMa Disp (stat, p)	1.16, 0.27	3.36, 0.14	0.79, 0.30	1.41, 0.27	2.24, 0.17
DHARMa Out (stat, p)	1.00, 0.51	0.00, 1.00	1.00, 0.51	0.00, 1.00	1.00, 0.51
DHARMa Quant (p)	0.212	0.138	0.316	0.310	0.074

Standard errors in parentheses. Significance *p < 0.05 *, p < 0.01 **, p < 0.001 ***. lh:* distance to the nearest hydrant; *la:* structure area *lf:* distance to the nearest fire station; *lt:* total suppression time; *Hyd-to-str:* hydrant to structure access.

Across the five models, total suppression time emerged as the most consistent predictor of loss severity. Once time-of-day controls were introduced, incidents beginning at dawn, relative to the afternoon baseline, were also associated with substantially higher expected losses, while outbuildings were associated with significantly lower expected losses than the residential baseline. By contrast, property area was positive in the simpler specifications but became less precisely estimated in the richer models. The coefficient for the log of total suppression time is large and highly significant in every specification, ranging from 1.213 to 1.330. In the preferred specification (Model 3), the suppression-time coefficient is 1.220, implying a strong positive association between longer operational duration and higher expected loss. This implies that a 10% increase in suppression time is associated with roughly a 12% increase in expected loss, and that doubling suppression time is associated with an expected loss about 2.3 times as large. This effect remains stable across specifications, indicating that operational duration is the most consistent correlate of loss severity once an incident occurs.

Other covariates show more limited or context-dependent associations. Distances to hydrants, to fire stations, and hydrant-to-structure access compliance are not statistically different from zero. This suggests that while hydrant networks are critical for fire response, proximity alone does not fully capture their role in explaining variation in loss magnitude once an incident is underway. To better interpret the null distance coefficients, Figure 3.5 summarizes the distribution of nearest-hydrant distances based on road-network distance. The dashed line denotes the 500 ft (152.4 m) mark. The distribution is concentrated at relatively short distances, with a median of 363.7 ft (110.9 m), an interquartile range of 213.1-543.8 ft (65.0-165.8 m), and 70.0% of incidents occurring within 500 ft of a hydrant. In addition, 42.2% of incidents occur within 300 ft (91.4 m). This range of variability can explain the inability of proximity to directly capture hydrant efficacy. Accordingly, the null coefficient is better interpreted as limited identifiability for the measured proximity proxy than as evidence that hydrant proximity is unrelated to loss severity.

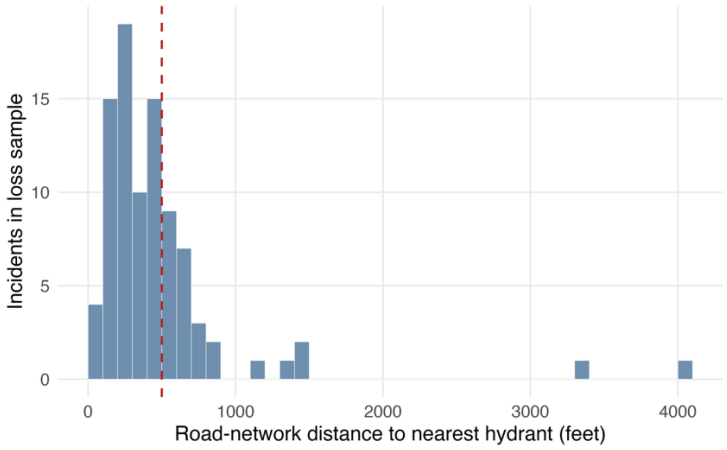


Figure 3.5. Distribution of incident-to-nearest-hydrant distance.

Time-of-day effects are more pronounced. Holding other included covariates constant, incidents beginning at dawn are associated with expected losses approximately 3.9 to 4.3 times those of afternoon incidents across Models 3-5. Regarding property type, commercial

and institutional categories are not statistically distinguishable from the residential baseline, whereas outbuildings are associated with significantly lower expected losses. This likely reflects the smaller size and lower economic value of outbuildings relative to the residential baseline.

Given the limited positive-loss sample of 90 incidents across 54 block groups, coefficient stability in the fully adjusted Gamma mixed model (Model 5) was assessed using a 500-resample nonparametric bootstrap (Table 3.4). Model 5 estimates 24 parameters, corresponding to approximately 3.75 observations per parameter, which warrants caution regarding finite-sample sensitivity. All bootstrap resamples converged, although only 109 refits (21.8%) yielded a positive-definite Hessian, indicating that the most complex specification is numerically sensitive. Among the coefficients examined, suppression duration was the most stable predictor, while property area showed moderate stability. By contrast, the distance-related coefficients were materially less stable, with wide intervals and lower sign stability. These results suggest that the fully adjusted loss model should be interpreted cautiously, with the strongest support concentrated in suppression duration and, to a lesser extent, property area. Despite the robustness of the suppression-time coefficient, it should be interpreted as an association rather than a causal effect, since more severe incidents may themselves require longer suppression. The comparatively low stability of the distance-related coefficients is consistent with the limited variability in nearest-hydrant distance within the loss-model sample. Because the observed distances are concentrated within a relatively short range, the model has limited leverage to identify a stable distance effect, making those coefficients more sensitive to sample variation.

Table 3.4. Coefficient stability assessment for Model 5.

Coefficient	Estimate	95% bootstrap CI	Sign stability

Total suppression time	1.326	[0.452, 1.948]	99.10%
Property area	0.215	[-0.103, 1.441]	91.70%
Distance to closest fire station	0.233	[-1.135, 2.209]	74.30%
Distance to closest hydrant	-0.495	[-1.849, 0.412]	85.30%

Model fit and diagnostics broadly support these conclusions. Information criteria improve as key covariates are added, with Model 3 attaining the lowest AIC among the reported specifications and thus providing the best overall balance of fit and parsimony. Models 4 and 5 add further temporal controls and preserve the main substantive pattern, namely a strong association with suppression duration, a positive dawn effect, and weak distance-related terms. The random intercept for GEOID remains empirically important throughout. The ICC declines from 0.60 in Model 1 to approximately 0.40 in the richer specifications, indicating that observed predictors explain part, but not all, of the between-place variability. Likewise, marginal R^2 increases across specifications, while conditional R^2 remains higher, showing that the GEOID random intercept continues to capture meaningful place-specific heterogeneity beyond the observed covariates.

3.5. Discussion

Several aspects require further discussion. Firstly, there are several considerations associated with modeling insights. Prevention and outreach efforts would be most effectively prioritized in dense urban areas where incident intensity is concentrated, while expectations that hydrant counts will reduce incident occurrence should be tempered. Because higher losses are strongly associated with longer suppression time, investment in measures that shorten the time needed to control a fire, such as staffing, dispatch, access, alternate water supply, pressure reliability, and operational preplans, may help reduce damage. The positive association

between dawn incidents and loss severity suggests that shifts, coverage, or alerting protocols in the early morning hours warrant closer attention.

Furthermore, there is a very important aspect in the practical implications of the results. The fact that the proxies used to measure the importance of hydrant infrastructure were not directly explanatory of the losses should be interpreted carefully. This null association should not be interpreted as evidence that hydrants are unimportant. Rather, it suggests that simple spatial availability metrics (water access to structure/proximity) may not capture the mechanisms by which water-supply systems improve outcomes. In this dataset, context reveals the nuances of these results. Within the loss-model sample ($n = 90$), hydrant coverage is already dense. The median distance from an incident to the closest hydrant is 363.7 ft (110.9 m), and 70% of the incidents occurred within 500 ft (152.4 m) of a hydrant. With such limited variation in hydrant distance, there is little statistical leverage to detect an effect, even if hydrants matter operationally. In addition, responding apparatus typically provide an immediate initial water supply from onboard tanks (often on the order of hundreds of gallons, depending on engine type), allowing crews to begin suppression while a sustained hydrant supply is established. From the dataset, there was no evidence of fire spread between units, which is consistent with a system that generally contains incidents effectively. A more informative interpretation is that hydrant systems may influence losses through mechanisms that proximity alone cannot capture, such as whether adequate flow and pressure can be delivered when needed, how reliable the system is under demand, and the operational constraints crews face in establishing a sustained water supply. System layout and the placement of water supply infrastructure have been shown to be crucial to determine whether protection requirements can be met (Raczek & Miotk, 2024). In that light, it is not surprising

that operational time is such a strong predictor in the loss models. Response and suppression durations likely reflect (among other things) how quickly a sustained water supply is secured and the incident is brought under control. Accordingly, hydrant planning remains essential for mitigation, but its benefits in this setting may be realized primarily through faster suppression and reduced escalation.

Secondly, the modifiable areal unit problem (MAUP) is a matter of further discussion for the negative binomial regressions. The spatial scale at which the socioeconomic variables were considered was the Census group level, which revealed that at this scale, population and house density were the primary factors driving incident intensity. However, at other scales, other variables can also play a significant role, and since these variables are not present at a more aggregated spatial scale, some insights might not be identified. This is also noted and discussed in previous works (Corcoran et al., 2007a), where the strength of the relationships between population characteristics and fire rate variations was dependent on the unit of analysis. For this reason, additional regressions were performed in which the space was partitioned into grids of 500 m x 500 m, 725 m x 725 m, and 1 km x 1 km. Census variables were interpolated from the census block group, and the remaining variables (related to hydrant infrastructure) were aggregated at this level. The significance of population and the number of housing units remained, and income at these levels was also significant, as shown in Table 3.5, indicating that at these spatial scales, areas with lower income are associated with higher fire incidence.

Table 3.5. Poisson models with different grid sizes.

y: Incident rate	**500 m**		**725 m**		**1000 m**	
Term	**Model 1**	**Model 2**	**Model 3**	**Model 4**	**Model 5**	**Model 6**
Hydrant spacing (m)	-0.00004	-0.00004	-0.00003	-0.00003	-0.00013	-0.00013

	(-0.00006)	(-0.00006)	(-0.00006)	(-0.00005)	(-0.00008)	(-0.00009)
log(Population)	0.478***	—	0.549***	—	0.604***	—
	(-0.056)		(-0.056)		(-0.061)	
log(Housing units)	—	0.502***	—	0.581***	—	0.637***
		(-0.059)		(-0.059)		(-0.063)
log(Income)	-0.537***	-0.539***	-0.489***	-0.512***	-0.583***	-0.610***
	(-0.128)	(-0.127)	(-0.137)	(-0.134)	(-0.137)	(-0.134)
AIC	1344.9	1344.5	1034.3	1029.8	826.7	815
Dispersion (Pearson φ)	0.885	0.884	0.996	0.988	1.227	1.195
Pseudo-R^2 (McFadden)	0.624	0.624	0.711	0.713	0.77	0.773
Sample size (N)	953	953	568	568	370	370

Standard errors in parentheses. Significance *$p < 0.05$ *, $p < 0.01$ **, $p < 0.001$ ***.*

Thirdly, it is consistent with the literature that incident intensity is associated with house and population density. Incidents are more likely to occur where residential and human activity revolve. However, other socioeconomic variables can untangle which characteristics of the population are associated with nuances of this intensity, and, in a larger sample, this can be further studied.

Fourthly, there are some aspects regarding point pattern analysis assumptions and diagnostics that need to be carefully noted. The bivariate cross-functions for incidents and hydrants were computed in the plane, whereas hydrants are constrained to street networks. Computing a linear-network cross-K (assuming that both patterns are constrained to the road network) produces the curve depicted in Figure 3.6, lying above the simulation envelope over most distances, indicating stronger incident-hydrant co-location than expected under a simple random-on-network null. However, this interpretation has important limitations. To compute the linear-network cross-K, incident locations must be projected onto the road network, even though fire incidents occur at structures rather than anywhere along the road centerlines. This suggests a new research avenue for assessing the co-location of patterns across different

spatial domains, i.e., when one pattern can occur *anywhere* in space and another is restricted to a linear network.

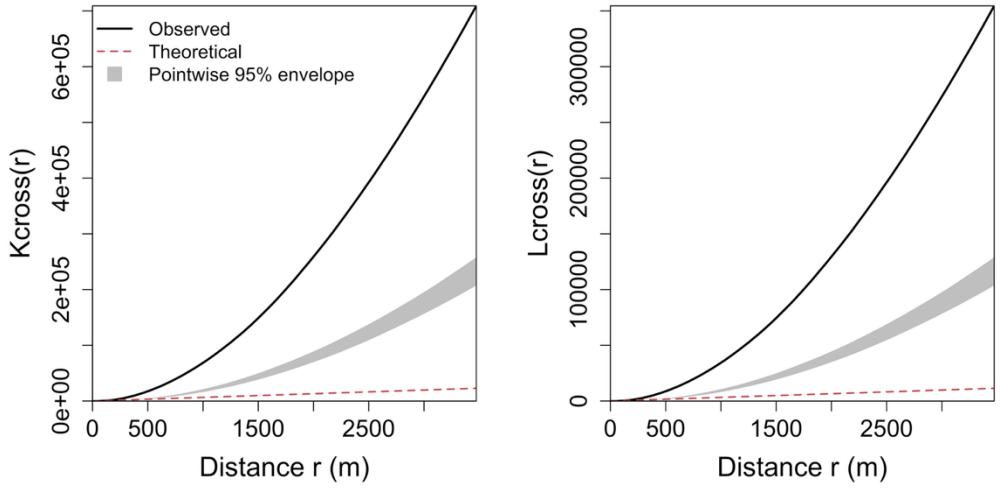


Figure 3.6. Linear-network Cross K and L functions for the study region.

Finally, several measurements introduce unavoidable uncertainty. Hydrant variables capture presence and proximity, but not flow, pressure, operability, valve size, or main diameter. These unobserved attributes likely influence performance and operational time to control a fire. Incident loss values reflect assessed or reported losses and may contain measurement error or under/over reporting. Temporal covariates (e.g., dawn) may capture detection and mobilization delays or reflect other causes of fire (fire while people were asleep, under the influence of narcotics or alcohol, etc.) rather than intrinsic fire behavior. The loss models were estimated on the subset of incidents with complete loss data, and unobserved confounding (e.g., construction materials, interior contents, wind, and weather at ignition) cannot be excluded. Also, sample sizes were limited in some subregions and for some loss categories, which constrains precision.

Notwithstanding these caveats, the main findings were consistent across analytic lenses. Incidents cluster with urban concentration, hydrant-related variables do not independently explain incident intensity at the block-group scale, and once incidents occur, higher losses are most consistently associated with longer suppression duration, with additional evidence of a dawn effect and more limited evidence for property area. These results provide an empirical basis for prioritizing density-focused prevention and mitigation focused on operational time in fire-prone urban regions.

3.6. Conclusions

Although wildfires are the primary concern for the spread of fire from wildland to urban areas in at-risk regions, they can also occur in urban settings under the right environmental conditions and spread across communities due to inherent vulnerability. This chapter shows how spatial statistical tools can help characterize where structure fires concentrate, the drivers of concentration, and which factors are most strongly associated with losses once an incident occurs, with particular attention to how hydrant infrastructure relates to these outcomes. The results suggest that incident intensity is primarily related to the concentration of people and structures, while loss severity is most consistently associated with operational duration. Property area shows a positive association in simpler loss specifications, but that relationship is less stable once richer temporal controls are added. In addition, incidents beginning near dawn are associated with substantially higher expected losses than afternoon incidents in the richer loss specifications. These findings support prioritizing prevention and outreach in high-density areas at neighborhood-relevant scales and strengthening measures associated with time-to-control, e.g., staffing, access, dispatch efficiency, and water supply reliability, especially for larger properties where potential losses are greater. Importantly, the lack of a

direct association between hydrant proximity/access measures and loss magnitude should not be interpreted as indicating that hydrants are unimportant. Instead, it is consistent with a setting where hydrant access is generally already present for most incidents, so the measured distance proxies provide limited leverage for explaining variation in loss magnitude. In that sense, the null distance effect may reflect a system that meets baseline coverage needs, while variation in losses is associated with how quickly a sustained water supply is established and the incident brought under control. Although the association between loss severity and suppression duration and exposed property scale is not unexpected, the result remains informative because it clarifies which variables carry the strongest empirical signal in the loss models after adjustment for the other covariates. Suppression duration, in particular, was the most stable predictor. However, this finding should be interpreted cautiously, as suppression duration may also reflect the incident's underlying severity or complexity. Thus, its value is less as a causal estimate than as an indicator of the operational conditions under which larger losses are observed.

Future research could extend the present framework in three directions. First, the empirical components analyzed here, namely incident concentration and conditional loss severity, could serve as building blocks for more comprehensive urban fire-risk measures that integrate observed fire patterns, defensive infrastructure, and broader exposure and vulnerability conditions. Second, preparedness and response planning merit closer attention, including the role of evacuation training and exercises as complementary risk-reduction measures. Planned procedures may not unfold as intended under real emergency conditions, and historical incident data could support comparative, including non-parametric, evaluations of alternative response and evacuation configurations. Third, from a methodological perspective, the

bivariate component could be extended to assess co-location between spatial patterns defined across different spatial domains, particularly when one process can occur throughout planar space while another is constrained to a linear network. Such extensions would help connect the present analysis of hydrant infrastructure, incident occurrence, and loss severity to broader questions of fire-risk assessment, preparedness, and the effectiveness of emergency management.

4. Strengthening Urban Defense Through Strategic Hydrant Additions

4.1. Introduction

Fire represents an ongoing threat to communities worldwide, driven by diverse causes. Regardless of the origin, the primary concerns after ignition are potential for fire spread and resulting losses of life and property. These concerns are particularly critical in regions prone to wildfires, especially at the wildland-urban interface (WUI). Ignitions originating in wildland fuels can transition into urban conflagrations. Additionally, structure fires too can escalate into conflagration, where strong winds can intensify flames and carry embers significant distances (Filkov et al., 2023). Recent catastrophic events have highlighted this vulnerability. The Lahaina Fire in 2023 (Maui, Hawaii) quickly spread through the community, resulting in over 100 casualties, destroyed more than 2,200 structures and displaced thousands, with lasting economic impacts (Baker, Browning, et al., 2023; Baker, Khurana, et al., 2023). Similarly, the 2017 Tubbs Fire destroyed the Coffey Park neighborhood (Santa Rosa, California), with 22 fatalities and more than 5,600 structures lost. More recently, the 2025 Palisades and Eaton fires in Los Angeles County, California, destroyed 16,251 structures and damaged 2,047 more, with 31 fatalities (CAL FIRE, 2025a). Similarities across these tragedies is proximity to the WUI, drought stressed vegetation and extreme fire weather conditions. Communities in urbanized areas adjacent to wildlands face greater risk when climate, environment and human factors combine. Notably, this combination has contributed to the increasing intensity and severity of California wildfires in recent years. Indeed, 14 of the state's 20 most destructive fires have occurred within the last ten years (CAL FIRE, 2025b). While wildfires can spread into urban settings, structure fires remain a persistent concern. In the United States, the U.S. Fire Administration estimated

344,600 residential building fires in 2023, resulting in 2,890 deaths, 10,250 injuries, and approximately $11 billion in property losses (U.S. Fire Administration, 2024). Historically significant urban fires, such as the London Fire of 1666 and the Great Chicago Fire in 1871 witnessing thousands of lost structures and hundreds of casualties (Chhetri et al., 2018; Garrioch, 2016), demonstrate that uncontrolled fire can spread aggressively.

Hydrants have emerged as critical infrastructure in response to past devastating urban fires, serving as the primary point of access to a municipal water supply for suppression operations (Wyss & Burns, 1958; Figueroa et al., 2024). Their significance in safeguarding lives, structures, and property has led to the development of systematic placement standards. Such standards encode spatial expectations (distances, service areas, and coverage) that reflect how cities are planned and how fire protection has evolved as a public service (Murray et al., 2025). In fire-prone regions, these spatial requirements are even more consequential, as response systems must operate under high-hazard conditions amid growing exposure at the WUI (Murray et al., 2023). Hydrant spacing standards serve as a key guideline, reflecting operational capabilities of firefighting equipment, including firehose connections from hydrants to engines and from engines to structures (King, 1926; California Fire Code, 2022; Montecito Fire Department, 2022; International Code Council, 2024). In California, these standards are not uniform. The California Fire Code (2022) regulates hydrant location and spacing based on building characteristics, including construction materials, structure size, and suppression features such as sprinklers. For example, a residential building of less than 3,600 ft^2 (335 m^2) constructed with Type V-B materials (wood walls and frames) requires hydrant spacing of no more than 500 ft (152 m) whereas a commercial building of less than 50,000 ft^2 (4,645 m^2) equipped with sprinklers and fire-resilient construction (e.g., Type A-I enhanced

or Type I-B basic) requires spacing of no more than 750 ft (229 m). In areas with less development, hydrants must be spaced every 1,000 ft (305 m) to address transportation-related hazards.

Spacing provisions are also linked to water main hydraulic performance. Code guidelines are intended not only to support coverage but also avoid pressure drops that can limit effective water flow during suppression operations (Kaufman & Rosencrants, 2015).

At the local scale, jurisdictions may further amend or refine state standards to reflect regional conditions and development patterns. In coastal Santa Barbara County, regional regulations generally follow the state baseline but modify requirements in specific contexts. For instance, Montecito requires hydrants near structures not exceeding 3,600 ft² (335 m²) to be spaced at no more than 300 ft (91 m) in commercial zones, while spacing in residential areas remains at 500 ft (152 m) (Montecito Fire Department, 2022). In addition to spacing requirements, the code also specifies "frontage" access criteria, defining coverage as the maximum allowable distance from any point along a street frontage (i.e., the portion of the street directly in front of a property) to its nearest hydrant. This coverage distance is often half of the mandated spacing standard (see Table C102 in California Fire Code, 2022).

The reality is that not all street frontages are covered, nor are all areas in compliance with stipulated maximum spacing. Figueroa et al. (2024) identified portions of the street network in Santa Barbara that do not comply hydrant spacing standards, representing areas of increased potential vulnerability. This noncompliance is nuanced because not all areas face the same level of fire risk exposure. For instance, certain neighborhoods only slightly exceed mandated standards and fire spread is unlikely, whereas others exhibit significant noncompliance in spacing limits and are at high risk of fire. Heffernan et al. (2026) found that fire incident

frequency in Santa Barbara is strongly related to local conditions, with higher frequency associated with housing and population density and greater losses associated with longer suppression times. Areas noncompliant with hydrant spacing and/or coverage standards therefore represent increased vulnerability to fire spread, making hydrant infrastructure upgrades and extension a priority.

Hydrant coverage and spacing are often conflated, even though they are distinct codes that correspond to very different spatial concepts (Figueroa et al., 2024). Coverage is often interpreted as a service area from a hydrant, but code mandates define coverage in terms of the maximum allowable distance from street frontage to the nearest hydrant. This chapter adopts this code-based interpretation of coverage. Despite progress in hydrant diagnostics, jurisdictions still face a critical planning question: once gaps in service and spacing are identified, where should new hydrants be located to achieve compliance? This research proposes a framework to strategically site hydrants along a road network in order to improve frontage coverage while accounting for tradeoffs in spacing compliance. This is accomplished by conceptualizing hydrant siting as a continuous maximal covering location problem along the street network, drawing on covering-model theory and continuous/network extensions (see Wei et al., 2014, Wei & Murray, 2015; Wei, 2016; Church & Murray, 2018). The remainder of this chapter is organized as follows. Section 4.2 reviews relevant background. Section 4.3 presents an optimization model for strategic hydrant siting. Section 4.4 reports application results for a coastal community in Santa Barbara County. Section 4.5 discusses planning implications, limitations, and directions for future work. Finally, section 4.6 offers concluding remarks.

4.2. Background

The question of where fire hydrants should be placed has long been a concern in urban planning in order to ensure protection, safety and security of people and property. Hydrant placement must provide adequate protection for structures and property, a need especially acute in densely populated urban areas (Corcoran et al., 2007a; Heffernan et al., 2026). Much of the existing literature has therefore focused on using spatial analytical methods to disclose, map, or diagnose service gaps. GIS frameworks are commonly used to assess hydrant access. For example, Raškauskaite & Grigonis (2019) present a structured approach for mapping hydrant accessibility and delineating unprotected territories. Other studies demonstrate that accessibility should be evaluated along the street network rather than estimated using Euclidean distance, as this can reveal areas with limited coverage (Lee et al., 2021) and identify noncompliant street segments in terms of average spacing at the hydrant, neighborhood, and regional levels (Figueroa et al., 2024). Okon & Njoku (2018) evaluate hydrant adequacy relative to standards, observing deficiencies that further motivate system improvements. Indirectly, GIS has also been utilized for hydrant placement by supporting the assessment of building conditions and urban form to produce spatial fire risk surfaces (Abrar et al., 2024; Ferreira et al., 2016; Ji et al., 2010), offering mitigation guidance (Pratiwi et al., 2024). More recent studies extend this line of work by using machine learning to predict fire severity for resource allocation, incorporating GIS-derived variables such as proximity to stations/hydrants and neighborhood characteristics (Lee et al., 2025). This body of work has focused on diagnosing inadequate service rather than prescribing how to mitigate vulnerabilities.

A smaller body of research has examined hydrant placement more directly using optimization, yet existing approaches differ substantially in how space is represented, how service demand is derived, and what performance standards are considered. Genetic algorithm heuristics have been used to identify candidate hydrant network configurations to reduce average distance to hydrants, intended to improve emergency access (Esquivel-Saldaña et al., 2021). Other work highlights that Euclidean distance is often not well suited for hydrant planning in complex urban settings and proposes alternative spatial metrics that better capture access around buildings (Kalach et al., 2020). Optimization approaches have been applied in other related contexts, including hydrant placement for ship design (Gomułka, 2023) and irrigation systems where hydrant-like outlets are located using integer programming with network shortest-path distances relied upon (González Villa & García Prats, 2012; González-Pavón et al., 2025). Additional studies involve hydrant selection from an existing set to mitigate fire in real time (Nerantzis & Stoianov, 2023), identify hydrants for flow testing to improve calibration (Wu & Song, 2014), and select hydrants to flush in order to reduce contamination risks (Shoorangiz et al., 2023; Alnajim & Abokifa, 2025;).

Hydrant placement is constrained by locational factors as well as technical and engineering considerations. Terrain, pressure, flow, and the underlying water distribution system all influence whether a hydrant can provide adequate service. A hydrant system is expected to deliver adequate flow while limiting pressure losses under periods of demand, which is why standards and engineering guidance relate hydrant effectiveness to hydraulic performance (Wyss & Burns, 1958). As a result, the ability to meet spacing and access requirements can be constrained by the underlying water distribution system and pressure/flow behavior during extreme demand conditions (Kanta & Brumbelow, 2013). This

association is important for planning because it shows that adding hydrants is not always straightforward. Location of hydrants is also constrained by spatial features, including not closer than 3 ft to driveways, trees, streetlights, signs or other obstructions (Ventura County Fire Protection District, 2011). Candidate locations must ultimately be evaluated against feasibility considerations.

Overall, research that treats hydrant network configuration and structure as a geographic planning problem remains narrow. Existing studies have contributed methods for diagnosing hydrant access, assessing spacing deficiencies, evaluating fire-risk surfaces, and placement using heuristics. These approaches do not, however, directly address street frontage coverage to a hydrant nor budgetary considerations. No methods have yet been developed and applied to support integrated hydrant coverage and spacing compliance. This research addresses these gaps for reducing noncompliance of fire hydrant coverage and spacing. Covering models provide a natural framework for hydrant planning because they formalize distance-based service requirements when only a limited number of facilities can be added. The classic covering family, including set covering and maximal covering, has a long history in spatial analysis and emergency service provision. They are well suited to evaluate and achieve code standards (Church & Murray, 2018). For hydrant planning, however, the key challenge is that feasible locations are not arbitrary points in space. Hydrants exist along streets in the public right-of-way, making candidate location continuous along road-network arcs. Continuous and network-based coverage research shows that discretizing a continuous problem can introduce representation error and that candidate site generation can affect coverage outcomes (Wei, 2016; Wei & Murray, 2015), so significant attention must be paid to this issue. Work on continuous arc covering directly addresses this issue by allowing facilities to be located

anywhere along network arcs and by providing approaches that reduce or eliminate representation error (Wei et al., 2014). These advances support framing hydrant siting as a continuous, road-constrained covering problem and provide a foundation for explicitly connecting code-based requirements to network-based placement decisions.

4.3. Methods

A broad set of spatial analytic tools has been developed to guide infrastructure siting, with spatial optimization and location analytics being at the heart of these approaches relied upon to support the design, maintenance and extension of service systems. Overviews of related methods can be found in ReVelle and Eiselt (2005) and Murray (2020). In this chapter, spatial optimization is used to identify strategic locations for siting new hydrants with the intent of most reducing coverage and spacing noncompliance. Spatial optimization and geographic information systems (GIS) can be used in tandem to support associated decision making, but hydrant additions are not straightforward as several factors must be considered. First, hydrant placement is restricted to the road network, and theoretically hydrants can be placed anywhere along approved street segments. This makes the problem continuous in nature. Second, there is generally a budget constraint, meaning that only a limited number of new hydrants can be sited. Third, frontage access (coverage) and average spacing are part of fire code guidelines, requiring an integrated assessment process. Lastly, housing and population density correlate highly with fire incidents (Heffernan et al., 2026), suggesting that hydrant prioritization should reflect spatial variation in exposure. Given these considerations, the continuous space maximal covering location problem (CSMCLP) provides a foundation for hydrant siting on a road network as it accounts for different demand weights, budgetary limitations and coverage and spacing compliance in accordance with code guidelines. The maximal covering location

problem (MCLP) first introduced by Church and ReVelle (1974) is a logical beginning. It is discrete in nature with the aim to site a predefined number of facilities in order to maximize service coverage. Potential facility sites are identified in advance as is the coverage standard. Consider the following notation:

I: set of demand points (indexed by i).

J: set of potential (hydrant) locations (indexed by j)

a_i: demand associated with demand i.

d_{ij}: distance between demand i and location j.

S: service access (or coverage) standard.

$\Omega_i = \{j \in J | d_{ij} \leq S\}$.

Decision variables:

$y_i = 1$ if demand point i is covered by a sited hydrant, and 0 otherwise.

$x_j = 1$ if potential location j is selected for hydrant placement, and 0 otherwise.

In the hydrant access context, the demand are the structures (and population) to be served, potential locations are sites for hydrant placement and the service standard is the spacing and/or frontage code requirement of hydrants. Based on this notation, the discrete version of the MCLP can be structured.

$$\text{Max} \sum_{i \in I} a_i y_i \qquad (4.1)$$

Subject to

$$\sum_{j \in \Omega_i} x_j \geq y_i, \quad \forall i \qquad (4.2)$$

$$\sum_{j} x_j = p \qquad (4.3)$$

$$x_j = \{0,\ 1\}\ \forall j\ , y_i = \{0,\ 1\}\ \forall i \qquad (4.4)$$

The objective (4.1) seeks to maximize the coverage of demand to the greatest extent. Constraints (4.2) ensure that demand can only be counted as covered if at least one selected facility lies within the service standard. Constraint (4.3) stipulates that only p facilities (hydrants) are to be selected, enforcing the budget on facilities sited. Constraints (4.4) impose binary restrictions on decision variables.

The MCLP, (4.1)-(4.4), formalizes a common planning problem, seeking to strategically locate a limited number of facilities that provide coverage, according to a service standard, to the greatest possible demand. As structured, (4.1)-(4.4) represents the case where potential locations for new hydrants are discrete and identified in advance. Demand in the hydrant siting context is interpreted as the portions of the road network containing structures that are not served (noncompliant) by the existing hydrant system. The parameter p represents a budget, limiting the number of sited hydrants based on budgetary constraints in terms of average installation cost.

To address the continuous nature of allowing facilities to be placed anywhere in space, implying an infinite number of potential locations, extension of the MCLP is necessary. In the

context of hydrant siting, potential locations and demand are not discrete because the road network comprises an infinite number of points where hydrants can be placed, and there are also infinite points that need to be covered. Church (1984) suggested an approach for addressing continuous space siting, with subsequent work by Murray and Tong (2007) and Wei and Murray (2015). A review may be found in Church and Murray (2018). Consider the following additional notation:

Φ: road network.

K = set of facility locations.

k = index of facility locations.

$w(g)$: weight associated with demand location g.

$\mathbb{1}(\cdot)$: indicator function for binary coverage within standard S.

d_{kg}: distance between location k and demand point g (network distance).

Relying on this notation, the continuous variant of the MCLP can be formulated as:

$$\max_{K,|K|=p} \int_{\Phi} w(g)\ \mathbb{1}\left(\min_{\mathrm{k}\in\mathrm{K}} d_{\mathrm{kg}} \leq S\right) \mathrm{dg} \quad (4.5)$$

This continuous formulation maximizes coverage when demand is distributed along a one-dimensional object, the road network street segments. Objective (4.5) is equivalent to integrating demand density over the union of facility service areas intersected with the demand region, as specified in Wei & Murray (2015). In practice, Objective (4.5) cannot be solved directly in its continuous form because the set of potential facility locations is infinite.

For network-based demand, Church and Meadows (1977) introduced the network intersect point set (NIPS) as a finite candidate set for unrestricted facility siting along network arcs under maximum service-distance criteria. Church (1984) later introduced a finite dominating set (FDS) for transforming the planar (continuous) MCLP into the discrete MCLP, (4.1)-(4.4), while ensuring that the optimality of (4.5) is maintained. He introduced the circle intersection point set (CIPS), proving that it contains an optimal solution to (4.5) when demand is represented as discrete points. To accommodate other demand representations, such as line or polygon-based demand, Murray and Tong (2007) extended this approach, referred to as the polygon intersection point set (PIPS). After discretizing the problem, the MCLP, (4.1)-(4.4), can solve the continuous extension reflected in (4.5). Demand associated with hydrant siting is a discrete set of arcs, i.e., I is the collection of uncovered road segments, and a_i is the associated weight for those road segments. Issues of spatial representation are considered in Wei (2016).

The above discussion suggests that the continuous siting problem in (4.5) can actually be solved as a discrete variant of the MCLP, (4.1)-(4.4), with potential facilities sites being a FDS, namely PIPS, CIPS, or NIPS, depending on demand representation. To address hydrant coverage and spacing, demand in objective (4.1) takes two forms: (i) prioritizing added protection where structures are present and (ii) prioritizing the reduction of noncompliant average spacing, i.e., covering the spacing gaps, consistent with spacing guidelines. As a result, objective (4.1) becomes the following multiple objectives:

$$\text{Max} \sum_{i \in I} \beta_i \, y_i \qquad (4.6)$$

$$\text{Max} \sum_{i \in I} \delta_i y_i \qquad (4.7)$$

where β_i and δ_i represent structure counts and spacing vulnerability, respectively. With two objectives, instead of finding a single optimal solution for each instance of p, trade-off solutions now result given a compromise of one objective against the other. These trade-offs form a Pareto frontier. Cohon (1978) discusses different approaches to solving multi-objective problems in order to find the solutions that constitute the Pareto solution set. One approach is the ε-constraint method, which is often preferred because of nonconvexities arising from integer requirements. In this case, objective (4.7) is considered a constraint in the following way:

$$\sum_{i \in I} \delta_i y_i \geq \varepsilon \qquad (4.8)$$

By varying ε and solving each unique problem instance, the model produces a set of nondominated solutions that makes the trade-off between two objectives explicit. Here, ε is varied across a range, the lower value obtained when primarily considering objective (4.7) and the higher when objective (4.6) is considered.

Central to applying (4.6) subject to (4.2)-(4.4) and (4.8) is the ability to derive the FDS (finite dominating set). This candidate construction follows the NIPS logic (see Church and Meadows, 1977, 1979). GIS is crucial because it allows continuously distributed demand to be represented as discrete objects, i.e., points, lines, or polygons. Discrete demand objects enable the derivation of discrete potential facility locations that adequately represent continuous space (see Church and Murray, 2018). Murray and Tong (2007) outline a general process for identifying a FDS, involving three steps: (i) identifying the demand objects that

need to be covered, (ii) deriving covering boundaries around these demand objects, and (iii) finding the intersection points of the overlapping covering boundaries, where these resulting points represent the FDS. Figure 4.1 illustrates the process to obtain an FDS.

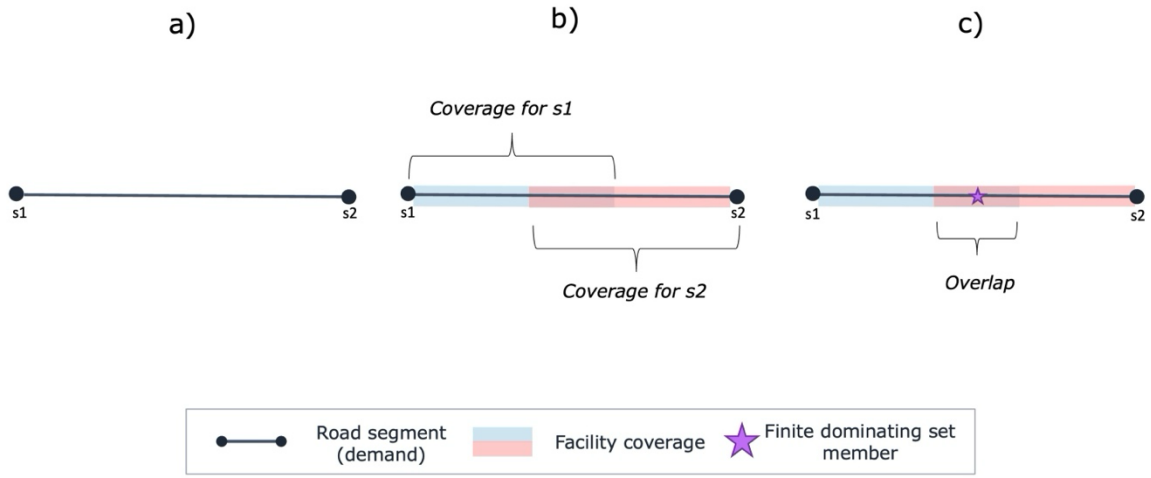


Figure 4.1. Steps to derive an FDS. a) Identify demand objects. b) Derive a service standard. c) Determine the FDS members based on the overlapping area of the service standard buffers.

Figure 4.1a illustrates the identification of spatial objects representing demand, where the nodes of the segment are labeled as $s1$and $s2$. Figure 4.1b shows the coverage area for the segment, with buffers generated from $s1$and $s2$ using road-network distance. Finally, Figure 4.1c depicts the FDS derivation. In the example, a candidate is derived from the center point of the overlap between these coverage buffers. Any point within the overlapping area would cover both nodes, thus at least one point of this overlapping area would be sufficient to be a member of the FDS. The resulting FDS therefore represents the set of potential candidate locations. Once demand and candidate locations are discretized, the MCLP formulated in (4.6), (4.2)-(4.4), and (4.8) can be solved computationally.

4.4. Application results

Montecito Fire Protection District in coastal Santa Barbara County, California, depicted in Figure 4.2, was interested in exploring hydrant spacing and coverage noncompliance issues in their community. Montecito is situated along Pacific Ocean at the base of the Santa Ynez Mountains. This area is within and surrounded by the WUI, best characterized as fire-prone and subject to strong downslope wind events (e.g., Sundowners). Seasonal vegetation dryness, drought, climate change, etc. make fire spread a serious issue and complicate suppression efforts (Murray et al., 2021; Filkov et al., 2023). Efforts to more completely understand fire related vulnerabilities in Montecito are therefore critical, necessitating the evaluation hydrant service deficiencies and developing strategies for hydrant investment prioritization under code-driven safety standards.

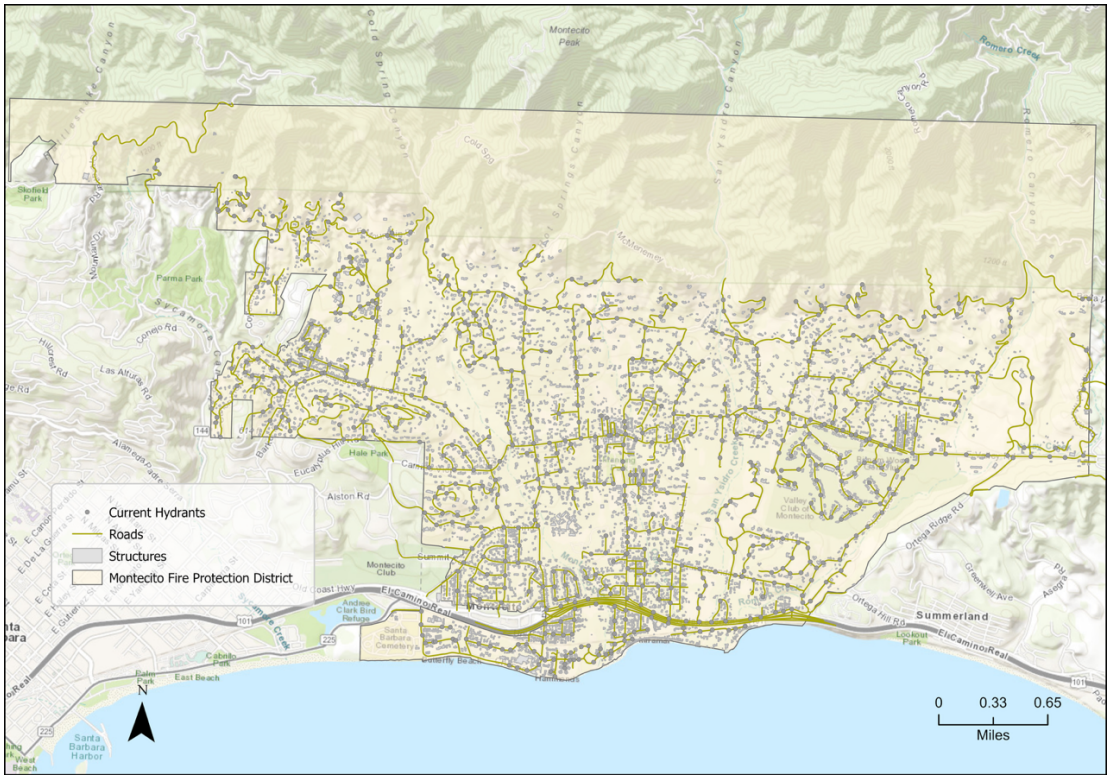


Figure 4.2. Hydrant distribution in Montecito.

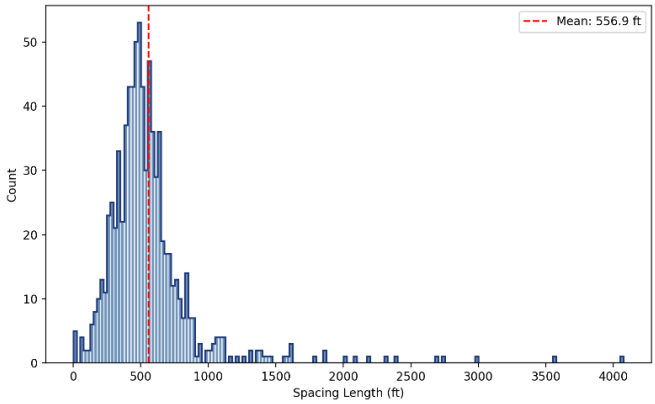
The data used for the analysis include road centerlines and hydrant locations, both provided by Santa Barbara County, and building footprints greater than 450 square ft in size, obtained from the USA Structures dataset through FEMA (Federal Emergency Management Agency et al., 2024). The boundary of Montecito Fire Protection District was relied upon, available from Santa Barbara County Fire and Conservation Biology Institute (2021). Analysis, modeling, and mapping were carried out using Python. All spatial layers were projected to a common coordinate reference system (EPSG:2229; U.S. feet). The road network totals approximately 96.18 mi (154.78 km) and includes 723 existing hydrants.

The specification of β_i and δ_i associated with structure counts and spacing vulnerability were derived as follows. Exposure associated with built development was based on structures projected to the road network (accounting for frontage). In this case, structures were linked to the road network via spatial projection within a fixed tolerance of 250 ft (76.2 m). The demand set I then is limited to only uncovered road segments, with β_i indicating the number of associated structures. Of the 4,695 in the study region, 1,448 (30.84%) were not within the mandated distance standard of 250 ft to a hydrant. Average hydrant spacing that exceeds 500 ft is noncompliant. Distances outside the middle range (below the 25th percentile or above the 75th percentile) were assigned priority weights of 1, while distances within the middle range are assigned linearly increasing weights from 1 to 100:

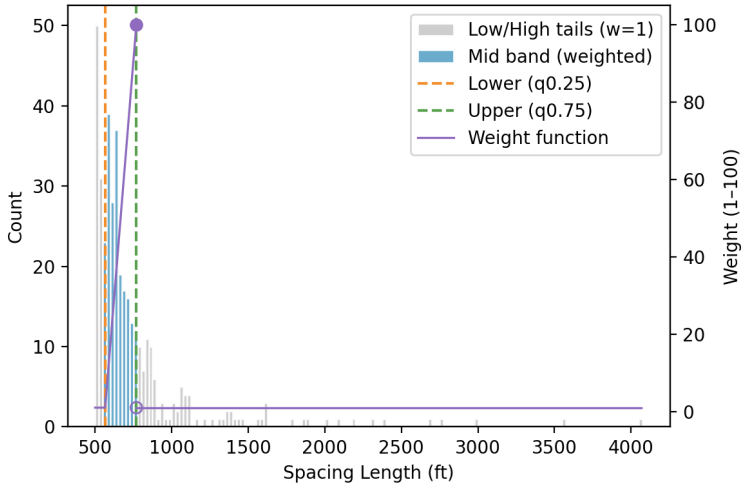
$$\delta_i = \begin{cases} 1 + 99 * \dfrac{l - q_{0.25}}{q_{0.75} - q_{0.25}}, & \text{if } q_{0.25} \le l \le q_{0.75} \\ 1, & \text{otherwise} \end{cases} \qquad (4.9)$$

where l is the length of the spacing path above the standard, and $q_{0.5}$ and $q_{0.75}$ are the 25th and 75th percentiles, respectively.

Under the baseline configuration, spacing diagnostics with a standard of 500 ft (152.4 m) show substantial noncompliance. For the region, 808 spacing paths were derived, and out of these, 403 are compliant, resulting in a compliance rate of 49.9%. The average spacing of the region is 556.9 ft, while the maximum spacing across all the paths is 4,067.4 ft. The distribution of the spacing paths is shown in Figure 4.3a. This distribution is clearly right skewed, with spacing paths clustering near the standard, while a smaller number of extreme gaps form a long tail. Given that the spacing weight is constructed from the noncompliant spacing paths, Figure 4.3b shows the resulting weighting scheme.



a) Baseline spacing path distribution



b) Weighting scheme for the paths out of compliance

Figure 4.3. Spacing distribution in the study region and weighting scheme.

Existing hydrants cover 66.7% of the road network under the adopted service-distance standard of 250 ft (76.2 m). Figure 4.4 depicts the spatial baseline conditions for both coverage and spacing. The spacing paths show the direct relation of hydrants where the standard is not compliant. These baseline conditions serve as a reference point for interpreting improvements as the hydrant budget increases. Although baseline road-network coverage is incomplete, not every road segment has the same level of exposure or potential benefit from added hydrant access. In particular, code-based frontage guidance is most consequential where streets front structures and people, rather than along segments with little or no adjacent development. In parallel, spacing remains a separate compliance objective. Even where frontage coverage can be improved, hydrant spacing is an independent code concept and a practical guideline that jurisdictions are expected to meet. For these reasons, the demand definitions used in this chapter serve to reflect how hydrant investments are typically prioritized in practice.

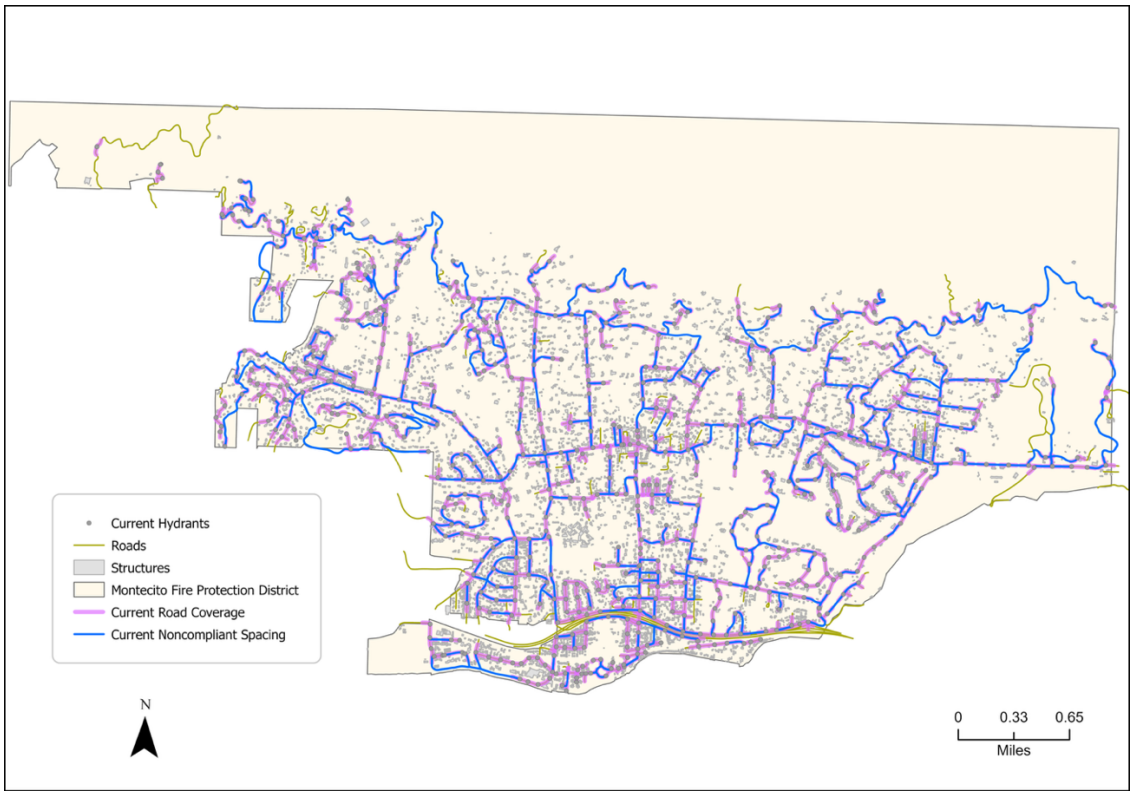


Figure 4.4. Spatial baseline conditions: coverage and noncompliant spacing paths.

Since the discrete representation of demand has the potential to affect any devised result, the discretization of demand, as discussed in section 4.3, must be sufficiently detailed. The idea is to split the road segments strategically to keep the problem size manageable. As mentioned previously, candidate locations (set J) are derived by finding a FDS based on road-network distance. Figure 4.1 illustrated this process, where at least one point in the overlapping service areas can serve as members of the FDS. In this application, endpoints of overlap intervals were used. Any point in the overlapping region provides natural candidate sites because a hydrant placed at such locations can simultaneously cover multiple uncovered segments. These candidate points are inserted into the network by splitting edges at candidate locations, ensuring that candidates remain constrained to road geometry and that coverage can be evaluated using network distance.

The FDS included 7,394 potential locations. To keep the problem size manageable, it was crucial to split the road network strategically, and such process involved several steps. First, existing hydrants were added to the network as nodes by splitting road segments at hydrant locations, resulting in a graph with 1,422 segments. After splitting edges at the baseline service boundary and discretizing only the uncovered road portions into segments no longer than 50 ft, the demand graph contained 5,583 segments. The FDS was then calculated and added to the graph as nodes. Once the candidate locations from the FDS were inserted, the total number of edges in the final graph was increased to 8,625 segments. After baseline coverage was evaluated, the remaining uncovered portion of the network formed the demand surface for optimization. This uncovered set consisted of 6,889 segments. The final demand length

averaged 25.7 ft with a standard deviation of 10.24 ft, a minimum length of 0.18 ft and a maximum of 50.28 ft.

All problem instances were solved using Gurobi (13.0.0) on a MacBook Pro M2 laptop with 16 GB memory. Table 4.1 summarizes the MCLP for the bi-objective spatial optimization formulation under different budget scenarios (p hydrant additions ranging from 1 to 20). The model considered 7,394 potential locations (FDS) and contained 6,890 rows (constraints), and 14,283 columns (decision variables). It solved to optimality in less than one second in all cases. For each scenario, the table reports the number of nondominated solutions found, the best structure-based objective, the best structure coverage evaluating the solution associated with the best structure-based objective, the best spacing-based objective, the best spacing coverage evaluating the best spacing-based solution, the average solution time, and the ε step used to generate the tradeoff set. In total, for each scenario of p, 100 model instances were generated.

Table 4.1. Summary of bi-objective results for different hydrant addition scenarios

p	Nondominated solutions	Best structure-based objective	Best structure coverage† (%)	Best spacing-based objective	Best spacing coverage‡ (%)	Average solution time (s)	Step (ε)
1	6	31	2.14	3,321.17	2.43	0.38	33.55
3	22	66	4.56	7,962.38	5.82	0.22	80.43
5	40	98	6.77	12,157.69	8.88	0.22	122.8
7	49	130	8.98	16,072.41	11.75	0.23	162.35
9	55	159	10.98	19,704.85	14.4	0.24	199.04
10	57	173	11.95	21,382.28	15.63	0.23	215.98
11	60	187	12.91	23,059.35	16.85	0.24	232.92
13	63	213	14.71	2,6271	19.2	0.24	265.36
15	65	237	16.37	29,461.97	21.53	0.23	297.6
17	66	261	18.02	32,545.24	23.78	0.23	328.74
20	65	294	20.3	36,881.3	26.95	0.21	372.54

†Computed evaluating best structure-based solution geographically. ‡Computed evaluating best spacing-based solution geographically.

Each planning scenario presented in Table 4.1 can be interpreted. For instance, for $p = 20$, of the 100 generated solutions with a ε step of 372.54, only 65 are unique and optimal in the Pareto sense. Among these, the best structure-based objective, i.e., the solution that totally favors the coverage for structures, shows that 294 structures can be covered, which represents 20.3% of the required structure coverage. The solution that mainly focuses on improving average spacing shows that adding 20 hydrants would contribute to covering the 26.95% of vulnerable areas that need improved spacing. On average, all the solutions for this scenario were found in 0.21 seconds. Since each scenario encompasses a set of solutions, these can be visualized in terms of the corresponding tradeoff solution identified. For example, again looking into the bi-objective results for p=20 scenario, there is a clear tradeoff between improving structure coverage and improving spacing coverage. Figure 4.5 shows the Pareto curve for the 65 unique solutions identified, where these 65 nondominated solutions reveal the tradeoff between both objectives. Each solution in Figure 4.5 has a distinct associated spatial configuration. As structure coverage increases, spacing coverage declines, meaning that improvements in one objective has implications for the other objective. The two highlighted solutions illustrate this well. The star-designated solution sits near the middle bend of the frontier, at roughly 15% structure coverage and 21% spacing coverage, and therefore represents a more balanced compromise. By contrast, the diamond-designated solution shifts toward stronger structure protection, reaching 18% structure coverage, but spacing coverage drops to roughly 13%. In practical terms, this means that gaining a few additional percentage points of structure protection requires giving up a more noticeable amount of spacing performance.

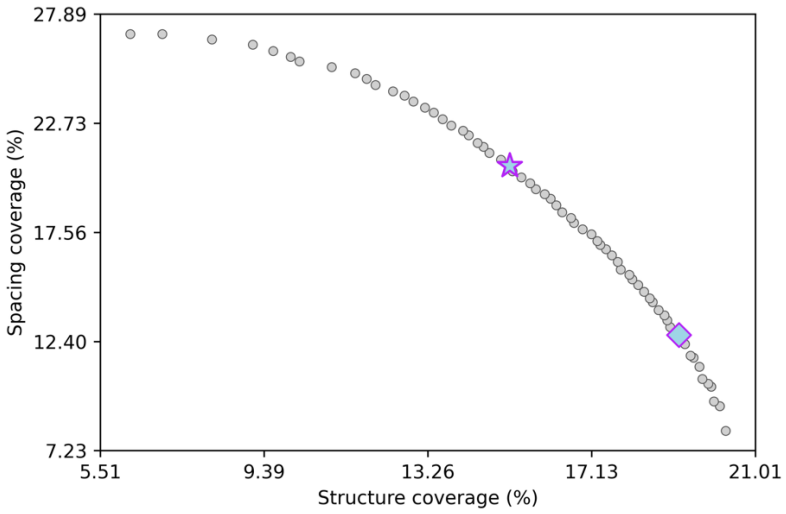


Figure 4.5. Pareto frontier for the 20-hydrant addition scenario.

As each solution is distinct, the star-designated solution in Figure 4.5 is shown spatially in Figure 4.6, and similarly the diamond-designated solution is presented in Figure 4.7. Several recommended locations occur in similar corridors across both solutions, especially in the southern and central portions of Montecito, suggesting that some hydrant additions remain high priority regardless of the planning emphasis. At the same time, the star-designated solution spreads more locations toward the periphery, where spacing deficiencies remain more consequential, while the diamond-designated solution is more concentrated in the denser built environment and along the southern corridor, where added frontage protection benefits more structures. This contrast reflects different allocation of 20 hydrants with the same average budget. In this way, the associated maps complement Table 4.1 by showing that the tradeoffs are geographic, changing how the benefits of new hydrant infrastructure are distributed across the community depending on the planning scenario.

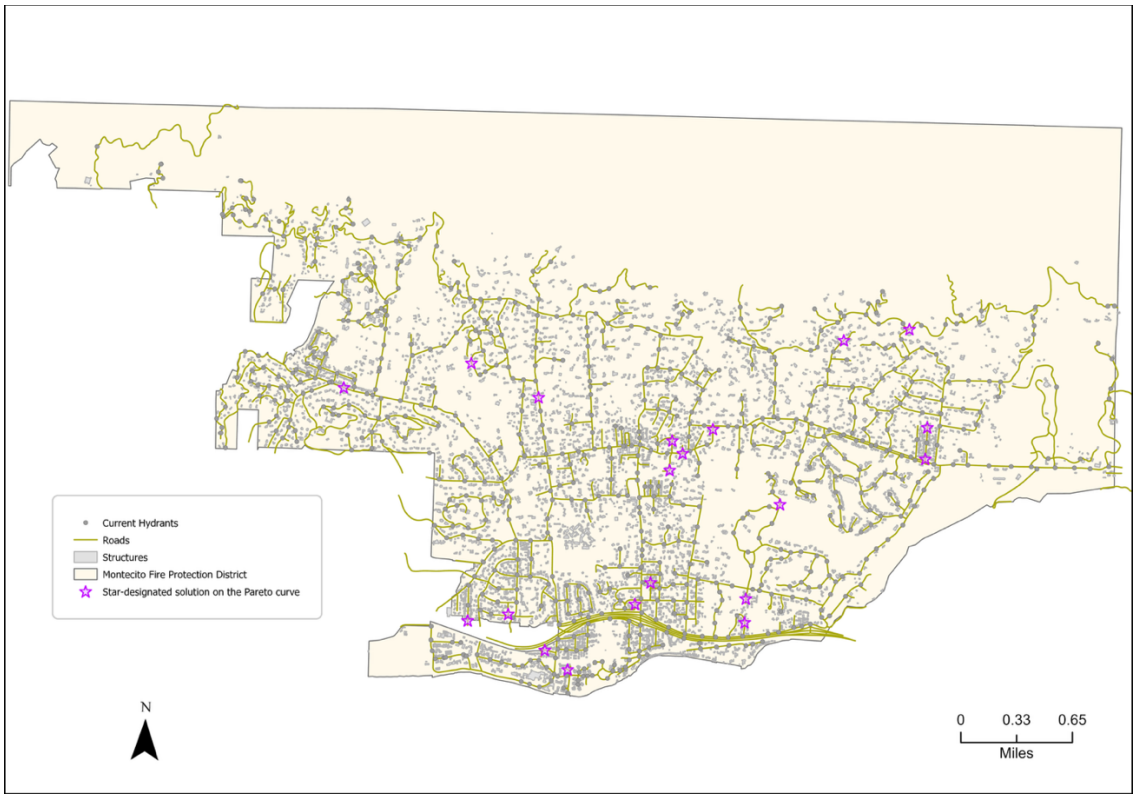


Figure 4.6. Spatial tradeoff solution (star in Figure 4.5).

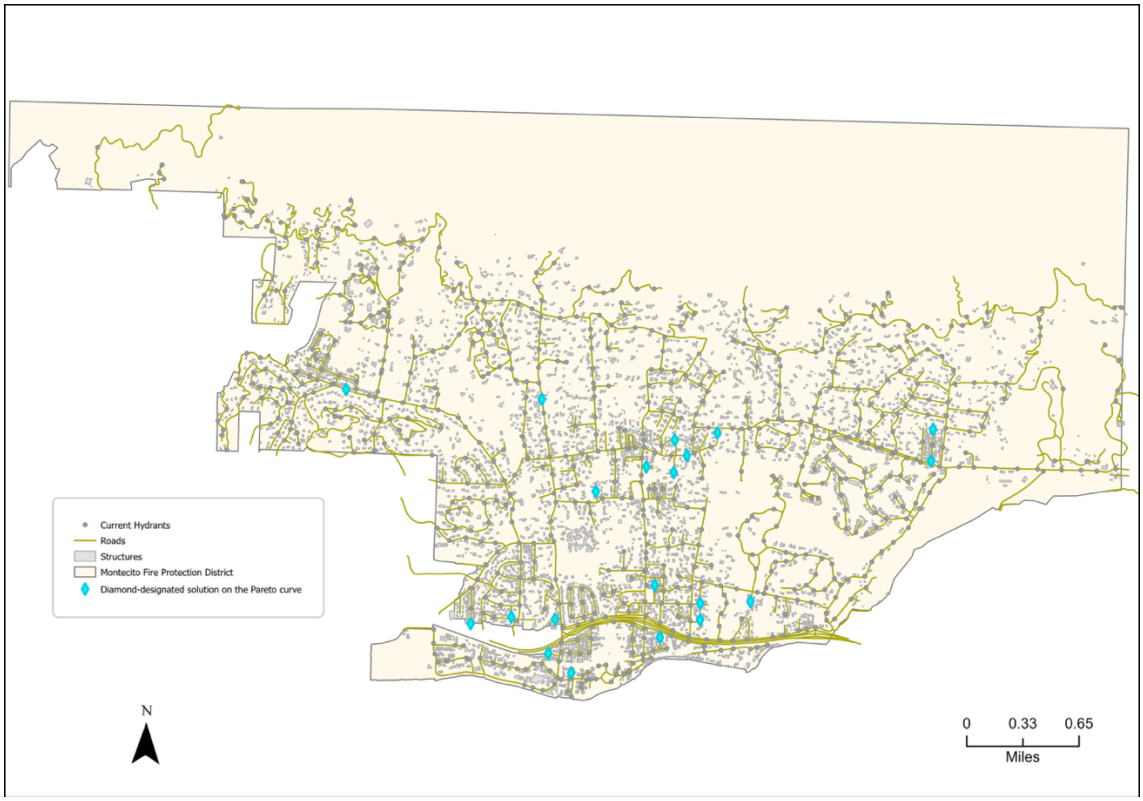


Figure 4.7. Spatial tradeoff solution (diamond in Figure 4.5).

Figure 4.8 presents the spatial solutions associated with extreme solutions of the tradeoff curve (i.e., when structure frontage coverage equals 20.3% and spacing coverage is overlooked, and when the spacing coverage is at 26.95% and the structure coverage is overlooked). The purple stars indicate the selected locations with the best structure coverage, while the blue stars represent the locations that achieve the best spacing coverage objective.

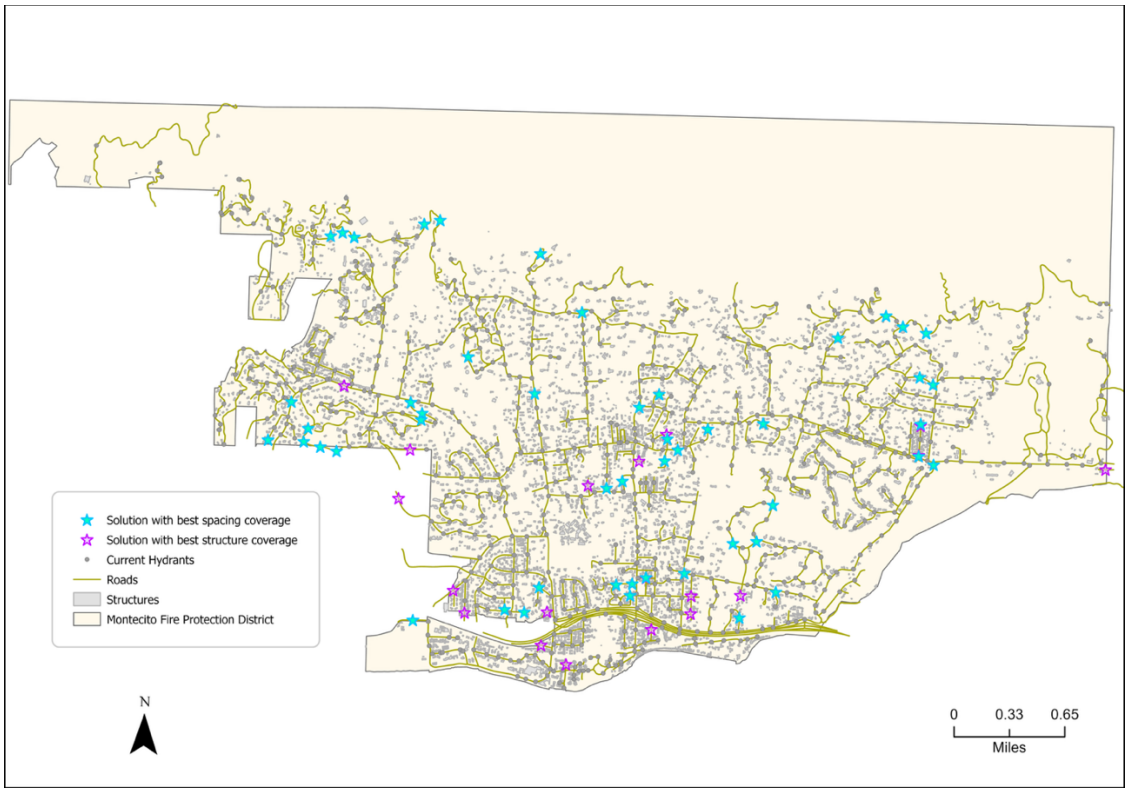


Figure 4.8. Associated spatial solutions when recommending 20 hydrant additions for the best values of both objectives.

One observation that reinforces the necessity of a bi-objective spatial optimization framework is taken from the extreme solutions under each budget scenario. Going back to baseline conditions in terms of road coverage and average spacing only, the improvements to these baseline conditions if hydrants are added according to the best objective values are shown in Table 4.2. In other words, Table 4.2 compares the road coverage and average spacing after adding hydrants considering the extreme solutions only. Road coverage is very similar

under both planning instances. However, average spacing improvements across the region differ significantly. Of course, the spacing-weighted demand model instance reveals greater average spacing improvements across all instances p. This does not imply that the structure-weighted demand model is inferior to its counterpart instance. Instead, it highlights the spatial disparity in locations when different priorities are considered in the planning process. This is why the spatial solutions differ in Figure 4.8 in the $p = 20$ scenario. When structure coverage is prioritized, the solutions tend to move towards denser and more developed areas. On the other hand, when spacing coverage is preferred, the solutions are located towards more peripheral areas where spacing noncompliance is greater. Those spatial differences, along with the results in Table 4.2, make the tradeoff visible and reinforced the adoption of a bi-objective spatial optimization framework to produce more nuanced scenarios.

Table 4.2. Road coverage and spacing outcomes for different hydrant addition scenarios for best structure and spacing objectives

	Best structure-based objective value				**Best spacing-based objective value**			
p	**Total road coverage**	**Road coverage added**	**Avg. spacing (ft)**	**Avg. spacing improvement (ft)**	**Total road coverage**	**Road coverage added**	**Avg. spacing (ft)**	**Avg. spacing improvement (ft)**
1	66.7%	0.1%	549.71	0.07	66.8%	0.1%	549.35	0.42
5	67.1%	0.4%	548.71	1.06	67.2%	0.5%	546.44	3.34
8	67.4%	0.7%	548.72	1.05	67.5%	0.8%	544.26	5.51
10	67.6%	0.9%	548.00	1.77	67.7%	1.0%	543.45	6.32
12	67.8%	1.1%	547.31	2.46	67.9%	1.2%	542.40	7.37
14	68.0%	1.3%	547.22	2.55	68.1%	1.4%	542.12	7.65
17	68.3%	1.6%	546.82	2.96	68.3%	1.6%	541.09	8.68
20	68.6%	1.9%	544.66	5.12	68.6%	1.9%	539.89	9.88

4.5. Discussion

Several matters of discussion are worth mentioning. First, although the placement of new hydrant infrastructure must satisfy hydraulic requirements for fire flow and pressure, which can constrain where new hydrants are feasible (Kanta & Brumbelow, 2013), this chapter did not address that part due to data unavailability. Therefore, the demand set may differ from that considered in the present chapter due to the infeasibility that those variables could reveal. Another consideration concerns budget conditions. In this chapter, hydrants were assumed to have the same average installation cost. But in reality, given flow constraints and the distance to the underlying water mains, installation costs vary (e.g., they can range from USD $10,000 to $55,000). Operational realities also matter. Hydrants may be out of service, access can be blocked, and extreme events can disrupt the water distribution network.

Second, spacing was considered indirectly in the bi-objective MCLP formulation, since spacing calculations are endogenous. To calculate average spacing, identifying hydrant neighbors (from a source hydrant to its neighbor hydrants to establish the spacing relation) is crucial (see Figueroa et al., 2024). Once a new hydrant is placed, the average spacing calculation at the hydrant level changes because it must account for hydrant neighbors. Consequently, all the relationships involving hydrant neighbors are affected, posing a challenge to the adoption of a spatial optimization model that directly addresses the placement of new hydrants to minimize the average hydrant spacing. This is especially significant given the vast number of calculations involved. Therefore, the simplification taken for spacing may carry some uncertainty. Structure weight also carries some uncertainty. The structure weights used assume that the structure count projected to the road network is a reasonable proxy for

exposure, but it does not account for occupancy, building vulnerability, vulnerable population occupancy, or critical facilities.

Lastly, although this chapter is intended as a decision-support framework, its results should be interpreted in light of several uncertainties. These do not invalidate the approach, but they define how the outputs should be used and what aspects are most important to test in future applications. One consideration is data uncertainty. Hydrant inventories might not be perfect. Positional error, missing hydrants, and uncertain operability can all affect diagnostics of the baseline scenarios and, therefore, influence which gaps are prioritized. Similarly, road network data can contain connectivity issues, private roads, unmapped roads, etc., that influence shortest-path distances. Because this study measures service distance along the network, connectivity errors can matter more than they would in a Euclidean buffer analysis. Structure datasets may also contain uncertainty. Footprint completeness, geometry generalization all influence which segments are treated as high-exposure demand. Another source of uncertainty is regarding model representation. Although hydrant placement is continuous along streets, it must be represented through a finite candidate set. Even though the discretization of the road segments was rigorous and met the discretization criteria to minimize error, there could still be some minor error. This is a standard issue in continuous coverage problems as discretization makes computation feasible, but it can introduce representation effects.

4.6. Conclusions

Hydrants are among the most critical pieces of response infrastructure for structure fire suppression because they provide distributed access to a pressurized water supply once an incident occurs, supporting the protection of life, infrastructure, and property. Modern

placement guidance emerged from lessons learned during catastrophic urban fires, where rapid spread and limited suppression capacity led to severe losses. Despite progress in hydrant diagnostics, jurisdictions still face the same planning question. Once gaps in service are identified, where should new hydrants be located? This chapter addressed this question by introducing a spatial optimization framework that prioritizes candidate hydrant locations along the road network to improve frontage access and reduce the most consequential spacing gaps, as defined by the code guidelines about hydrant placement and distribution.

The Montecito community in Santa Barbara was studied to strategically add hydrants to reduce average spacing noncompliance, while also providing sufficient coverage to the community, i.e., hydrant service in areas where there are indeed settlements/structures. Baseline conditions in terms of coverage and average spacing for the community indicated incomplete service relative to code intent, including 66.7% road-network coverage under the adopted service distance and spacing-path noncompliance under a 500 ft threshold. The modeling framework developed in this chapter addressed this gap by linking code-informed service standards to a road-network bi-objective maximal covering formulation, thus treating coverage and spacing as separate planning objectives. Depending on the planning goal, the additions can favor one of the objectives, but the planner would know exactly how the other objective is being compromised, providing a clearer picture for the decision-making process through the tradeoff curves and associated solutions in space. The results reinforce a simple point that is easy to lose in practice. Coverage and spacing are not the same planning objective, even though they are often treated as interchangeable in some research studies and even in day-to-day compliance conversations. The difference could be treated as minor technicality,

but it is a planning choice that changes where installations are prioritized and how benefits are distributed across space.

The proposed framework can be expanded to other jurisdictions. Core data needs such as roads, hydrant locations, and a representation of exposed structures or demand are common. The most local component is the interpretation of standards, e.g., service distance, spacing thresholds, and any jurisdictional amendments. Those values can be adjusted without changing the model structure. Importantly, the approach does not replace engineering design, but it provides a structured pre-design step that narrows the search space to a small set of high-priority locations and provides justification for why those sites were identified.

This chapter contributes a practical, transferable workflow for hydrant prioritization that moves beyond diagnosing gaps by identifying high-priority locations for new hydrants along the street network under budget constraints (only a limited number of hydrants could be placed). The approach is readily portable to other jurisdictions with hydrant inventories, road networks, and code thresholds, and it provides a replicable basis for prioritizing hydrant investments and documenting compliance improvements. Future work could extend this framework in several directions. First, coupling the siting model with hydraulic data (e.g., pressure-driven fire-flow feasibility) would allow candidate locations to be filtered based on system performance. Second, additional aspects could be incorporated to reflect implementation realities, such as variability in installation costs, constructability, robustness to hydrant outages, network disruptions, and social factors such as social vulnerability. Lastly, alternative representations of exposure and demand, such as parcel-level occupancy or incident likelihood surfaces, could be used to refine weighting beyond structure counts alone.

5. Conclusions

This dissertation developed spatial analytic methods to support fire response preparedness and infrastructure planning in fire-prone urban and wildland-urban interface (WUI) communities. While the empirical chapters focus on fire hydrant infrastructure, the broader concern is how spatial data, road-network analysis, statistical modeling, and spatial optimization can be used to evaluate fire-safety conditions and support decisions about limited infrastructure resources. This dissertation's framework progresses from diagnostic assessment to empirical analysis of structure fire incidents and their associated losses, ultimately leading to strategic infrastructure prioritization. This chapter summarizes the major findings of the dissertation, discusses its contributions, and identifies challenges and extensions for future research.

5.1. Summary

Chapter 1 introduced the motivation for this dissertation, focusing on the need for spatial analytic approaches that support fire response preparedness in fire-prone communities. The chapter described the importance of fire response infrastructure in urban and WUI-adjacent communities (understood as denser developed areas not considered as WUI, but near it), reviewed the research context, identified key analytical and planning problems, and outlined the dissertation's research objectives. In particular, Chapter 1 framed the dissertation around three related problems: how to evaluate existing fire response infrastructure, how to understand observed structure-fire patterns and losses, and how to support infrastructure planning when resources are limited.

Chapter 2 developed an advanced spatial analytics approach for assessing hydrant spacing along road networks. The chapter addressed limitations of traditional GIS approaches,

particularly Euclidean buffers and simplified service-area methods, which do not adequately capture the street network relationships required to identify assess hydrant distribution according to code standards. The chapter introduced a method for evaluating hydrant spacing and applied it to coastal Santa Barbara County accounting for complexities of the road network and determining hydrant neighbors when the relationship is ambiguous. Results showed that spacing can be measured at the individual spacing, hydrant, neighborhood, and community scales. The application in the region revealed that hydrant spacing standards are not always maintained and that violations occur in spatially clustered pockets. This chapter established the diagnostic foundation of the dissertation by showing that fire response infrastructure must be evaluated using spatial methods that reflect actual road-network connectivity that go beyond simplified distance approximations.

Chapter 3 examined historical structure fire incidents in urban areas of Santa Barbara County to better understand where fires occur and which factors are associated with loss once an incident occurs. The analysis combined spatial mapping, point pattern analysis, count models, and loss models. Results showed that structure fire incidents cluster around major activity centers and that population and housing density are important predictors of incident occurrence. For loss severity, suppression duration was the most stable predictor, with additional evidence that property area and incident timing were relevant in some model specifications. Hydrant proximity and code-compliant access were not independently associated with loss magnitude after controlling for operational factors and property characteristics. This finding should not be interpreted as evidence that hydrants are unimportant but instead it suggests that in this empirical setting, where current hydrant access is often already present where fire incidence were present, variation in loss is more closely

associated with operational duration and incident conditions than with proxies that represent hydrant presence in form of distances.

Chapter 4 developed a bi-objective spatial optimization framework for strategic hydrant additions. The chapter addressed the planning problem that follows from Chapters 2 and 3. Once infrastructure gaps are identified according to spacing and structure frontage coverage, where should new hydrants be prioritized? Consequently, the model was designed to improve frontage coverage while also accounting for spacing compliance under budgetary considerations. Applied to the Montecito Fire Protection District, the framework demonstrated how candidate hydrant additions can be prioritized along a road network using structure-weighted and spacing-weighted demand. Results showed that the two objectives can lead to different spatial priorities, making tradeoffs visible for planners and decision makers. This chapter extended the dissertation from assessment and explanation to prescriptive planning support.

With these chapters, the dissertation shows how spatial analytic methods can support fire response preparedness across a sequence of planning tasks, contributing an integrated approach for moving from spatial diagnosis to empirical understanding and then to decision-making support.

5.2. Contributions

This dissertation contributes to GIScience, location science, and fire response planning by developing spatial analytic methods for evaluating infrastructure, interpreting structure-fire outcomes, and supporting strategic investment decisions. The contributions are methodological, empirical, and practical. Together, they show how spatial data and spatial

modeling can be used to improve understanding of fire response systems in complex urban and WUI-adjacent communities.

This dissertation advances an emerging research direction at the intersection of GIScience, location science, and fire-response infrastructure planning. Figure 5.1 summarizes the dissertation's contributions to fire-response planning.



Figure 5.1. Dissertation contributions to fire response.

The first contribution comes from a technical and methodological perspective, as this dissertation extends GIScience and location science by adapting spatial analytics and spatial optimization methods to a class of fire response infrastructure problems that has received limited formal treatment. In GIScience, the dissertation advances network-based infrastructure assessment by showing that code-based fire response standards cannot be represented adequately through Euclidean buffers, generic service areas, or simple proximity measures. In location science, the dissertation extends covering models to a road-constrained, code-driven infrastructure setting where potential facility locations are continuous along network arcs, demand is distributed along road segments, and planning objectives are not

reducible to a single measure of access. In doing so, the dissertation moves fire response infrastructure analysis beyond descriptive mapping and toward a reproducible decision-support framework that links network representation, empirical fire outcomes, and strategic infrastructure prioritization. From other angles, there are also several contributions.

The second contribution is conceptual. This dissertation clarifies distinctions among related fire-response concepts. Hydrant spacing and frontage coverage are related but not interchangeable. Spacing concerns the relationship between neighboring hydrants along the road network. Coverage concerns whether street frontage or structures are within an allowable distance of a hydrant. Regarding the study of fire incidence patterns, important concepts are also clarified. Incident occurrence concerns where fires happen. Loss severity concerns what happens once an incident occurs. Treating these concepts separately allows the dissertation to avoid a common analytical shortcut that some research has taken, assuming that a single proximity measure explains all dimensions of fire risk, response, and loss.

The third contribution is empirical. The dissertation provides evidence from fire-prone communities in Santa Barbara County that can enhance fire-response planning in the region. Chapter 2 identifies spatial variation in hydrant spacing compliance across the coastal Santa Barbara region revealing areas with fire response vulnerability. Chapter 3 shows that structure-fire incident occurrence is associated with density, while loss severity is more closely related to suppression duration and incident-level characteristics than to hydrant proximity alone. Chapter 4 builds on Chapters 2 and 3 by demonstrating how to address vulnerabilities identified in Chapter 2 while considering structure density, a significant finding from Chapter 3. It proposes a method to enhance preparedness in the region through strategic hydrant additions under various planning scenarios and objectives. These findings provide a

more nuanced empirical basis for fire response planning as they demonstrate that effective decision-making support requires interpreting infrastructure, urban form, and operational conditions altogether.

Considering the above, the fourth contribution is then practical. The dissertation provides approaches that can be useful for fire departments, emergency services, planners, public works agencies, water agencies, and policymakers. Fire departments and emergency services can use these methods to identify areas where infrastructure conditions warrant closer review, to evaluate code-related gaps, and to communicate infrastructure needs with a stronger foundation. Urban planning and public works agencies can use the framework to coordinate fire safety goals with land development, capital improvement planning, and water-system planning. Policymakers and community organizations can use the results to support targeted outreach and resource allocation in areas where fire exposure, population density, infrastructure gaps, and response challenges overlap.

The broader impacts of this dissertation are connected to the communities and agencies that must prepare for and respond to fire hazards. The Santa Barbara coastal region includes dense urban centers, WUI-adjacent neighborhoods, high-value residential areas, student communities, workers in tourism, education, agriculture, and service sectors, and residents who may have fewer resources for preparedness and recovery. Fire preparedness in such a region goes beyond being a technical problem. It is also a community planning problem involving infrastructure, land development, emergency response capacity, and unequal exposure to risk. By making fire response infrastructure and incident patterns more visible, the methods developed in this dissertation can support more transparent planning and help agencies identify where preparedness investments may be most needed.

This dissertation's main contribution is to provide analytical tools that help decision makers better understand existing conditions, evaluate where gaps may exist, and compare planning alternatives. In this way, the dissertation supports more defensible fire safety planning. The ultimate beneficiaries include not only technical users of the models, but also residents and communities whose safety depends on well planned, well maintained, and well-coordinated response infrastructure.

5.3. Challenges and extensions

There are several challenges faced in this dissertation that suggest directions for future research. These challenges relate to data inputs, spatial representation, code interpretation, statistical modeling, hydraulic feasibility, implementation, and transferability. Addressing these issues would strengthen the analytical framework and expand its usefulness for planning and emergency management.

A first challenge concerns the spatial data used to represent hydrants, roads, structures, incidents, and communities. The analyses rely on the accuracy and completeness of hydrant locations, road centerlines, structure footprints, incident records, jurisdictional boundaries, and associated socioeconomic or land-use data. Errors or omissions in any of these inputs can affect spacing assessment, incident modeling, and optimization results. Future work could evaluate how uncertainty in hydrant locations, road geometry, structure projection, and incident geocoding affects the results. Sensitivity analysis would be especially useful for understanding which data inputs most strongly influence identified infrastructure gaps and candidate improvement locations.

A second challenge concerns the translation of fire-code standards into spatial metrics. Fire area, building type/land use, and construction materials determine flow. This flow

determines the required maximum separation between hydrants and frontage coverage. For the purpose of this dissertation, assumptions regarding property fire area and building materials were made according to what is typical for a type of structure in the region. Future research could determine spacing in a more accurate way if information regarding flow is available. Also, in other geographic contexts that require alternative code assumptions, future research can evaluate different code standards and examine how local amendments change the spatial distribution of identified gaps. Such work would be valuable for jurisdictions that must interpret state or international standards under local development and infrastructure conditions.

A third challenge concerns the empirical modeling of structure fire incidents and losses. Chapter 3 analyzes observed incident concentration and loss severity using available records, but the loss-model sample is smaller than the full incident dataset and should be interpreted cautiously. In addition, suppression duration is strongly associated with loss severity, but it may also reflect the underlying complexity or severity of the incident. Future research could incorporate additional operational data, including dispatch time, arrival time, staffing, equipment, water supply establishment, and fire flow conditions. These additions would help distinguish between factors that describe incident severity and factors that may be actionable through response planning.

A fourth challenge concerns implementation. The optimization framework in Chapter 4 identifies candidate locations for strategic hydrant additions, but these locations should be interpreted as pre-design priorities rather than literal recommendations. Actual hydrant installation requires hydraulic review, pressure and flow analysis, water-main capacity assessment, right-of-way review, terrain and constructability analysis, cost estimation, and

coordination with water agencies and local jurisdictions. Future work should integrate spatial optimization with hydraulic modeling and capital planning. This would allow candidate hydrant additions to be evaluated not only by spatial benefit, but also by engineering feasibility and implementation cost.

Beyond challenges, there is a possible extension regarding ignition probability. Chapter 3 analyzed observed structure-fire incidents, their concentration, and conditional loss severity. However, it did not estimate the underlying probability that an ignition occurs at a given location or time. Therefore, the observed incident pattern was treated as the available empirical realization of a broader ignition and response process. The implicit assumption regarding ignitions is then that reported incidents provide a reasonable empirical basis for analyzing observed fire patterns and losses. This was appropriate for the chapter's objective of explaining observed fire patterns and losses, but future work could extend the analysis by estimating ignition probability more directly. Incorporating such probabilities could also strengthen the hydrant location framework in Chapter 4 by prioritizing additions in places where ignition is more likely to occur, moving the analysis toward a more explicit risk-based planning framework.

There are also other research avenues that this dissertation opens. First, the work can be extended by connecting the dissertation's infrastructure-focused methods with broader vulnerability and resilience planning. The dissertation focuses on hydrant infrastructure, structure-fire incidents, and strategic additions, but fire preparedness also depends on social vulnerability, evacuation constraints, household resources, communication capacity, land use, building materials, vegetation, and community-level preparedness. Future work could incorporate variables such as income, renter status, age, vehicle access, language access,

disability, and evacuation limitations into fire response infrastructure planning. This would help connect technical infrastructure analysis with planning oriented in equity and targeted community outreach.

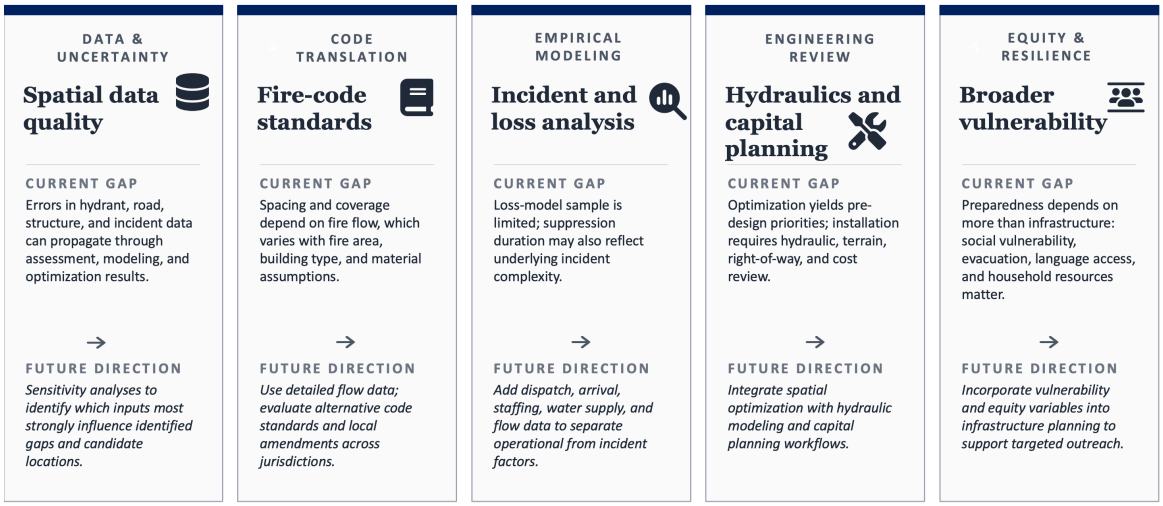


Figure 5.2. Current challenges and future research avenues.

Figure 5.2 summarizes and illustrates the presented gaps and how each of them presents an avenue for future research. Overall, this dissertation demonstrates the value of spatial analytic methods for fire response preparedness and infrastructure planning. By assessing hydrant spacing, examining structure fire incidents and losses, and developing an optimization framework for strategic hydrant additions, the dissertation provides quantitative support for identifying infrastructure gaps and prioritizing improvements in fire-prone communities. More broadly, it shows that fire safety planning benefits from methods that connect spatial data, empirical evidence, and decision support. In communities where urban development, WUI exposure, and limited infrastructure resources intersect, such tools can help make preparedness planning more transparent, targeted, and defensible.

References

Abrar, A., Kamal, A. S. M. M., & Fahim, A. K. F. (2024). Fire risk vulnerability and safety assessment of Farmgate area using fire risk index, Dhaka City and optimization of fire hydrant placement. *Progress in Disaster Science*, *24*, 100384.

Alexandre, P. M., Stewart, S. I., Mockrin, M. H., Keuler, N. S., Syphard, A. D., Bar-Massada, A., Calyton, M. K., & Radeloff , V. C. (2016). The relative impacts of vegetation, topography and spatial arrangement on building loss to wildfires in case studies of California and Colorado. *Landscape Ecology*, *31*(2), 415–430.

Alnajim, K., & Abokifa, A. A. (2025). Operational response to contamination in water distribution systems: A multi-objective Bayesian optimization approach. *Frontiers in Water*, *7*, 1547112.

Anselin, L. (2022). Spatial econometrics. In S. J. Rey & R. S. Franklin (Eds.), *Handbook of Spatial Analysis in the Social Sciences* (pp. 101–122). Edward Elgar Publishing.

Ardianto, R., & Chhetri, P. (2019). Modeling spatial-temporal dynamics of urban residential fire risk using a Markov chain technique. *International Journal of Disaster Risk Science*, *10*(1), 57–73.

Asgary, A., Ghaffari, A., & Levy, J. (2010). Spatial and temporal analyses of structural fire incidents and their causes: A case of Toronto, Canada. *Fire Safety Journal*, *45*(1), 44–57.

Asgary, A., Naini, A. S., & Levy, J. (2012). Modeling the risk of structural fire incidents using a self-organizing map. *Fire Safety Journal*, *49*, 1–9.

Baik, J., & Murray, A. T. (2024). Emergency response planning: A framework to assess hydrant-structure access. *Transactions in GIS*, *28*(7), 2412–2424.

Baker, M., Browning, K., & Bogel-Burroughs, N. (2023, August 14). As inferno grew, Lahaina's water system collapsed. *The New York Times* (https://www.nytimes.com/2023/08/13/us/lahaina-water-failure.html, accessed 04/25/26)

Baker, M., Khurana, M., Lai, K. K. R., Mellen, R., Reneau, N., Saget, B., Shao, E., Singhvi, A., & Smart, C. (2023, November 1). Inside the deadly Maui inferno, hour by hour. *The New York Times* (https://www.nytimes.com/interactive/2023/11/01/us/hawaii-maui-fire-timeline.html, accessed 04/25/26)

Besag, J. (1977). Contribution to the discussion on Dr Ripley's paper. *Journal of the Royal Statistical Society Series B: Statistical Methodology*, *39*, 193–195.

Bispo, R., Vieira, F. G., Bachir, N., Espadinha-Cruz, P., Lopes, J. P., Penha, A., Marques, F. J., & Grilo, A. (2023). Spatial modelling and mapping of urban fire occurrence in Portugal. *Fire Safety Journal, 138*, 103802.

Burke, M., Driscoll, A., Heft-Neal, S., Xue, J., Burney, J., & Wara, M. (2021). The changing risk and burden of wildfire in the United States. *Proceedings of the National Academy of Sciences*, *118*(2), e2011048118.

CAL FIRE. (2025a). *2025 incident archive* (https://www.fire.ca.gov/incidents/2025, accessed 4/25/26)

CAL FIRE. (2025b, February 9). *Top 20 most destructive wildfires* (https://www.fire.ca.gov/our-impact/statistics#:~:text=California%20Wildfires, accessed 4/25/26)

California Fire Code. (2022). *2022 California Fire Code, Title 24, Part 9*. International Code Council.

Carpinteria-Summerland Fire Protection District. (2021). Fire protection water supply: Development Standard #2. Carpinteria-Summerland Fire Protection District (https://s3.amazonaws.com/siteninja/multitenant/assets/32817/files/original/CSFPD_Std2.pdf, accessed 03/05/26)

CBS News. (2026, April 25). 2 massive Georgia wildfires destroy more than 120 homes, scorch over 40,000 acres. *CBS News* (https://www.cbsnews.com/news/georgia-wildfires-destroy-homes-scorch-acres/, accessed 05/10/26)

Ceyhan, E., Ertuğay, K., & Düzgün, Ş. (2013). Exploratory and inferential methods for spatio-temporal analysis of residential fire clustering in urban areas. *Fire Safety Journal*, *58*, 226–239.

Chhetri, P., Corcoran, J., Ahmad, S., & KC, K. (2018). Examining spatio-temporal patterns, drivers and trends of residential fires in South East Queensland, Australia. *Disaster Prevention and Management: An International Journal*, *27*(5), 586–603.

Chicago Architecture Center. (2025). The Great Chicago Fire of 1871. In *Architecture Encyclopedia* (https://www.architecture.org/online-resources/architecture-encyclopedia/the-great-chicago-fire-of-1871, accessed 01/20/26)

Church, R. L. (1984). The planar maximal covering location problem. *Journal of Regional Science*, *24*(2), 185–201.

Church, R. L., & Meadows, M. E. (1977). Results of a new approach to solving the p-median problem with maximum distance constraints. *Geographical Analysis*, *9*(4), 364-378.

Church, R. L., & Meadows, M. E. (1979). Location modeling utilizing maximum service distance criteria. *Geographical Analysis*, *11*(4), 358-373.

Church, R. L., & Murray, A. T. (2018). *Location covering models: History, applications and advancements*. Springer International Publishing.

Church, R., & ReVelle, C. (1974). The maximal covering location problem. *Papers of the Regional Science Association*, *32*, 101–118.

City of Los Angeles. (2016). *LAFD Fire Code Chapter 5, Section 507.3.2: Fire service features: Fire hydrant systems* (https://up.codes/viewer/los_angeles/ca-fire-code-2016/chapter/5/fire-service-features#new_507.3.2, accessed 04/20/24)

City of Los Angeles Department of Public Works. (2024). Tree spacing guidelines. *Bureau of Street Services* (https://streetsla.lacity.org/sites/default/files/BSS_TREE_SPACING_GUIDELINES.pdf, accessed 04/21/24)

City of Medford. (2024). *Medford, WI Code of Ordinances, Chapter 9.4: Fire Prevention and Protection, Section 9.4.28: Hydrant Locations* (https://codelibrary.amlegal.com/codes/medford/latest/medford_wi/0-0-0-2344, accessed 04/21/24)

Cohon, J. L. (1978). *Multiobjective Programming and Planning*. Academic Press.

Conservation Biology Institute. (2020). *Santa Barbara County Building Footprints.* Data Basin (https://sbcblueprint.databasin.org/datasets/e0cc067522204c70bfb3baae2c, accessed 08/20/23)

Corcoran, J., Higgs, G., Brunsdon, C., Ware, A., & Norman, P. (2007a). The use of spatial analytical techniques to explore patterns of fire incidence: A South Wales case study. *Computers, Environment and Urban Systems*, *31*(6), 623–647.

Corcoran, J., Higgs, G., Brunsdon, C., & Ware, A. (2007b). The use of Comaps to explore the spatial and temporal dynamics of fire incidents: A case study in South Wales, United Kingdom. *The Professional Geographer*, *59*(4), 521–536.

Corcoran, J., Higgs, G., & Higginson, A. (2011a). Fire incidence in metropolitan areas: A comparative study of Brisbane (Australia) and Cardiff (United Kingdom). *Applied Geography*, *31*(1), 65–75.

Corcoran, J., Higgs, G., Rohde, D., & Chhetri, P. (2011b). Investigating the association between weather conditions, calendar events and socio-economic patterns with trends in fire incidence: An Australian case study. *Journal of Geographical Systems*, *13*(2), 193–226.

Diggle, P. J. (1985). A kernel method for smoothing point process data. *Journal of the Royal Statistical Society: Series C (Applied Statistics)*, *34*(2), 138–147.

Diggle, P. J. (2013). *Statistical Analysis of Spatial and Spatio-temporal Point Patterns (3rd ed.)*. Chapman & Hall/CRC.

Esquivel-Saldaña, G., Domínguez-Honorio, E., & Gutiérrez-Gutiérrez, J. (2021). Genetic algorithm for the strategic location of a network of fire hydrants. *Ingeniare. Revista Chilena de Ingeniería*, *29*(4), 661–667.

Federal Emergency Management Agency, Oak Ridge National Laboratory, & U.S. Geological Survey. (2024). *USA Structures*.

Ferreira, T. M., Vicente, R., Raimundo Mendes da Silva, J. A., Varum, H., Costa, A., & Maio, R. (2016). Urban fire risk: Evaluation and emergency planning. *Journal of Cultural Heritage*, *20*, 739–745.

Figueroa, V. E., Murray, A. T., & Funk, T. (2024). Supporting fire response: Advanced spatial data analytics for hydrant access assessment. *Transactions in GIS*, *28*(8), 2559–2573.

Filkov, A. I., Tihay-Felicelli, V., Masoudvaziri, N., Rush, D., Valencia, A., Wang, Y., Blunck, D. L., Valero, M. M., Kempna, K., Smolka, J., De Beer, J., Campbell-Lochrie, Z., Centeno, F. R., Ibrahim, M. A., Lemmertz, C. K., & Tam, W. C. (2023). A review of thermal exposure and fire spread mechanisms in large outdoor fires and the built environment. *Fire Safety Journal*, *140*, 103871.

Flexer, G. G. (1966). From fire plug to fire hydrant. *Journal AWWA*, *58*(11), 1417–1428.

Forkuo, E. K., & Quaye-Ballard, J. A. (2013). GIS based fire emergency response system. *International Journal of Remote Sensing and GIS*, *2*(1), 32–40.

Garrioch, D. (2016). 1666 and London's fire history: A re-evaluation. *The Historical Journal*, *59*(2), 319–338.

Getis, A. (2009). Spatial weights matrices. *Geographical Analysis*, *41*(4), 404–410.

Getis, A., & Aldstadt, J. (2004). Constructing the spatial weights matrix using a local statistic. *Geographical Analysis*, *36*(2), 90–104.

Gilbert, S. W., & Butry, D. T. (2018). Identifying vulnerable populations to death and injuries from residential fires. *Injury Prevention*, *24*(5), 358–364.

Gomułka, P. (2023). Computer-aided system for layout of fire hydrants on boards designed vessel using the particle swarm optimization algorithm. *Polish Maritime Research*, *30*, 4–16.

González Villa, F., & García Prats, A. (2012). Using location-allocation algorithms to distribute multioutlet hydrants in irrigation networks design. *Journal of Irrigation and Drainage Engineering*, *138*(4), 304–309.

González-Pavón, C., Palau, C. V., Manzano-Juárez, J. M., Guillem-Picó, S., & Balbastre-Peralta, I. (2025). Optimization of multioutlet hydrant location and pressurized irrigation network layout using the GRASP metaheuristic. *Journal of Agricultural Engineering*, *56*, 1633.

Goodhue, R. F. (1941). Insurance requirements for water works properties. *Journal AWWA*, *33*(6), 1058–1068.

Grant, G., Brenton, J., & Drysdale, D. (2000). Fire suppression by water sprays. *Progress in Energy and Combustion Science*, *26*(2), 79–130.

Grattan, S. (2026, January 22). Why Chile's wildfires are spreading faster and burning hotter. *AP* (https://apnews.com/article/chile-wildfires-climate-change-plantations-drought-448d20e4fb24aca74458db739a20b318, accessed 05/10/26)

Guldåker, N. (2020). Geovisualization and geographical analysis for fire prevention. *ISPRS International Journal of Geo-Information*, *9*(6), 355.

Guldåker, N., & Hallin, P. O. (2014). Spatio-temporal patterns of intentional fires, social stress and socio-economic determinants: A case study of Malmö, Sweden. *Fire Safety Journal*, *70*, 71–80.

Halim, S. Z., Quddus, N., & Pasman, H. (2021). Time-trend analysis of offshore fire incidents using nonhomogeneous Poisson process through Bayesian inference. *Process Safety and Environmental Protection*, *147*, 421–429.

Hall, S. (2025, November). *Fire loss in the United States during 2024*. National Fire Protection Association.

Heffernan, V., Murray, A. T., Baylis, K., & Church, R. L. (2026). Urban safety and the role of hydrant structure and configuration. *Scientific Reports*. Advance online publication. doi: 10.1038/s41598-026-45799-1.

Himoto, K., & Tanaka, T. (2008). Development and validation of a physics-based urban fire spread model. *Fire Safety Journal*, *43*(7), 477–494.

Hossain, M. R., & Smirnov, O. (2023). Analyzing the risk factors of residential fires in urban and rural census tracts of Ohio using panel data analysis. *Applied Geography*, *151*, 102863.

Hu, J., Shu, X., Xie, S., Tang, S., Wu, J., & Deng, B. (2019). Socioeconomic determinants of urban fire risk: A city-wide analysis of 283 Chinese cities from 2013 to 2016. *Fire Safety Journal*, *110*, 102890.

International Code Council. (2024). 2024 *International Fire Code*. International Code Council (https://codes.iccsafe.org/content/IFC2024V2.0, accessed 05/20/2024)

Jackson, L. A. (1944). Historical development of the fire hydrant. *Journal AWWA*, *36*(9), 928–956.

Jain, S., & McLean, C. R. (2006). An integrating framework for modeling and simulation for incident management. *Journal of Homeland Security and Emergency Management*, *3*(1).

Jeong, D., Kim, B., & Shin, D. (2018). Analysing spatial pattern of fire factor using text mining. *Journal of the Korean Society for Geospatial Information Science*, *26*(2), 67–75.

Ji, Y., Gu, H., & Li, B. (2010). Urban fire risk evaluation of Xuzhou city based on GIS. *2010 18th International Conference on Geoinformatics*, 1–6.

Juran, J. M. (1975). The non-Pareto principle; mea culpa. *Quality Progress*, *8*(5), 8–9.

Kalach, A. V., Rodin, V. A., & Sinegubov, S. V. (2020). Optimizing fire-fighting water supply systems using spatial metrics. *Journal of Computational and Engineering Mathematics*, *7*(4), 3–16.

Kanta, L., & Brumbelow, K. (2013). Vulnerability, risk, and mitigation assessment of water distribution systems for insufficient fire flows. *Journal of Water Resources Planning and Management*, *139*(6), 593–603.

Kaufman, M. M., & Rosencrants, T. (2015). GIS method for characterizing fire flow capacity. *Fire Safety Journal*, *72*, 25–32.

KC, K., & Corcoran, J. (2017). Modelling residential fire incident response times: A spatial analytic approach. *Applied Geography*, *84*, 64–74.

Keeley, J. E., & Syphard, A. D. (2021). Large California wildfires: 2020 fires in historical context. *Fire Ecology*, *17*(1), 22.

Keeley, J., & Syphard, A. (2016). Climate change and future fire regimes: Examples from California. *Geosciences*, *6*(3), 37.

Kelly, H., Clare, J., Wuschke, K., & Garis, L. (2019). Opportunity and rationality as an explanation for suspicious vehicle fires. *Crime Science*, *8*(1), 8.

Kimmel, S., Mallory, J., & Walker, B. (2004). Pine Ridge Trailer Court: Water distribution system. In *Purdue University*. Engineers Without Borders.

King, F. H. (1926). The spacing of fire hydrants. *Journal (American Water Works Association)*, *15*(3), 224–226.

Lee, Y. H., Kim, M. S., & Lee, J. S. (2021). Firefighting in vulnerable areas based on the connection between fire hydrants and fire brigade. *Sustainability*, *13*(1), 98.

Lee, S. L., Hsu, M. H., Wang, Y. F., & Wang, M. Y. (2025). Forecasting urban fire severity for enhanced emergency response and resource allocation. *Scientific Reports*, *15*(1), 42165.

LeSage, J. P., & Fischer, M. M. (2008). Spatial growth regressions: Model specification, estimation and interpretation. *Spatial Economic Analysis*, *3*(3), 275–304.

Lestari, F., Kim, K., Adiwibowo, A., Octaviani, D. F., Fisher, M., & Yamashita, E. (2022). Improving service coverage and response times for three-wheeled mobile fire units on Pari Island, Indonesia. *Transportation Research Record*, *2677*(1), 682–693.

Li, S., Dao, V., Kumar, M., Nguyen, P., & Banerjee, T. (2022). Mapping the wildland-urban interface in California using remote sensing data. *Scientific Reports*, *12*(1), 5789.

Littell, J. S. (2018). Drought and fire in the western USA: Is climate attribution enough? *Current Climate Change Reports*, *4*(4), 396–406.

Maranghides, A., Link, E. D., Nazare, S., Hawks, S., McDougald, J., Quarles, S. L., & Gorham, D. J. (2022). *WUI Structure/parcel/community fire hazard mitigation methodology*. Washington, DC: US Department of Commerce, National Institute of Standards and Technology.

Maranghides, A., & Mell, W. (2011). A case study of a community affected by the witch and Guejito wildland fires. *Fire Technology*, *47*, 379–420.

McElroy, S. (1865). Papers on hydraulic engineering. *Journal of the Franklin Institute*, *79*(2), 81–92.

Mohammadi, A., Shahparvari, S., Kiani, B., Noori, S., & Chhetri, P. (2023). An analysis of spatio-temporal patterns of fires in an Iranian city. *Indoor and Built Environment*, *32*(1), 183–199.

Montecito Fire Department. (2022). *Development Standard #4a: Water Supply Requirements* (https://s3.amazonaws.com/siteninja/multitenant/assets/33145/files/original/2022_Development_Standard_4a_Water_Supply_Requirements_-_Final.pdf, accessed 01/10/26)

Moritz, M. A., Batllori, E., Bradstock, R. A., Gill, A. M., Handmer, J., Hessburg, P. F., Leonard, J., McCaffrey, S., Odion, D. C., Schoennagel, T., & Syphard, A. D. (2014). Learning to coexist with wildfire. *Nature*, *515*(7525), 58–66.

Murray, A. T. (2018). Evolving location analytics for service coverage modeling. *Geographical Analysis*, *50*(3), 207–222.

Murray, A. T. (2020). New geography location analytics. In *Handbook of Regional Science* (pp. 1–20). Springer Berlin Heidelberg.

Murray, A. T., Baik, J., Echeverri Figueroa, V., Rini, D., Moritz, M. A., Roberts, D. A., Sweeney, S. H., Carvalho, L. M. V., & Jones, C. (2023). Developing effective wildfire risk mitigation plans for the wildland urban interface. *International Journal of Applied Earth Observation and Geoinformation*, *124*, 103531.

Murray, A. T., Carvalho, L., Church, R. L., Jones, C., Roberts, D., Xu, J., Zigner, K., & Nash, D. (2021). Coastal vulnerability under extreme weather. *Applied Spatial Analysis and Policy*, *14*, 497–523.

Murray, A. T., & Feng, X. (2016). Public street lighting service standard assessment and achievement. *Socio-Economic Planning Sciences*, *53*, 14–22.

Murray, A. T., Rini, D., Sweeney, S. S., Roberts, D. A., Moritz, M. A., Baik, J., Figueroa, V. E., & Zheng, Z. (2025). Geographic fire response standards emerging from human–environment interactions. *Annals of the American Association of Geographers*, *115*(9), 2048–2070.

Murray, A. T., & Tong, D. (2007). Coverage optimization in continuous space facility siting. *International Journal of Geographical Information Science*, *21*(7), 757–776.

National Board of Fire Underwriters. (1942). Standard schedule for grading cities and towns of the United States with reference to their fire defenses and physical conditions. *Journal AWWA*, *34*(10), 1–78.

National Fire Protection Association. (2024). *NFPA 1, Fire Code*. National Fire Protection Association.

Nerantzis, D., & Stoianov, I. (2023). Optimization-based selection of hydrants and valves control in water distribution networks for fire Incidents management. *IEEE Systems Journal*, *17*(1), 134–145.

Okabe, A., Satoh, T., Furuta, T., Suzuki, A., & Okano, K. (2008). Generalized network Voronoi diagrams: Concepts, computational methods, and applications. *International Journal of Geographical Information Science*, *22*(9), 965–994.

Okon, I., & Njoku, C. G. (2018). The location of fire hydrants and implications to fire disaster management in Calabar, Cross River State, Nigeria. *IOSR Journal of Humanities and Social Science (IOSR-JHSS)*, *23*(7), 42–55.

Pratiwi, H. A. N., Rachmansyah, A., Efani, A., Wardana, F. C., & Dhana, F. R. (2024). Fire disaster mitigation strategy in Malang City using a Geographic Information System

(GIS) approach. *Jurnal Pendidikan Geografi: Kajian, Teori, Dan Praktek Dalam Bidang Pendidikan Dan Ilmu Geografi*, *29*(2), 9.

Price, O. F., Whittaker, J., Gibbons, P., & Bradstock, R. (2021). Comprehensive examination of the determinants of damage to houses in two wildfires in eastern Australia in 2013. *Fire*, *4*(3), 44.

Raczek, J., & Miotk, M. (2024). Theoretical modelling of efficient fire safety water networks by certified domination. *Scientific Reports*, *14*(1), 21574.

Radeloff, V. C., Mockrin, M. H., Helmers, D., Carlson, A., Hawbaker, T. J., Martinuzzi, S., Schug, F., Alexandre, P. M., Kramer, H. A., & Pidgeon, A. M. (2023). Rising wildfire risk to houses in the United States, especially in grasslands and shrublands. *Science*, *382*(6671), 702–707.

Rahman Tishi, T., & Islam, I. (2019). Urban fire occurrences in the Dhaka Metropolitan Area. *GeoJournal*, *84*(6), 1417–1427.

Raškauskaitė, R., & Grigonis, V. (2019). An approach for the analysis of the accessibility of fire hydrants in urban territories. *ISPRS International Journal of Geo-Information*, *8(12),* 587.

Reuters. (2026, February 11). Record heat and raging fires ring in 2026 across the Southern Hemisphere. *Reuters* (https://www.reuters.com/sustainability/cop/record-heat-raging-fires-ring-2026-across-southern-hemisphere-2026-02-11, accessed 05/10/26)

ReVelle, D. O., & Eiselt, H. A. (2005). Location analysis: A synthesis and survey. *European Journal of Operational Research*, *165*(1), 1–19.

Ripley, B. D. (1976). The second-order analysis of stationary point processes. *Journal of Applied Probability*, *13*(2), 255–266.

Ripley, B. D. (1977). Modelling spatial patterns. *Journal of the Royal Statistical Society Series B: Statistical Methodology*, *39*(2), 172–192.

Ripley, B. D. (1979). Tests of 'randomness' for spatial point patterns. *Journal of the Royal Statistical Society. Series B (Methodological)*, *41*, 368–374.

Rohde, D., Corcoran, J., & Chhetri, P. (2010). Spatial forecasting of residential urban fires: A Bayesian approach. *Computers, Environment and Urban Systems*, *34*(1), 58–69.

Ronan, T., & Teeuw, R. (2016). London's burning: Integrating water flow rates and building types into fire risk maps. *International Journal of Emergency Services*, *5*(1), 34–51.

Ronchi, E., Gwynne, S. M., Rein, G., Intini, P., & Wadhwani, R. (2019). An open multi-physics framework for modelling wildland-urban interface fire evacuations. *Safety Science*, *118*, 868–880.

Safar, M., Ibrahimi, D., & Taniar, D. (2009). Voronoi-based reverse nearest neighbor query processing on spatial networks. *Multimedia Systems*, *15*(5), 295–308.

Santa Barbara County Fire, & Conservation Biology Institute. (2021, July 7). *Local fire protection districts and fire stations, Santa Barbara County*. Data Basin.

Santa Barbara County Fire Department. (2023). Fire hydrants development standard 2. In *Chapter 4, Section 4.2.* Fire Prevention Division (https://sbcfire.com/wp-content/uploads/2023/07/Fire-Hydrant-Spacing-and-Flow-Rates.pdf, accessed 04/23/26)

Scott, D. W. (1992). *Multivariate density estimation: Theory, practice, and visualization*. Wiley.

Sheather, S. J., & Jones, M. C. (1991). A reliable data-based bandwidth selection method for kernel density estimation. *Journal of the Royal Statistical Society Series B: Statistical Methodology*, *53*(3), 683–690.

Shoorangiz, M., Nikoo, M. R., Šimůnek, J., Gandomi, A. H., Adamowski, J. F., & Al-Wardy, M. (2023). Multi-objective optimization of hydrant flushing in a water distribution system using a fast hybrid technique. *Journal of Environmental Management*, *334*, 117463.

Shuo, Z., Jingyu, Z., Zhengxiang, Z., & Jianjun, Z. (2021). Identifying the density of grassland fire points with kernel density estimation based on spatial distribution characteristics. *Open Geosciences*, *13*(1), 796–806.

Sierra, S., & Feingold, L. (2022). Thousands of fire hydrants across east bay go uninspected annually, public records show. *ABC7 News* (https://abc7news.com/fire-hydrants-in-east-bay-ebmud-not-inspected-oakland-hills-fires/12466579, accessed 05/10/24)

Silverman, B. W. (1986). *Density estimation for statistics and data analysis*. Chapman and Hall.

Singh, P. P., Sabnani, C. S., & Kapse, V. S. (2021). Hotspot analysis of structure fires in urban agglomeration: A case of Nagpur City, India. *Fire*, *4*(3), 38.

Smith, C. (2020). *Chicago's Great Fire: The destruction and resurrection of an iconic American city*. Atlantic Monthly Press.

Syphard, A. D., Brennan, T. J., & Keeley, J. E. (2017). The importance of building construction materials relative to other factors affecting structure survival during wildfire. *International Journal of Disaster Risk Reduction*, *21*, 140–147.

Syphard, A. D., Radeloff, V. C., Keeley, J. E., Hawbaker, T. J., Clayton, M. K., Stewart, S. I., & Hammer, R. B. (2007). Human influence on California fire regimes. *Ecological Applications*, *17*(5), 1388–1402.

Taylor, M., Francis, H., Fielding, J., Jarman, I., & Etchells, T. (2024). A chaos theory view of accidental dwelling fire injuries. *Fire and Materials*, *48*(7), 715–724.

Todorović, S. K. (2020). *Modelling risk factors in urban residential fires in Helsinki*. Master's thesis, University of Helsinki.

U.S. Department of Transportation. (2015). Stops, spacing, location and design. *Federal Transit Administration*. Department of Transportation (https://www.transit.dot.gov/research-innovation/stops-spacing-location-and-design, accessed 08/20/23)

U.S. Department of Transportation. (2024). *Methods and practices for setting speed limits: Informational report* (https://highways.dot.gov/safety/speed-management/methods-and-practices-setting-speed-limits-informational-report/speed-1, accessed 05/10/26)

U.S. Fire Administration. (2024). *Residential fire estimate summaries (2014-2023)* (https://www.usfa.fema.gov/statistics/residential-fires/, accessed 07/20/24)

USDA Forest Service. (2024). *Wildland-urban interface growth in the U.S.* Department of Agriculture, Forest Service, Northern Research Station

Usui, H. (2022). Furthest neighbour distance distribution function: An application to evaluate the relationship between the density of city benches and the required continuous walking distance distribution. *Applied Spatial Analysis and Policy*, *15*(4), 1469–1492.

Ventura County Fire Protection District. (2011). Standard 14.5.3. Fire hydrants. *Fire Prevention Bureau*. Ventura County Fire Department (https://fire.venturacounty.gov/wp-content/uploads/2020/02/14.5.3-Fire-Hydrants.pdf, accessed 05/10/26)

Wang, K., Yuan, Y., Chen, M., & Wang, D. (2021). A POIs based method for determining spatial distribution of urban fire risk. *Process Safety and Environmental Protection*, *154*, 447–457.

Wang, Z., Zhang, X., & Xu, B. (2015). Spatio-temporal features of China's urban fires: An investigation with reference to gross domestic product and humidity. *Sustainability*, *7*(7), 9734–9752.

Wei, R. (2016). Coverage location models: alternatives, approximation, and uncertainty. *International Regional Science Review*, *39*(1), 48–76.

Wei, R., & Murray, A. T. (2015). Continuous space maximal coverage: Insights, advances and challenges. *Computers & Operations Research*, *62*, 325–336.

Wei, R., Murray, A. T., & Batta, R. (2014). A bounding-based solution approach for the continuous arc covering problem. *Journal of Geographical Systems*, *16*, 161–182.

Wielebski, Ł., & Medyńska-Gulij, B. (2013). Cartographic visualization of firehydrants accessibility for the purpose of decision making. *Geodesy and Cartography*, *62*(2), 183–198.

Wielebski, Ł., & Medyńska-Gulij, B. (2019). Graphically supported evaluation of mapping techniques used in presenting spatial accessibility. *Cartography and Geographic Information Science*, *46*(4), 311–333.

Wu, Z. Y., & Song, Y. (2014). Optimizing selection of fire hydrants for flow tests in water distribution systems. *Procedia Engineering*, *70*, 1745–1752.

Wyss, G. A., & Burns, W. J. (1958). Fire hydrant efficiency and standards. *Journal AWWA*, *50*(7), 951–964.

Xia, Z., Li, H., Chen, Y., & Yu, W. (2019). Detecting urban fire high-risk regions using colocation pattern measures. *Sustainable Cities and Society*, *49*, 101607.

Xiong, L., Bruck, D., & Ball, M. (2015). Comparative investigation of 'survival' and fatality factors in accidental residential fires. *Fire Safety Journal*, *73*, 37–47.

Yadav, A., & Patel, P. (2014). Assessment of water requirement and calculation of fire flow rates in water based fire fighting installation. *International Journal of Innovations in Engineering and Technology*, *4*(1), 5–12.

Zampella, A., Jr. (2017). Fire hydrants in residential areas. *Insurance Service Office, Inc.* (https://www.isomitigation.com/newsletter/fall-2017/fire-hydrants-in-residential-areas/ accessed 08/20/24)

Zhang, X., Yao, J., Sila-Nowicka, K., & Jin, Y. (2020). Urban fire dynamics and its association with urban growth: Evidence from Nanjing, China. *ISPRS International Journal of Geo-Information*, *9*(4), 218.

Zhang, Y. (2013). Analysis on comprehensive risk assessment for urban fire: The case of Haikou City. *Procedia Engineering*, *52*, 618–623.

Zigner, K., Carvalho, L. M. V., Jones, C., & Duine, G. (2022). Extreme winds and fire weather in coastal Santa Barbara County, CA: An observational analysis. *International Journal of Climatology*, *42*(1), 597–618.